1996

Electrical performance of RTV silicone rubber coatings for H.V. outdoor insulators.

Hui. Deng
University of Windsor

ELECTRICAL PERFORMANCE OF RTV SILICONE RUBBER COATINGS FOR H.V. OUTDOOR INSULATORS

by

Hui Deng

A Thesis
Submitted to the
Faculty of Graduate Studies and Research
Through the Department of Electrical Engineering in Partial Fulfilment of the Requirements for the Degree of Master of Applied Science at the University of Windsor

Windsor, Ontario, Canada
1995

ISBN 0-612-10988-7

Name Hui DENG

Dissertation Abstracts International and *Masters Abstracts International* are arranged by broad, general subject categories. Please select the one subject which most nearly describes the content of your dissertation or thesis. Enter the corresponding four-digit code in the spaces provided.

Mechanical and Aerospace Engineering
SUBJECT TERM

0544
SUBJECT CODE

UMI

Subject Categories

THE HUMANITIES AND SOCIAL SCIENCES

COMMUNICATIONS AND THE ARTS
Architecture 0729
Art History 0377
Cinema 0900
Dance 0378
Fine Arts 0357
Information Science 0723
Journalism 0391
Library Science 0399
Mass Communications 0708
Music 0413
Speech Communication 0459
Theater 0465

EDUCATION
General 0515
Administration 0514
Adult and Continuing 0516
Agricultural 0517
Art 0273
Bilingual and Multicultural 0282
Business 0688
Community College 0275
Curriculum and Instruction 0727
Early Childhood 0518
Elementary 0524
Finance 0277
Guidance and Counseling 0519
Health 0680
Higher 0745
History of 0520
Home Economics 0278
Industrial 0521
Language and Literature 0279
Mathematics 0280
Music 0522
Philosophy of 0998
Physical 0523
Psychology 0525
Reading 0535
Religious 0527
Sciences 0714
Secondary 0533
Social Sciences 0534
Sociology of 0340
Special 0529
Teacher Training 0530
Technology 0710
Tests and Measurements 0288
Vocational 0747

LANGUAGE, LITERATURE AND LINGUISTICS
Language
General 0679
Ancient 0289
Linguistics 0290
Modern 0291
Literature
General 0401
Classical 0294
Comparative 0295
Medieval 0297
Modern 0298
African 0316
American 0591
Asian 0305
Canadian (English) 0352
Canadian (French) 0355
English 0593
Germanic 0311
Latin American 0312
Middle Eastern 0315
Romance 0313
Slavic and East European 0314

PHILOSOPHY, RELIGION AND THEOLOGY
Philosophy 0422
Religion
General 0318
Biblical Studies 0321
Clergy 0319
History of 0320
Philosophy of 0322
Theology 0469

SOCIAL SCIENCES
American Studies 0323
Anthropology
Archaeology 0324
Cultural 0326
Physical 0327
Business Administration
General 0310
Accounting 0272
Banking 0770
Management 0454
Marketing 0338
Canadian Studies 0385
Economics
General 0501
Agricultural 0503
Commerce-Business 0505
Finance 0508
History 0509
Labor 0510
Theory 0511
Folklore 0358
Geography 0366
Gerontology 0351
History
General 0578
Ancient 0579
Medieval 0581
Modern 0582
Black 0328
African 0331
Asia, Australia and Oceania 0332
Canadian 0334
European 0335
Latin American 0336
Middle Eastern 0333
United States 0337
History of Science 0585
Law 0398
Political Science
General 0615
International Law and Relations 0616
Public Administration 0617
Recreation 0814
Social Work 0452
Sociology
General 0626
Criminology and Penology 0627
Demography 0938
Ethnic and Racial Studies 0631
Individual and Family Studies 0628
Industrial and Labor Relations 0629
Public and Social Welfare 0630
Social Structure and Development 0700
Theory and Methods 0344
Transportation 0709
Urban and Regional Planning 0999
Women's Studies 0453

THE SCIENCES AND ENGINEERING

BIOLOGICAL SCIENCES
Agriculture
General 0473
Agronomy 0285
Animal Culture and Nutrition 0475
Animal Pathology 0476
Food Science and Technology 0359
Forestry and Wildlife 0478
Plant Culture 0479
Plant Pathology 0480
Plant Physiology 0817
Range Management 0777
Wood Technology 0746
Biology
General 0306
Anatomy 0287
Biostatistics 0308
Botany 0309
Cell 0379
Ecology 0329
Entomology 0353
Genetics 0369
Limnology 0793
Microbiology 0410
Molecular 0307
Neuroscience 0317
Oceanography 0416
Physiology 0433
Radiation 0821
Veterinary Science 0778
Zoology 0472
Biophysics
General 0786
Medical 0760

EARTH SCIENCES
Biogeochemistry 0425
Geochemistry 0996
Geodesy 0370
Geology 0372
Geophysics 0373
Hydrology 0388
Mineralogy 0411
Paleobotany 0345
Paleoecology 0426
Paleontology 0418
Paleozoology 0985
Palynology 0427
Physical Geography 0368
Physical Oceanography 0415

HEALTH AND ENVIRONMENTAL SCIENCES
Environmental Sciences 0768
Health Sciences
General 0566
Audiology 0300
Chemotherapy 0992
Dentistry 0567
Education 0350
Hospital Management 0769
Human Development 0758
Immunology 0982
Medicine and Surgery 0564
Mental Health 0347
Nursing 0569
Nutrition 0570
Obstetrics and Gynecology 0380
Occupational Health and Therapy 0354
Ophthalmology 0381
Pathology 0571
Pharmacology 0419
Pharmacy 0572
Physical Therapy 0382
Public Health 0573
Radiology 0574
Recreation 0575
Speech Pathology 0460
Toxicology 0383
Home Economics 0386

PHYSICAL SCIENCES
Pure Sciences
Chemistry
General 0485
Agricultural 0749
Analytical 0486
Biochemistry 0487
Inorganic 0488
Nuclear 0738
Organic 0490
Pharmaceutical 0491
Physical 0494
Polymer 0495
Radiation 0754
Mathematics 0405
Physics
General 0605
Acoustics 0986
Astronomy and Astrophysics 0606
Atmospheric Science 0608
Atomic 0748
Electronics and Electricity 0607
Elementary Particles and High Energy 0798
Fluid and Plasma 0759
Molecular 0609
Nuclear 0610
Optics 0752
Radiation 0756
Solid State 0611
Statistics 0463

Applied Sciences
Applied Mechanics 0346
Computer Science 0984
Engineering
General 0537
Aerospace 0538
Agricultural 0539
Automotive 0540
Biomedical 0541
Chemical 0542
Civil 0543
Electronics and Electrical 0544
Heat and Thermodynamics 0348
Hydraulic 0545
Industrial 0546
Marine 0547
Materials Science 0794
Mechanical 0548
Metallurgy 0743
Mining 0551
Nuclear 0552
Packaging 0549
Petroleum 0765
Sanitary and Municipal 0554
System Science 0790
Geotechnology 0428
Operations Research 0796
Plastics Technology 0795
Textile Technology 0994

PSYCHOLOGY
General 0621
Behavioral 0384
Clinical 0622
Developmental 0620
Experimental 0623
Industrial 0624
Personality 0625
Physiological 0989
Psychobiology 0349
Psychometrics 0632
Social 0451

ABSTRACT

Room temperature vulcanizing (RTV) silicone rubber coating is increasingly being used by power utilities to overcome the contamination problems encountered with ceramic and glass insulators. Various formulations of the RTV coating systems were intensively investigated in an effort to optimize their electrical performance and in particular to extend their life.

The effects of the size of the particles of ATH filler on the life of RTV silicone rubber coating was studied in a salt-fog chamber. The median particle sizes examined were 1.0, 4.5, 13, 17 and 75 μm. The optimum size giving the lowest leakage current and the longest time to failure of the coating was determined. The particle size affected the roughness of the coating. This was determined by a high resolution surface roughness tester and a scanning electron microscope (SEM). The roughness was enhanced after a prolonged test in salt-fog. The leakage current affected the amount of silicone fluid on the surface. The amount of silicone fluid present on the surface after exposure to dry-band arcing in salt-fog was a function of the particle size. Measurements of surface roughness, the amount of silicone fluid on the surface, and the leakage current combined with theoretical analysis of the heat of conduction, lead to identification of the mechanisms by

which the size of the ATH particle impart resistance to tracking and erosion.

The influences of the coating thickness, different substrates, addition of silicone fluid to the coating system and different carrier solvents on the leakage current, pulse current count rates and the life of the RTV coatings were investigated. It was found that all these parameters affected the electrical performance in salt-fog. The optimum coating thickness was determined for a fixed substrate. Mechanisms by which these four parameters affected the performance are suggested and discussed.

The content of low molecular weight (LMW) silicone fluid and the diffusion of LMW from the bulk to the surface were determined, by using an extraction technique in an analytical hexane. This was in order to explore some of the factors governing the lifetime of the RTV coating. ATH filled RTV coatings having thicknesses from 0.17 to 0.99mm, ATH particle sizes from 1.0 to 75 μm and different carrier solvents were used. The roles of the LMW content and the diffusion process in the lifetime of the coating were evaluated for different formulations of RTV.

Dedicated to my parents and to my wife

ACKNOWLEDGEMENTS

I would like to express my sincere thanks to my supervisors, Dr. R. Hackam and Dr. E.A. Cherney, for their guidance, suggestions and their support throughout the course of this work.

I wish to thank Dr. R. Aroca of Chemistry & Bio-Chemistry Department and Dr. A. Watson of Electrical Engineering Department for their useful criticisms and suggestions throughout the course of this work.

I wish to thank the Natural Science and Engineering Research Council of Canada for providing the funds for this project.

I wish to thank CSL Silicones Inc., Guelph, Ontario, for providing the RTV silicone rubber materials for this study.

I wish to thank Mr. D. Liebsch, Central Research Workshop, and members of his staff for their assistance during this work.

I would also like to thank Mr. M. Fuerth in the Department of Chemistry for his technical assistance and permission to use FT-IR spectroscopy, Mr. A. Johns and Mr. J.M. Novosad in the Department of Electrical Engineering for their technical assistance, and Mr. J. Robinson in the Department of Engineering Materials for his assistance with the EDAX and SEM analysis.

TABLE OF CONTENTS

LIST OF FIGURES

LIST OF TABLES.

CHAPTER I

INTRODUCTION

Surface contamination and leakage current have caused operating problems for electrical utilities since electrical power was in its infancy. Even though porcelain and glass insulators can withstand substantial arcing without serious degradation, the effects of leakage current and flashover is a major practical limitation in the reliable supply of electrical power. A flashover in a substation may result in destruction of an insulator, circuit breaker lock-out or potential damage to equipment costing millions of dollars in equipment losses and replacement power.

The main problem with ceramic insulators is that they have high surface energy[1-3] and wet readily by allowing water to spread in a continuous film. There are many sources of natural contaminants in the outdoor environment such as sea salt, road salt, cement dust, fly ash, bird droppings, fertilizer and many types of industrial emissions[4-6]. These contaminants which deposit on the insulators encourage leakage current to develop, the effect of which can range from dry band arcing to flashover. On ungrounded wood structures, leakage currents can cause crossarm and pole top burnoffs while on steel structures, uncontrolled leakage current can develop into flashover. In either event, disruptions of the power system can occur.

1.1 TECHNOLOGIES AND INSULATOR CONTAMINATION MAINTENANCE PRACTICES

To prevent disruptions of the power system due to insulator contamination several technologies have been employed with varying degrees of success to reduce the incidence of insulator flashover. Changes to insulator design has been one method of modifying performance. The conventional approach has been to increase the leakage distance thereby decreasing the voltage stress across the surface of the insulator by either adding insulator sheds or by replacing the insulators with longer leakage path designs[7,8]. Although this technology is a cost effective one, it is one that can not be implemented in every case[9,10]. Another approach has been to apply a resistive glaze to porcelain insulators[11-19] thereby modifying the electrical stress and at the same time, increasing the surface temperature to prevent the condensation of moisture. Both technologies have had limited success.

Maintenance practices have also shown varying degrees of success to help prevent disruption of the power system due to insulator contamination. The most successful have been high-pressure cleaning techniques[11,20,21] either by water or dry-cleaning methods, using an abrasive medium such as crushed corn cobs or walnut shells sometimes admixed with lime. Most utilities regularly wash insulators to prevent flashover in very heavily polluted areas[22]. Both technologies are costly because they are labour-intensive and can require frequent repetition to be effective, and in many situations, are no longer cost effective.

Silicone compounds for outdoor insulation offer advantages over other methods of protection. The experience with grease-like coating materials for porcelain insulator over a 20 year period[20,21,23-26] has shown that as long as they maintain their water

repellency properties, they provide total protection of the insulator. When the grease-like materials reduce their water repellency, due to extended exposure to corona, ultraviolet light, water erosion and /or saturation with contaminants, the grease must be removed and reapplied at considerable expense in order to maintain protection. Non-ceramic insulators having silicone rubber weathersheds have been quite successful in maintenance of overhead lines for many years[22,27-29]. The silicone rubber gives the initial water repellent(hydrophobic) surface thereby preventing leakage current [27-31]. The silicone rubber filled with alumina trihydrate filler ($ATH{\cdot}3H_2O$) provides an arc resistant property, ensuring a long term ability to limit leakage currents and therefore prevent flashover [32-35]. Experience has shown that water washing of silicone rubber insulators may not be required[36].

Where silicone rubber insulators are either not available as direct replacements for porcelain and glass insulators, or too expensive, an alternative maintenance practice is to impart water repellency to the surface of ceramic insulators with a coating of room temperature vulcanizing (RTV) silicone rubber [10,37-40]. Though the concept that a water repellency surface is created by coating porcelain and glass insulators with RTV silicone rubber is relatively new, the liquid silicone RTV coatings have gained considerable popularity since the first field trial in 1974 with an experimental product [30] and the first large scale application in 1987 with a commercialized product[31].

1.2 CHARACTERISTICS OF RTV SILICONE RUBBER COATINGS

The usual RTV silicone rubbers are made from a basic polydimethylsiloxane (PDMS) molecules, as shown in Fig.1.1. The molecule of PDMS is mainly composed of methyl group (CH_3), oxygen (O) and silicone (Si). The RTV system contains PDMS

silicone polymer, cross-linking agent and catalyst, fumed silica reinforcer, ATH filler and special additives , all dispersed in a carrier solvent [10,41]. The vulcanization can be prevented if absolutely water-free conditions is assured. In this manner, this kind of RTV silicone rubber is suitable for long-term storage in moisture - impermeable containers. The liquid coating vulcanizes in the presence of atmospheric humidity forming a solid rubber coating with physical and electrical properties that vary considerably [10]. These properties are the result of the degree of cross-linkage, type of radical within the monomer molecule, and the amount of filler [10]. Special additives serve to achieve particular effects or improvements of these properties [41].

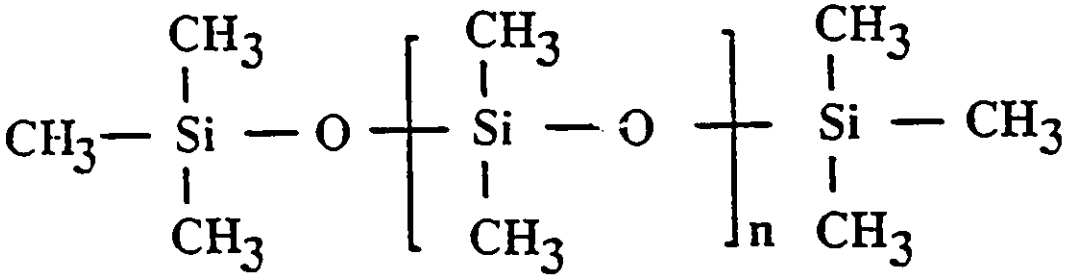

Figure 1.1 Chemical structure for PDMS

The solvent most often used is V&P naphtha which is flammable and therefore the coating with using this solvent can be applied to the insulators when the power system is de-energized. Other solvents such as 1,1,1 trichloroethane and anhydrous cyclohexane are also occasionally employed. RTV coating can be applied to ceramic insulators by dipping, painting or spraying [10,41]. The RTV coating can also be applied to many

organic polymer substrates, such as epoxy resin and EPDM rubber, due to its superior adhesive property. The liquid polymer layer, vulcanizes into a flexible layer when exposed to moisture in the air. The coating gives initial water repellency which prevents the formation of continuous water filming on the surface even when a layer of contamination has built-up on the surface and thus suppresses the leakage current and flashover. This concept of protection for ceramic insulators has been increasingly giving considerable interest as a maintenance tool of insulator contamination.

1.3 ELECTRICAL PERFORMANCE OF RTV COATINGS

Porcelain and glass insulators are coated with RTV silicone rubber to improve their contamination performance. The RTV coating provides hydrophobicity initially which prevents water filming and thus suppresses the development of leakage current and flashover. After a heavy and prolonged wetting, a continuous water filming is gradually formed and leakage current develops on the surface. The heat from the dry band arcing causes hydrolysis, scission and interchange of molecular bonds and removes hydrophobic methyl groups [3,38,42,43] resulting in aging of the coating. The RTV coating finally fails by erosion and tracking on the substrate. The various formulations of RTV coatings differ in their ability to impart resistance to dry band arcing although the base material in all cases is PDMS. High temperature vulcanizing (HTV) silicone rubber filled with alumina trihydrate (ATH) shows a better performance than with silica filler[34]. The concentration of [34,44] and the size of the ATH filler particles [45] also affect the life of RTV coating. Properly selected formulations of coatings which maintain a high resistance to damage from dry band arcing may have a longer life. This renders the occurrence of flashover, better reliability, and enhanced integrity of the power system. A

study of the degradation, erosion and lifetime of the RTV coatings in wet and contaminated conditions is necessary to determine the limitation on the application of the coating to outdoor insulation particularly in sea coast environments.

When the coating is covered with contaminants, the hydrophobicity is reduced on the surface of RTV. The low molecular weight (LMW) silicone fluid, which is inherently present in the coating, diffuses from the bulk to the surface of RTV and then surmounts the contamination layer [35,44,46,47]. The process of diffusion modifies the physical property of the contaminant giving it a hydrophobic quality. It has been reported that there was a reduction in the quantity of LMW on the surface of aged RTV when compared to virgin RTV [48]. The total content of LMW silicone fluid in the RTV coating was also reduced after an extended time of salt-fog testing at $0.5kV_{rms}$/cm and 250μS/cm[49]. The heat from the dry band arcing causes scissions of the long polymer chain into short chains which become more water soluble and more volatile[50]. The water washes the surface and removes some silicone fluid away from the coating. The contaminants also carry some silicone fluid from the surface when they are washed away by water or blown away by wind. As the silicone fluid is gradually depleted on the surface and in the bulk of RTV coating, the hydrophillic contamination absorbs more water and forms a thicker water film. Increased current then develops on the surface and the insulator eventually flashes over. Therefore the presence of sufficient quantity of LMW silicone fluid in the bulk of RTV coating and its ability to diffuse to the surface are of paramount interest in maintaining the hydrophobic properties of the coating and in order to achieve a long life of the coating. It is therefore desirable to evaluate the role of the LMW content and diffusion in affecting the life of RTV coatings.

1.4 RESEARCH OBJECTIVES

1. To investigate the role of the size of ATH particle filler in the development of leakage current and the life of RTV coatings.
2. To determine the optimum thickness of RTV coatings giving the best electrical performance.
3. To determine the influences of substrate type and solvent type on the leakage current and life of RTV coatings.
4. To study the mechanisms by which the addition of silicone fluid to RTV influence its electrical performance.
5. To determine the LMW content and diffusion in RTV coatings with various compositions.
6. To determine the surface roughness with various RTV formulations.
7. To examine the dependence of surface conditions (surface roughness and contact angles) on the development of leakage current.
8. To evaluate the role of LMW content and diffusion in the life of RTV coatings.
9. To uncover the role the thermal conductivity of RTV in imparting tracking and erosion resistance to the coatings.

CHAPTER II

EXPERIMENTAL SET UP

2.1 SALT-FOG CHAMBER

The commonly used artificial test methods are salt-fog and clean fog[51,52]. The salt-fog test is derived as a simple and direct method of measuring the ability of an insulator to withstand contaminant, without flashover, by subjecting it to an artificial salt water fog. The schematic diagram of the salt-fog chamber used in this study is shown in Fig.2.1[38,53]. It is fabricated of 3mm thick acrylic glass sheets and has the dimensions of 2.5m x 2.5m x 2.5m. Four nozzles are used in the fog chamber and these are fabricated from acrylic glass in accordance with IEC specifications[54]. The nozzles are symmetrically placed and face the specimens to provide uniform wetting of the specimens, as shown in Fig.2.2.

Saline water and compressed air were supplied through stainless steel lines. Water conductivity was measured by a conductivity meter(Horizon Model 1484) which was capable of measuring from 0 to 20,000μS/cm. The conductivity of the saline water was adjusted intermittently to maintain ±5% of the initial value. The saline water was supplied from a 250 litre reservoir tank. The tank was fabricated from XLPE and the salt water was handled by two corrosion resistant pumps, as shown in Fig.2.1. The saline water was not usually changed until all specimens had failed in the fog chamber. The saline water from the chamber was continuously filtered to remove the contaminant originating from the dry band arcing by placing a stainless steel mesh located at the bottom of the chamber and was collected in a small container. There is a water level switch in this container which turns on a pump when the container is full and turns it off when the container is empty. The function of the container is to retain the drained water from the fog chamber before its return to the main reservoir to prevent the pump from running on empty. The water flow rate is controlled using a flow meter (model CALQFLO) in series with the input water

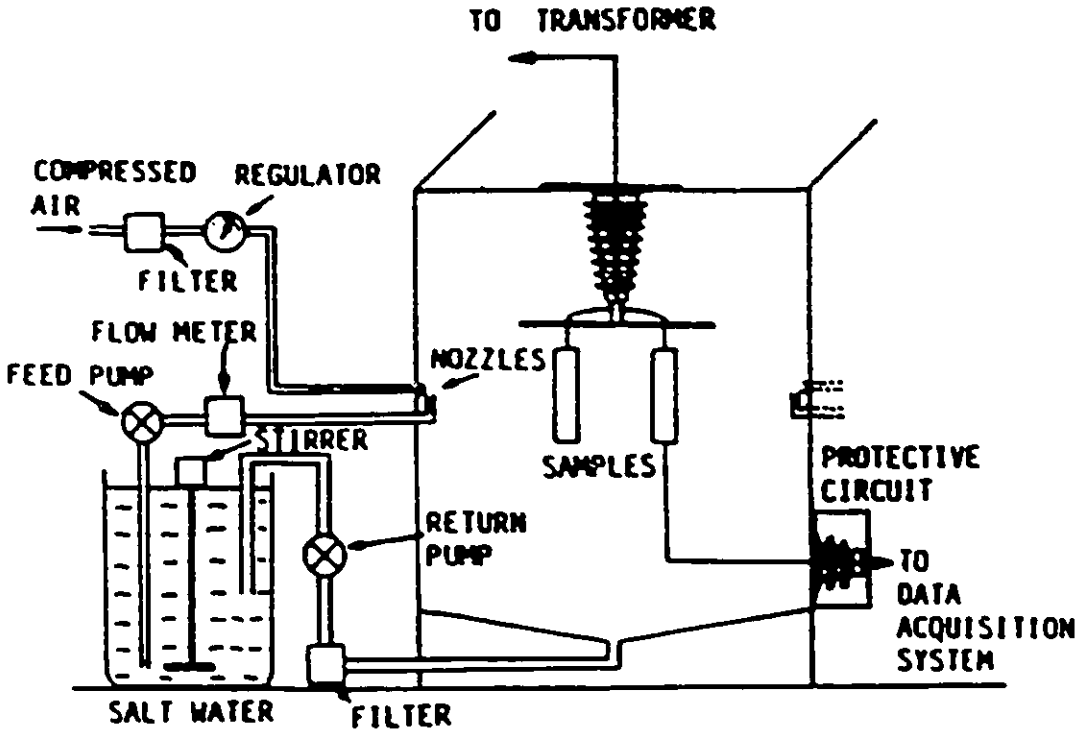

Figure 2.1 Schematic diagram of the salt-fog chamber

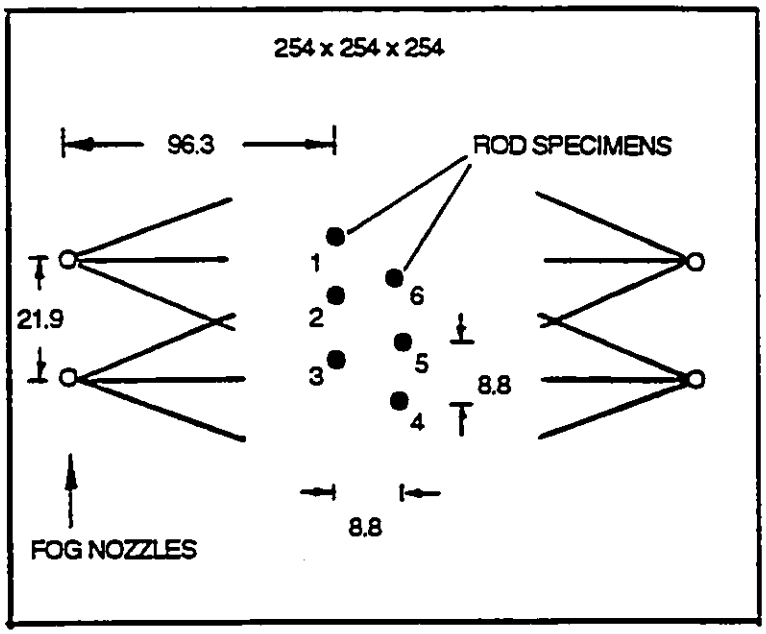

Figure 2.2 Arrangement of 4 IEC fog nozzles and 6 rods in the salt-fog chamber. Dimension are in cm. Diagram is not drawn to scale.

line. The flow rate of the water can be varied from 0 to 2.0 l/min. The compressed air can be varied from 0.1 to 0.65 MPa by an air regulator.

2.2 TEST SUPPLY

The test supply is a 14.4kV/208V, 37.5kVA, 60Hz, distribution transformer used in reverse. The primary is controlled by a 20kVA, 0-220V variac. The high voltage from the transformer is brought into the fog chamber through a 25kV wall bushing which is placed at the top of the chamber, as shown in Fig.2.1. The bushing is coated with silicone grease to prevent flashover through the surface. In the present study the applied voltage is constant and adjusted regularly to maintain a nominal voltage of 7.6±0.3 Kv_{rms} giving an average electric stress of 0.50±0.02kV_{rms}/cm to the 152mm long specimen.

2.3 DATA ACQUISITION SYSTEM

A data acquisition system is used to continuously monitor the leakage current through the surface of the specimens under test. It consists of a resistive high voltage divider, protective circuits, a reference signal circuit, analog-to-digital (A/D) converter(Mountain Computer Inc.), and a microcomputer (Apple II). A schematic diagram of the system is shown in Fig.2.3[55]. Details of the principles of the data acquisition system, algorithm of data acquisition software and the computer program for sampling the leakage current have been described in the dissertation by Kim[55] and only essential information necessary for the present study will be given here. The system employed an 8 bit, 16 channels A/D converter. Only 6 channels were used in the present study in order to increase the sampling speed. The microprocessor processes the instantaneous current to yield the peak and the average values on both the positive and

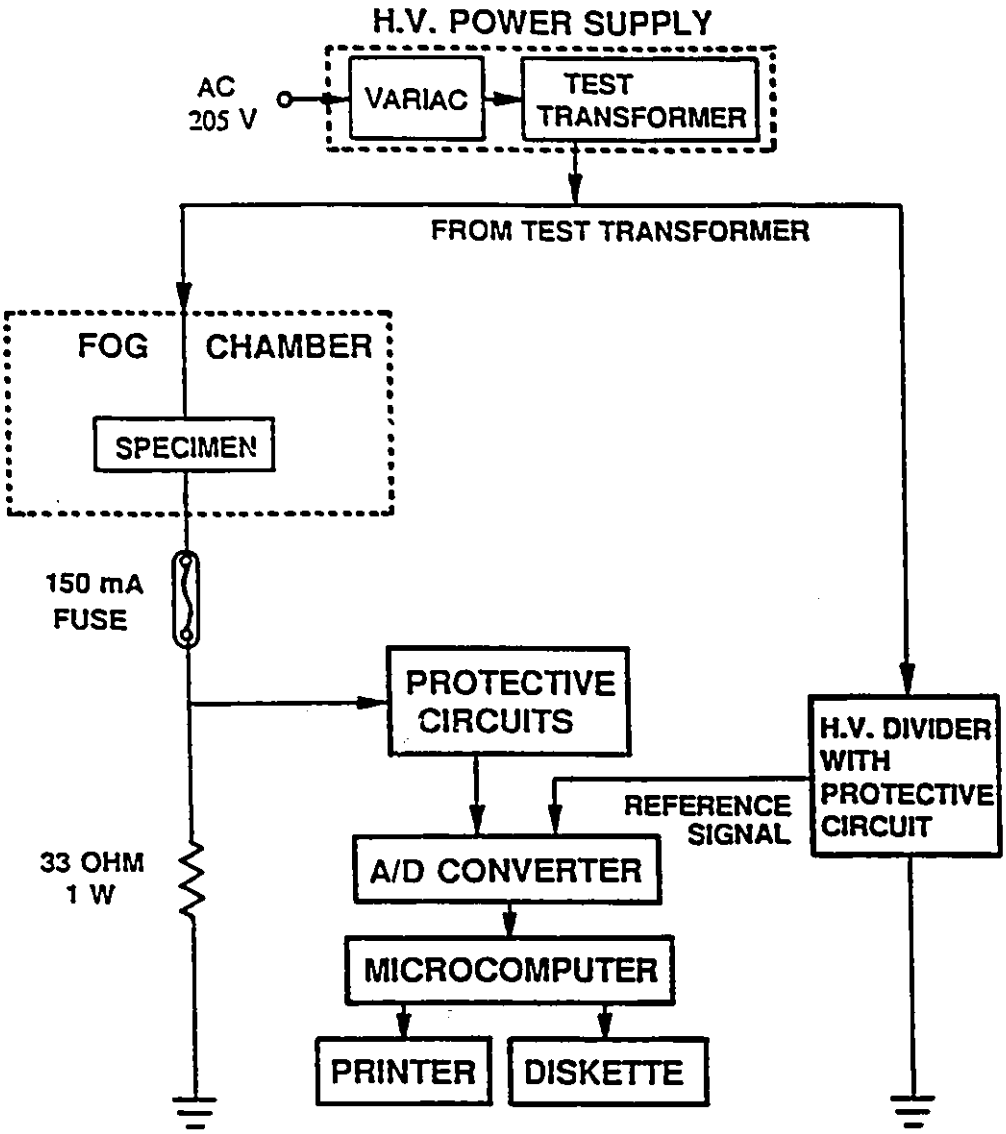

Figure 2.3 Schematic diagram of data acquisition system

the negative portions of the 60 Hz power frequency. The length of the sampling time varied from 10 minutes during the first hour of the test to one hour during the rest of the test which typically lasted up to 400 hours. The total charge flow across the specimens is continuously calculated by integrating the sampled current over specified periods. The average leakage current is defined as the value obtained by summing up the absolute values of all the current sampled during the positive (13 samples) and negative (13 samples) portions of the 60Hz power frequency, over a specified length of time, and then dividing by the total number of the sampled currents. The number of leakage current pulses was determined over a specified period and specified current limits in 15 ranges from 0 to 88mA. At the end of each desired test period, the data were stored in a floppy disk and a hard copy was printed.

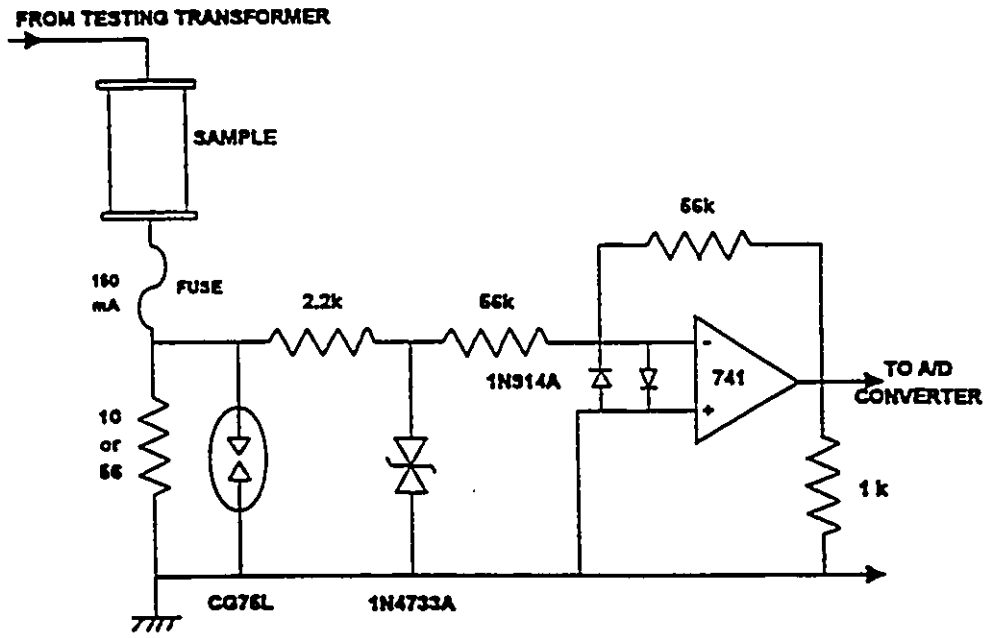

Figure 2.4 Protection circuit of the data acquisition system against flashover of the insulators being tested. Resistance values are in Ω.

2.4 ELECTRICAL PROTECTION

The data acquisition system is protected against an occasional flashover of either the insulator or coated rods. The input of the A/D converter and the microprocessor are protected using a combination of a fast acting low voltage (75V) gas filled spark gaps (CG75L), a Zener diode (IN4733A), a pair of back to back diodes (IN914A) and a combination of resistors to attenuate the initial energy of the flashover which may get through before the spark gap operates (a few nanoseconds). A standard operational amplifier (741) is employed to recover the original signal as shown in Fig.2.4[56]. A fast 150 Ma fuse wire enclosed in a glass tube is placed in series with each specimen, ensuring that the power supply to the other specimens is not interrupted when a single specimen is failed by flashover. The control variac is protected by a 50A fuse and a 50 A fast magnetic circuit breaker.

2.5 SPECIMENS

The RTV was formulated using a basic polydimethylsiloxane (PDMS) polymer system containing a fumed silica reinforcer, a polymerization catalyst and ATH filler, all dispersed in a carrier solvent[10]. The ATH filler was used in the RTV to enhance its resistance to damage from erosion. The improved performance with addition of ATH is due in part to its higher thermal conductivity than that of the base silicone rubber[57,58]. A constant concentration by weight of 90 parts of the ATH filler per one hundred (pph) of the silicone rubber was used in the present study. This concentration of the ATH filler was found to be close to the optimum level, which is in the range of 45 to 55% by weight, that gives both good dispersion in the RTV liquid and longest time to failure[44]. The RTV coatings were largely applied to polyester fibre glass reinforced plastic (FRP)

rods, 152mm length and 16mm in diameter in the present study. Uncoated FRP rods were chosen because they readily track and then flashover in salt-fog. This enabled the testing of the performance of RTV coatings of different formulations on a substrate which was, in the case of FRP, inherently much inferior than the coatings. This gives an accurate method to determine the length of time when the RTV silicone rubber coating has been substantially aged. The onset of failure of RTV coating occurs when sufficient erosion has occurred by the action of the dry band discharges which exposes the surface of the FRP. The latter fails by tracking and is followed with flashover. Contact to the RTV coating was made with two disk-type graphite electrodes 31.7mm in diameter and 3.2mm thick. The graphite electrodes were attached to the FRP rods using stainless steel screws.

2.6 THE POSITION OF RTV SPECIMENS IN FOG CHAMBER

The position of specimens in salt-fog chamber is shown in Fig.2.2. Six RTV specimens were tested simultaneously, three of which were tested at a fixed coating formulation (rods 1, 2 and 3 in Fig.2.2). Additionally three rods having identical formulation but different from the other group were placed together (rods 4, 5 and 6 in Fig.2.2). The uniformity of the salt-fog condition on the six specimens in the chamber was first determined before the onset of salt-fog test with the RTV coatings[45]. 6 identical rods of uncoated FRP were placed in the chamber in carefully selected positions until almost identical average leakage currents and current pulse count rate were developed in the rods. The time to failure in the 6 uncoated polyester FRP rods were in the range of 44±8h. This indicated that the variation of the fog conditions in the locations of the specimen was acceptably small and therefore the simultaneous testing of 6 coated rods could be reasonably assumed to be under the same fog condition for all specimens.

CHAPTER III

MEASUREMENT TECHNIQUES

3.1 MEASUREMENTS OF CONTACT ANGLE

Measurements of contact angle of a drop of water on organic polymers provides an indication of the state of the hydrophobicity of the surface[3,59,60]. When a water droplet is in contact with a solid, the angle formed between the tangent to the droplet and the horizontal surface is called the contact angle. The contact angle is dependent on the free energy of the surface and therefore the wettability of the solid surface is related to the contact angle. The free energy and the contact angle are inter-related via Yang's equation[3,61,62] and decreases with increasing surface free energy. A high energy surface, like glass, wets readily, allowing water to spread over it and has a contact angle of zero. The surface is completely wetted and is hydrophillic. On the other hand the low energy surface, like silicone rubber, repels water, the contact angle is large(>90°) and the surface is hydrophobic or water repellent.

In the present study, the contact angle was measured on a stable horizontal surface by a goniometer using a sessile drop having a volume of about 5µl of deionized distilled water (5.5µS/cm). The conductivity of the water droplet in the range 20-1000 µS/cm had no effect on the contact angle [46] and this conclusion was further confirmed and extended by the author to the range 5.5-10,000µS/cm. The contact angle depends on the volume of the droplet but in the range 2-9µl the contact angle has been reported to be independent of the volume[46]. In the this work the contact angle was also studied with droplets having various volumes in the range 5-30 µl. Two different surfaces, RTV silicone rubber and FRP polyester, were used. It was found that the contact angle was independent of the volume up

to 30 µl for both materials. The contact angle was determined within 30s after placing the water droplet on the surface in order that the measured values were not unduly influenced by a long duration of a presence of water on the surface[46]. The contact angle was determined at four equi-distance locations along the circumference of the cylindrical specimens, and at least 4 locations along the axis of the rod were investigated. Thus a total of at least 16 readings were taken for each specimen.

3.2 MEASUREMENTS OF SURFACE ROUGHNESS

The surface roughness of RTV specimen has a direct influence on the development of leakage current and the initiation of dry band discharges. Experiments have shown that the average leakage current and the current pulse counts increased with increasing surface roughness. In the present study the surface roughness was determined using both a roughness detector and a Scanning Electron Microscope (SEM). The average and the maximum roughness values of the RTV surface were determined by using a high resolution (±0.05µm) roughness detector type Surftest-212 (Mitutoyo, Japan). The average roughness is defined as the arithmetic average value of the profile of the roughness throughout the sampling length. The maximum roughness is defined as the value measured between the highest peak and the lowest valley. The sampling length was adjusted to 8mm along the length of the rod. Measurements of the surface roughness were conducted at 4-6 locations in each specimen. The profile of the surface roughness was determined by a roughness detector type Mitutoyo Surftest-III.

The SEM studies were conducted using an instrument type Semko Nano Lab7 with a 15keV electron beam, at a pressure of 10^{-4} to 10^{-3} Pa. The penetration of the electron beam into the surface of RTV specimens at this voltage was about 10µm. The specimens

were first coated with a conducting layer of carbon using a carbon arc, in vacuum, at a pressure of 10^{-4} to 10^{-2} Pa, to a thickness of about 20nm. In some cases the RTV specimens were coated with gold to a thickness of a few hundred A° to eliminate charging of the surface in the SEM. The size of the specimens was about 10mm x 10mm.

3.3 MEASUREMENTS OF FTIR-ATR

The principle of an infrared (IR) spectroscopy technique is that a light beam is passed through the entire thickness of the sample material and the transmission is measured as a function of the wavelength (or wave number). The wavelength of the infrared light in the range $2.5x10^{-4}$ - $5x10^{-3}$ cm (wave number 4000 to 200cm^{-1}) is mostly used[63]. Coupling with internal reflection[64-67], the conventional IR optical spectroscopy can be used in the study of the surface of organic materials. In this technique the specimen is in contact with an optically dense but transparent medium and then measuring the wavelength dependence of the reflectivity of the interface by introducing light into the dense medium.

Monitoring of the chemical changes on the surface of RTV coating due to dry band arcing under wet and contaminated conditions are useful to give indications of the changes that occur. Some of the changes at the surface of an aged coating are indicated by the formation of low molecular weight PDMS silicone fluid and the diffusion of the fluid from the bulk to the surface of the coating[43,48]. To measure the amount of silicone fluid on the surface of the coating and determine its dependence on the formulation of RTV, a Nicolet 5DX Fourier Transform Infrared (FTIR) spectrometer with an attenuated total reflection (ATR) attachment was employed using a KRS-5 (Thalium Bromoiodide) crystal. The silicone fluid was obtained by placing the specimen next to the

crystal and applying a predetermined pressure and then some of the silicone is transferred to the crystal which is determined using IR spectroscopy.

3.4 SPECIMEN WASHING

In order to conduct the measurements of surface roughness, FTIR-ATR and SEM on RTV specimens after salt fog the specimens were washed to remove the salt deposits using 5% acetic acid in an ultrasonic vibrator for 2 minutes and rinsed thoroughly with distilled water[53]. The mild acetic acid at the low concentration used did not react with the surface of the RTV coating since it was applied for a brief period of 2 minutes and was followed immediately by a thorough rinsing with distilled water to remove any residual traces of acetic acid. The acetic acid solution neither penetrate nor reacts with the RTV coating[42]. This was determined by FTIR studies, which showed complete lack of carbonyl (C=0) stretching frequency which would be expected from dissolution or derivatization. A derivatizing agent reacts with certain elements or group of elements and label the outcome of the reaction with a distinctive element or a compound.

CHAPTER IV

EVALUATION OF ELECTRICAL PERFORMANCE OF RTV SILICONE RUBBER COATINGS

4.1 INTRODUCTION

The various RTV coatings differ greatly in their ability to prevent leakage current and flashover although the base material in all case is PDMS. Coating composition is the key to their performance. Coatings that loose their hydrophobicity have a short life. These coatings become ineffective in a short time and fail to prevent flashover. Properly selected coatings which maintain their hydrophobicity have a long life in preventing flashover.

In this chapter, the effects of the size of particles of ATH filler, the coating thickness, substrate type, addition of silicone fluid to RTV formulation and carrier solvent type in RTV on performance and life time are studied. Mechanisms by which these parameters affect the performance are suggested and discussed.

4.2 RTV PERFORMANCE WITH SIZE OF ATH PARTICLES

4.2.1. Experimental Conditions

RTV coatings were applied to polyester fibre glass reinforced plastic (FRP) rods, 152mm length and 16mm in diameter. RTV formulations were made with ATH filler

having median particle sizes of 1.0, 4.5, 13, 17 and 75μm in a carrier solvent of 1,1,1 trichloroethane. These particle sizes were selected because they were commercially available. The size of the particle was obtained by x-ray sedimentation using a Micromeritics Sedigraph. The particle size distribution of the precipitated grade of ATH was relatively narrow. The concentration of the filler in RTV coatings was 90pph by weight. Three specimens were used for each size of particles. A saline water flow rate of 1.6±0.2 l/min and an air pressure of 0.65±0.02MPa (94.7±3psi) were used to generate the fog. The saline solution was obtained by adding table salt (NaCl) to the tap water which has a typical conductivity of 300±10μS/cm. The conductivity of the saline water was adjusted continuously to maintain a nominal conductivity of 1000±3% μS/cm. The temperature in the fog chamber was 24±2°C during the test.

4.2.2 Dependence of Leakage Current

Measurement of the contact angle on the surface of the coating before the salt-fog test showed that the contact angle was within 92-96° for all particle sizes of ATH from 1 to 75μm. This indicates that at the start of the salt-fog test the water repellency of the coatings was almost identical and independent of the particle size. However the development of leakage current depended on the size of the particle. Fig.4.1 shows the average leakage current as a function of test time in the fog chamber. After 2h of test, the leakage current was in the range 3-6mA for all sizes of ATH particles. The leakage current was lower for smaller particle sizes at the start of the test as indicated in Fig.4.1. The difference in the leakage current at the beginning is thought to be due to the roughness of the surface which was smoother for smaller sizes and rougher for larger sizes of ATH particles. Fig.4.1 also shows that the leakage current of the uncoated FRP

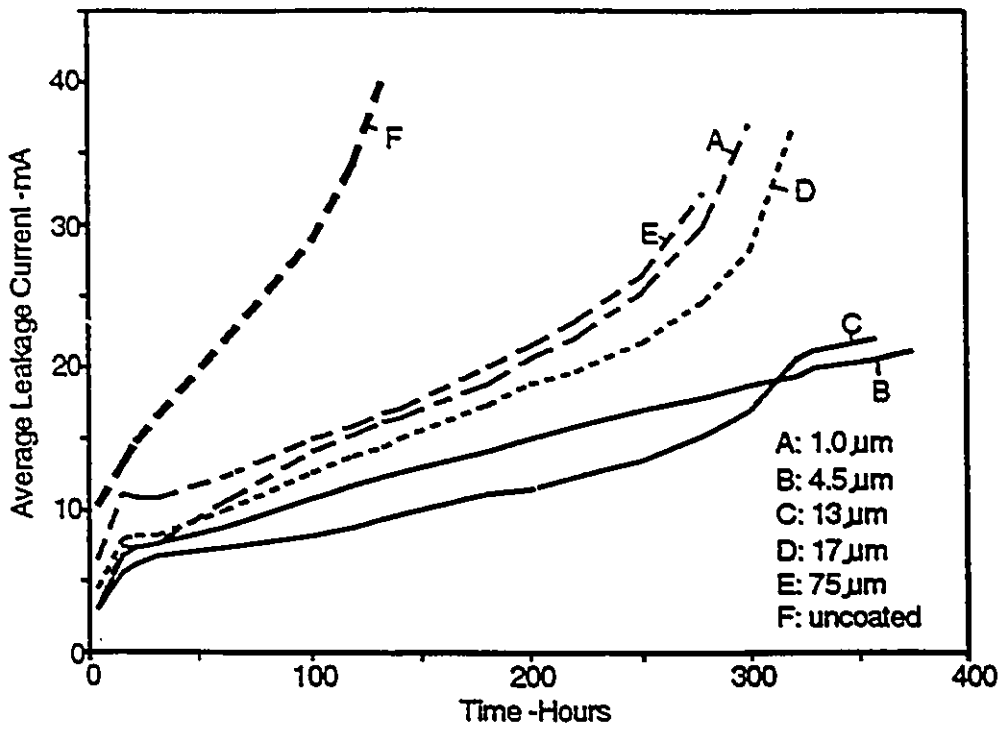

Figure 4.1 Average leakage current in ATH filled RTV coating having different sizes of particles of the filler. Conditions: concentration of filler. 90pph: conductivity of saline water. 1000µS/cm: voltage stress. 0.5kV$_{rms}$/cm.

rods is higher right from the start of the test and reaches 11mA after 2h. The coatings maintained a hydrophobic surface for about 14h for all particle sizes and then the surface become hydrophillic and dry band discharges developed. The leakage current developed more slowly for coatings with 4.5 and 13µm particles as shown in Fig.4.1. The possibility of having an optimum range of particle sizes to give longer time to the development of leakage current was further confirmed by measuring the current pulse counts during the salt-fog test for the different particle sizes.

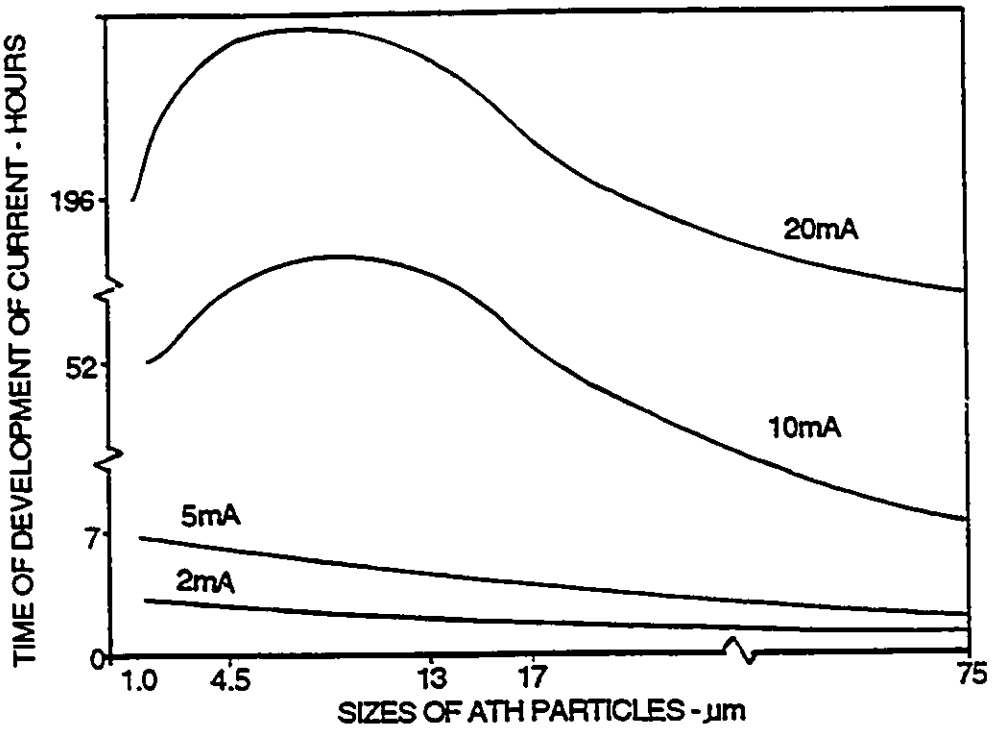

Figure 4.2 Time of development of different levels of leakage current as a function of size of ATH particle. Conditions are as in Fig.4.1.

Fig.4.2 shows the dependence of the time of development of different levels of leakage current on the size of the particle. It will be observed from Fig.4.2 that it takes longer time to develop a given level of leakage current at 4.5 and 13µm particle sizes. As the particle size increases above or decreases below these values the leakage current developed at successively shorter times.

Figs.4.3 and 4.4 show typical current pulse rates in the ranges 31-61mA and 62-74mA. respectively. in RTV coatings. Other current ranges show a similar behaviour. The current pulse developed more rapidiy and at a given time into the test a higher number of current pulse count was found for 1.0. 17 and 75µm sizes of ATH particles compared to 4.5 and 13µm. This indicates that the hydrophobicity of the surface was lost quickly

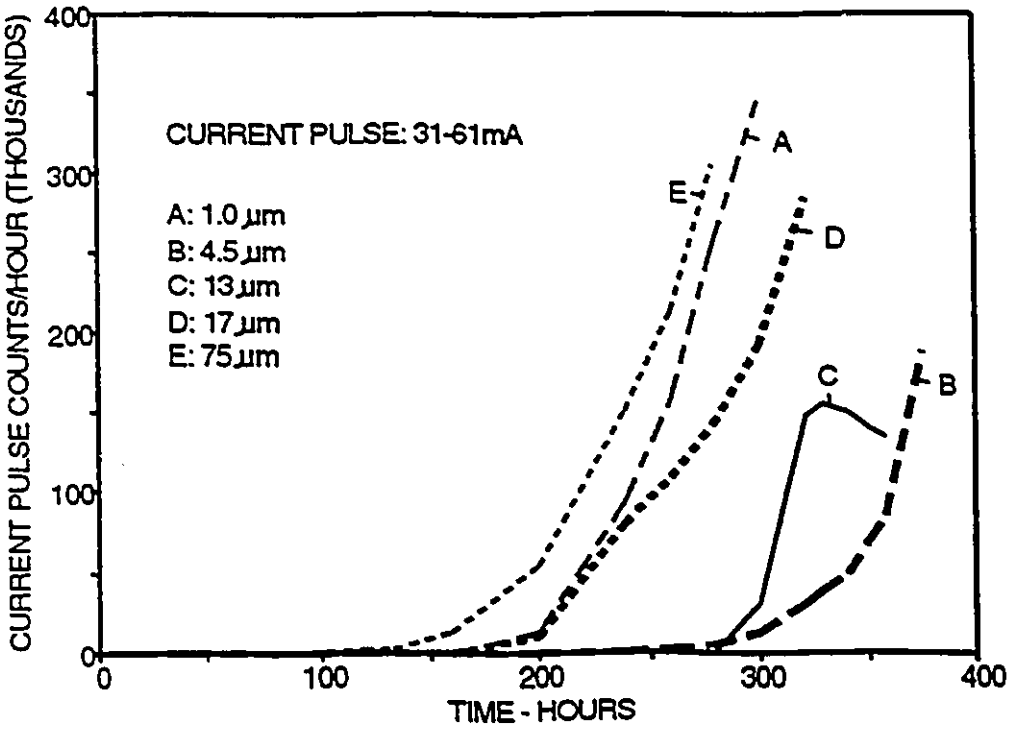

Figure 4.3 Current pulse count per hour having amplitudes in the range 31-61mA as a function of test time using different particle sizes. Conditions are as in Fig.4.1.

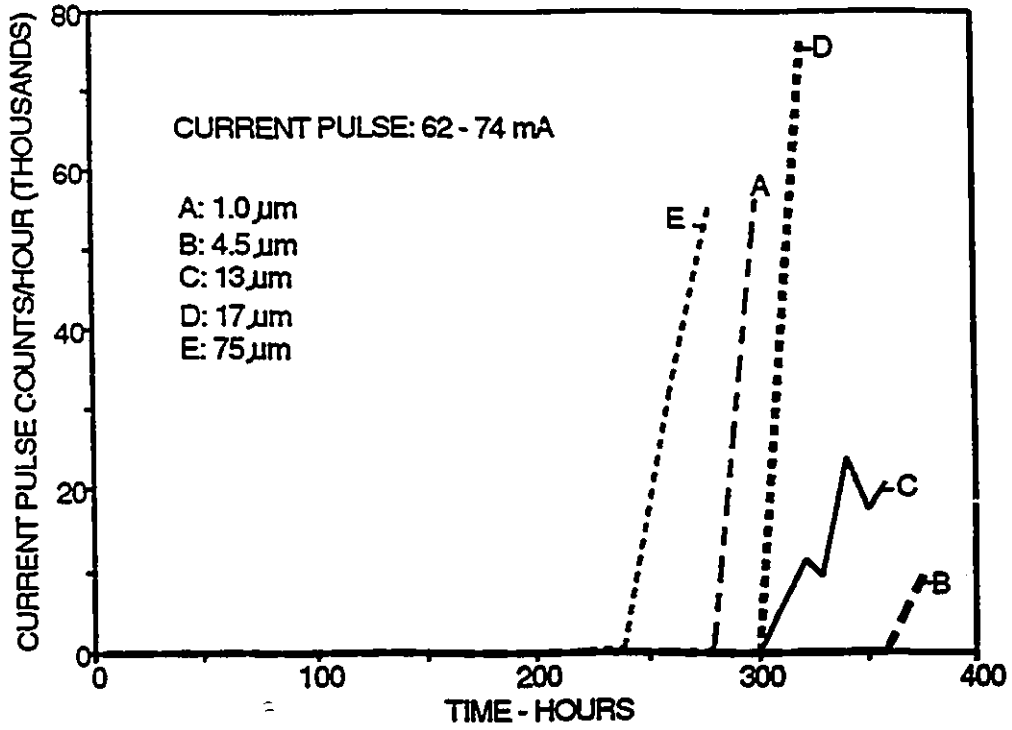

Figure 4.4 Current pulse count per hour having amplitudes in the range 62-74mA as a function of test time using different particle sizes. Conditions are as in Fig.4.1.

and earlier initiation of water filming occurred on the surface. This results in earlier dry band discharges and initiation of tracking and failure of the RTV coating. The coatings having 4.5 and 13μm of ATH particles show better performance as indicated by longer time to the onset of dry band discharges and lower current pulse counts. The accumulated damage from the heat of discharges determines the life of the coating. Therefore the variation of the current pulse counts is a measure of the aging. The role of the size of the ATH filler as it imparts resistance to erosion in the RTV coating may be ascertained from monitoring of the leakage current. This finding was reinforced further by the observed dependence of the time to failure of the coating as a function of the particle size of ATH.

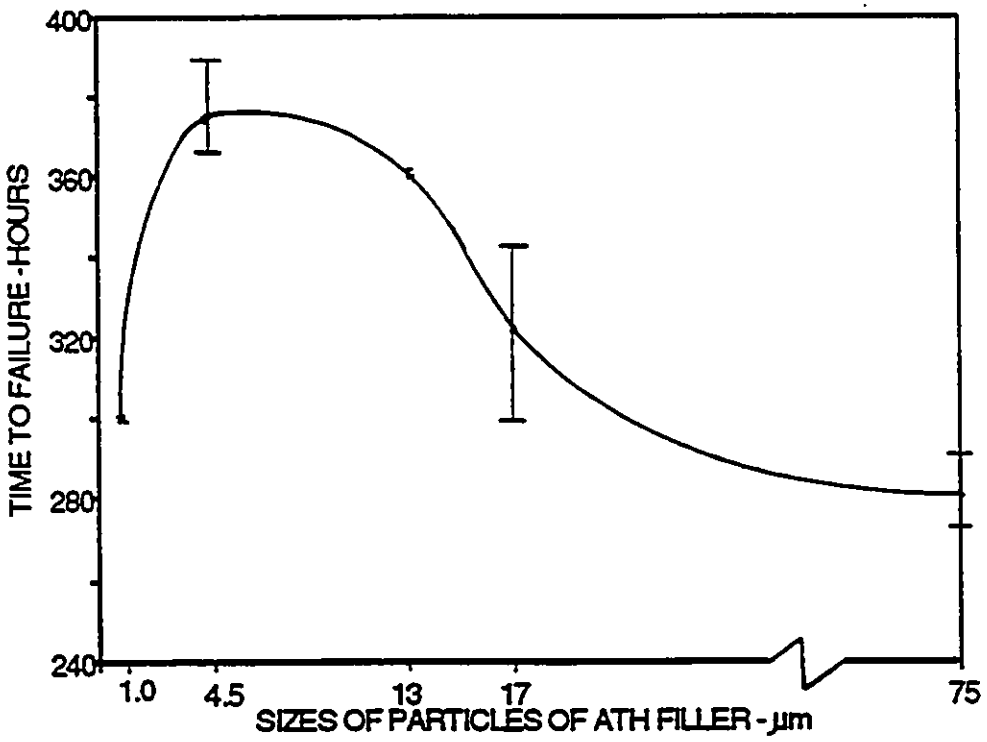

Figure 4.5 Time to failure of RTV coatings as a function of size of ATH particles. Conditions are as in Fig.4.1.

4.2.3. Dependence of Time to Failure

Failure of the specimens was determined when the leakage current exceeded 150mA as mentioned in Section 2.4, Chapter II. Fig.4.5 shows the time to failure due to erosion of the RTV coatings with various sizes of ATH particles and subsequent tracking of the FRP rods. The bars indicate the variations within each size of 3 specimens. A fixed 90 pph concentration of the filler of ATH was used for all particle sizes from 1 to 75μm. It can be seen from Fig.4.5 that the particle size affects the time to failure of the RTV coating. The ATH filler with particle sizes of 4.5 and 13μm impart a higher resistance to erosion than the other sizes. These provide less damage on the surface from dry band discharges and consequently give the longest time to failure, as shown in Fig.4.5.

4.2.4. Dependence of Surface Roughness

The development of leakage current and the initiation of dry band discharges are due to the loss of hydrophobicity resulting in water filming on the surface. These discharges affect the physical and chemical conditions on the surface which ultimately lead to erosion of the coating and failure. The particle size of the ATH filler in the RTV silicone rubber coatings is thought to have a direct influence on the roughness of the surface finish.

The measurements of the roughness and its dependence on the energized time of salt-fog test and on the size of ATH particles was made. The roughness of the surface of the coating was measured in virgin specimens with different sizes of particles of ATH and after subjecting them to 14h and 92h of salt-fog. To give reliable and better reproducibility extensive measurements of roughness were conducted in three different regions of the coated rod surface.

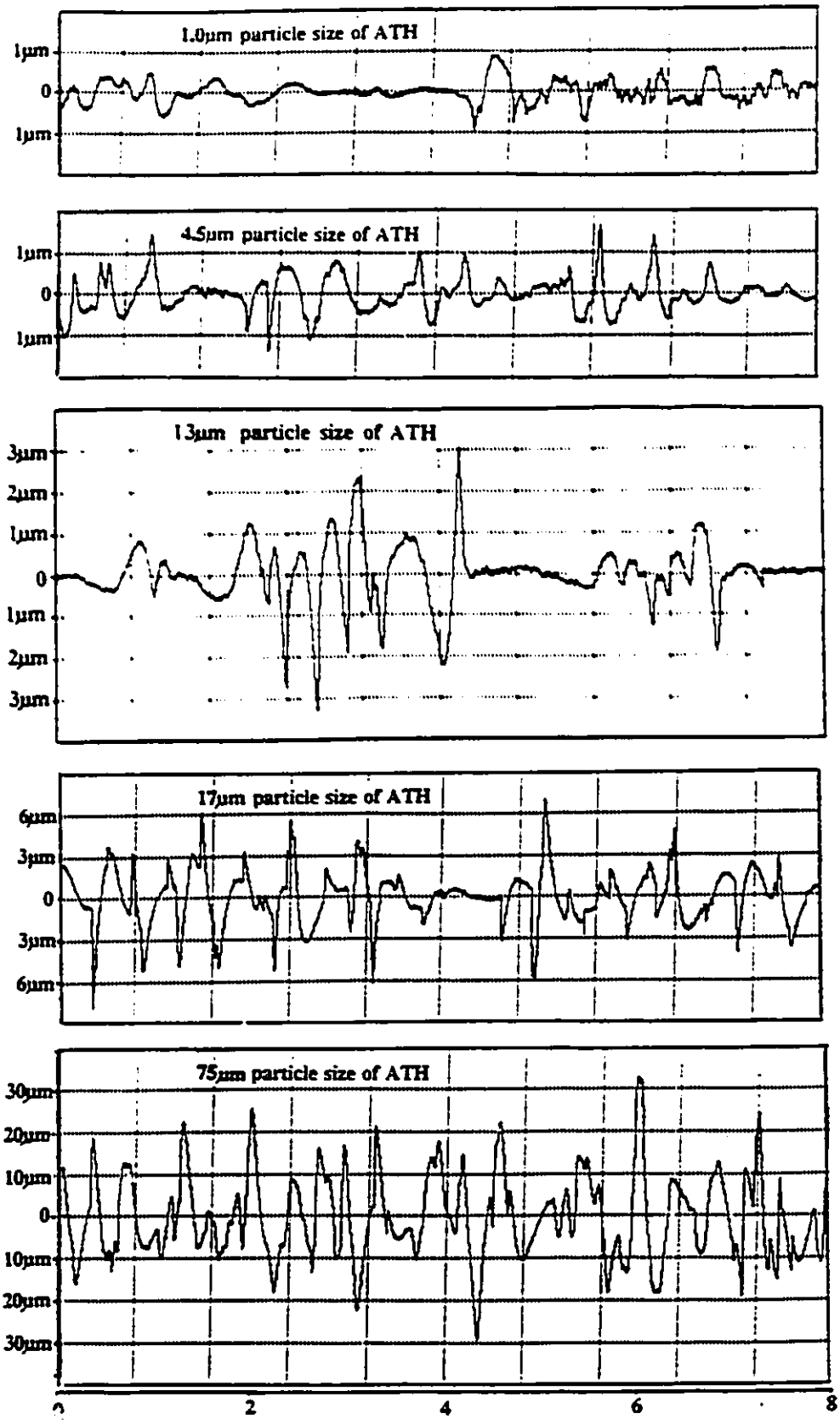

Figure 4.6 Roughness of the surface of ATH filled RTV coating for various sizes of ATH particles. Specimens were measured before salt-fog test. Concentration of filler 90pph.

4.2.4.1. Roughness of the surface before salt-fog test

Fig.4.6 shows a typical variation of the roughness of the surface as a function of distance within a length of 8mm of the specimen for various ATH particle sizes of the coatings. Fig.4.6 shows that the surface of the RTV coating became rougher with increasing particle size. It should be noted that the FRP rod before coating with RTV was very smooth and the average roughness (Ra) was 0.32±0.03μm.

The profile for the 1μm particle size specimen shown in Fig.4.6 is generally observed on the surface. However, for this size of particle, relatively large discontinuities were also observed on the surface and were confirmed with SEM studies. These are discussed in Sections 4.2.4.2 and 4.2.5. The dependence of Ra of the surface roughness of Fig.4.6 on the size of particle of ATH filler is shown in Fig.4.7 before and after different durations in the salt-fog. It can be seen from Figs.4.6 and 4.7 that the surface of the coating is rougher with larger ATH particles and this leads to higher leakage current at the beginning of the salt-fog test (<7h) as shown in Figs.4.1 and 4.2. Higher leakage currents lead to a more rapid loss of hydrophobicity and thus water filming and initiation of discharges on the surface.

Generally coatings with larger particle size have a shorter life. The largest time to failure for particle sizes in the range of 4.5 to 13μm was found and the coating with 1.0μm, 17μm and 75μm sizes of ATH particles failed in a shorter time. The mechanism of the failure of the coating with 1.0μm particle size which occurred after 300±1h (Fig.4.5) is thought to be due to the ATH particles flowing together to form an aggregate or a concentration as non-uniform surface in the virgin specimens and this under test conditions leads to hot spots when a dry band discharge occurs. The localized highly non-uniform surface has been found more frequently in the surface of the coating with 1.0μm

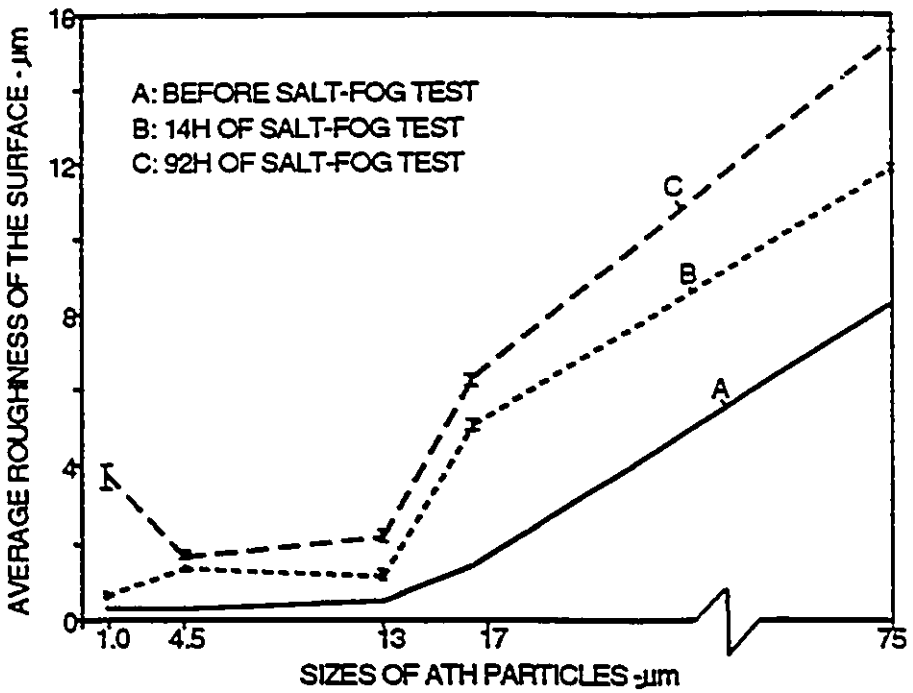

Figure 4.7 Variation of the average roughness of the surface Ra with test time as a function of size of ATH particles. Conditions of salt-fog test are as in Fig.4.6.

size of ATH particle. An example of this is shown in Fig.4.8 before the salt-fog test. A similar scan of the surface over an extended length showed that for the 1.0µm size of ATH there are many such large discontinuities. These might explain the larger leakage current, larger current pulse count and shorter lifetime which were observed with 1.0µm particle size. Fig.4.9 shows a typical of many such scans where there are on average between 5 to 8 such large discontinuities over 48mm distance on the specimens surface. Fig.4.10 shows an extended scan of a virgin coating having 13µm size of ATH particles which shows no evidence of aggregation of particles similar to that which is clearly demonstrated in Figs.4.8 and 4.9.

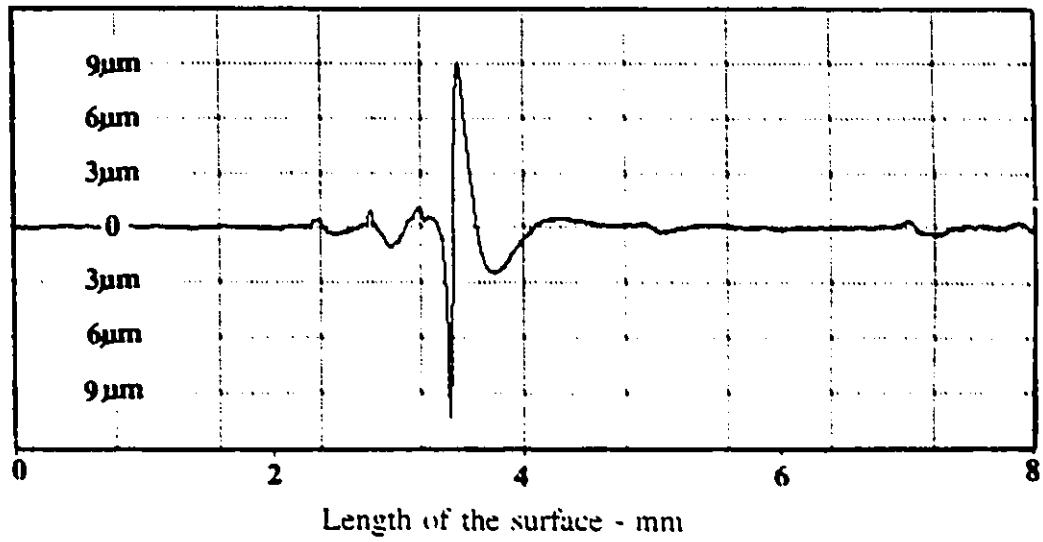

Figure 4.8 The largest non-uniform surface with 1.0µm particle size before salt-fog test due to aggregation of particles.

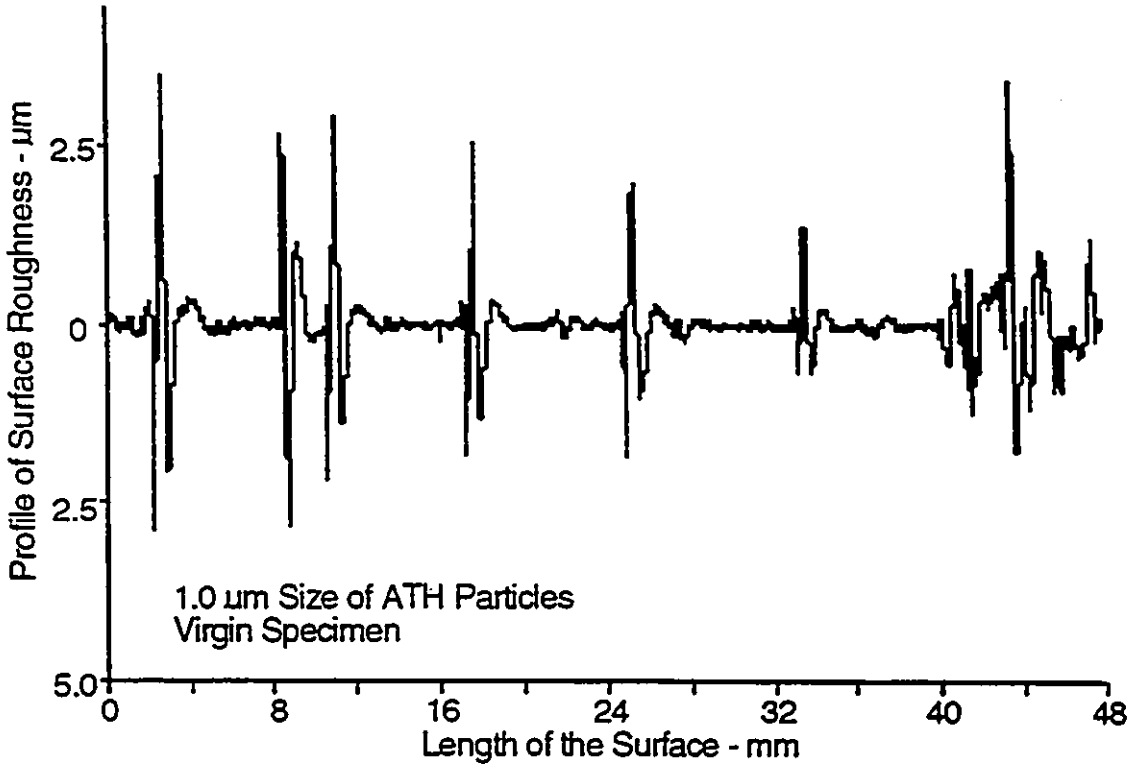

Figure 4.9 Typical roughness of the surface of a virgin RTV with 1.0µm median particle size of ATH showing the peak-to-valley heights of the discontinuities over an extended scan.

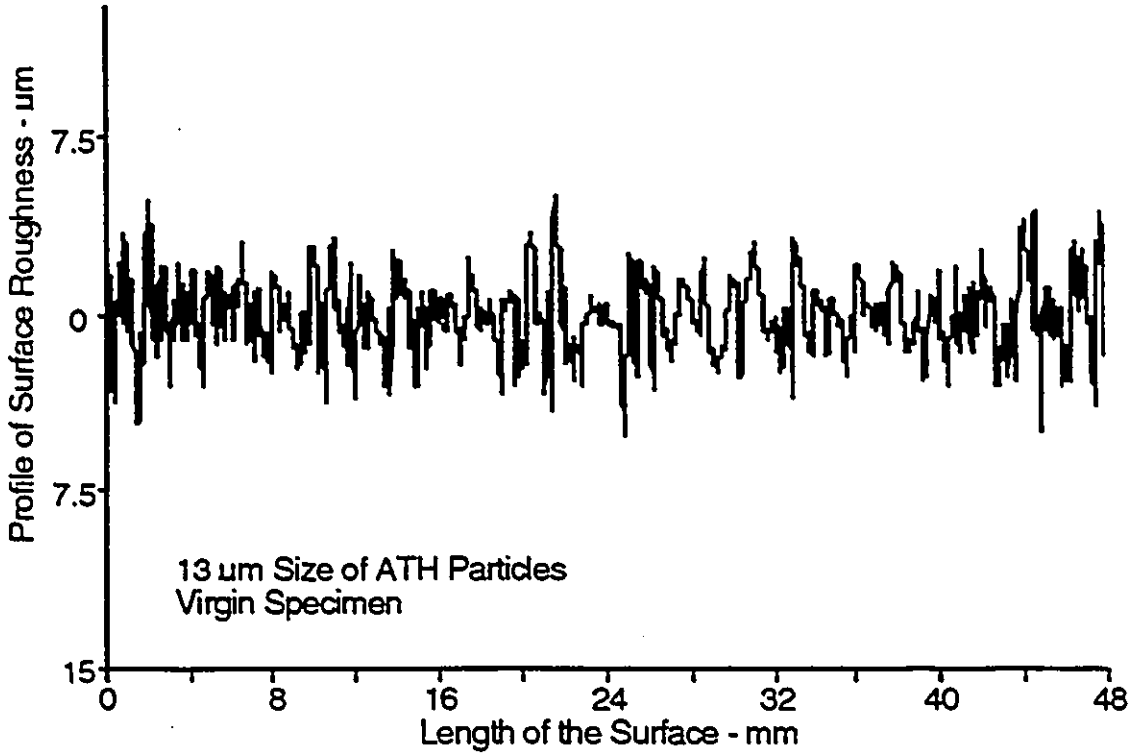

Figure 4.10 Typical roughness of a virgin RTV having 13μm size of ATH particles.

4.2.4.2. Roughness of the surface after salt-fog test

Fig.4.7 shows the dependence of the average roughness Ra on the test time as a function of particle size. After salt-fog, the surface roughness increased with increasing test time up to 14h for the particle sizes from 1 to 75μm. This is due to the higher leakage current which was developed across the coating and caused more damage on the surface from the dry band discharges. The roughness of the surface with 1.0 μm size of ATH particle increased rapidly with test time and became rougher than the surfaces with 4.5 and 13μm particle size after 92 hours. The largest roughness of the surface of the RTV coating with 1.0μm particle size as a function of distance within 8mm range of the surface after 92h of fog test is shown in Fig.4.11. A highly non-uniform surface of the

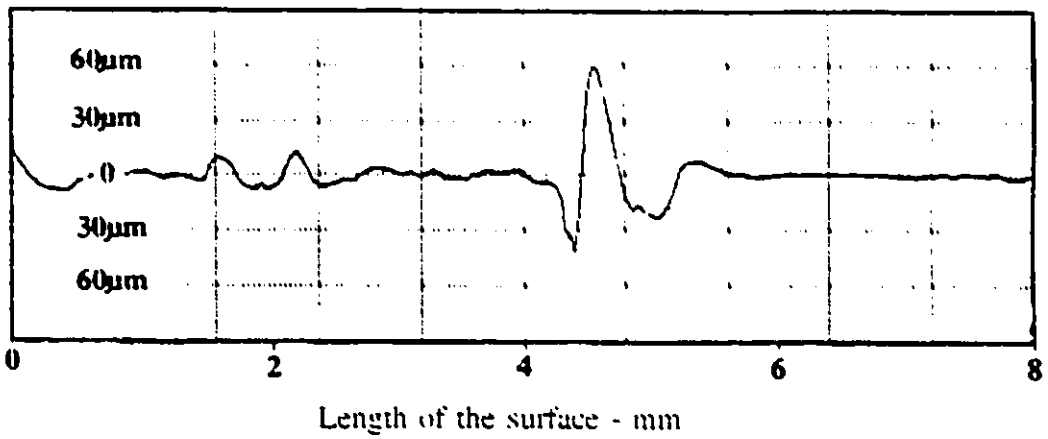

Figure 4.11 The largest non-uniform surface with 1.0µm particle size after 92h of salt-fog test. Conditions of test are as in Fig.4.1.

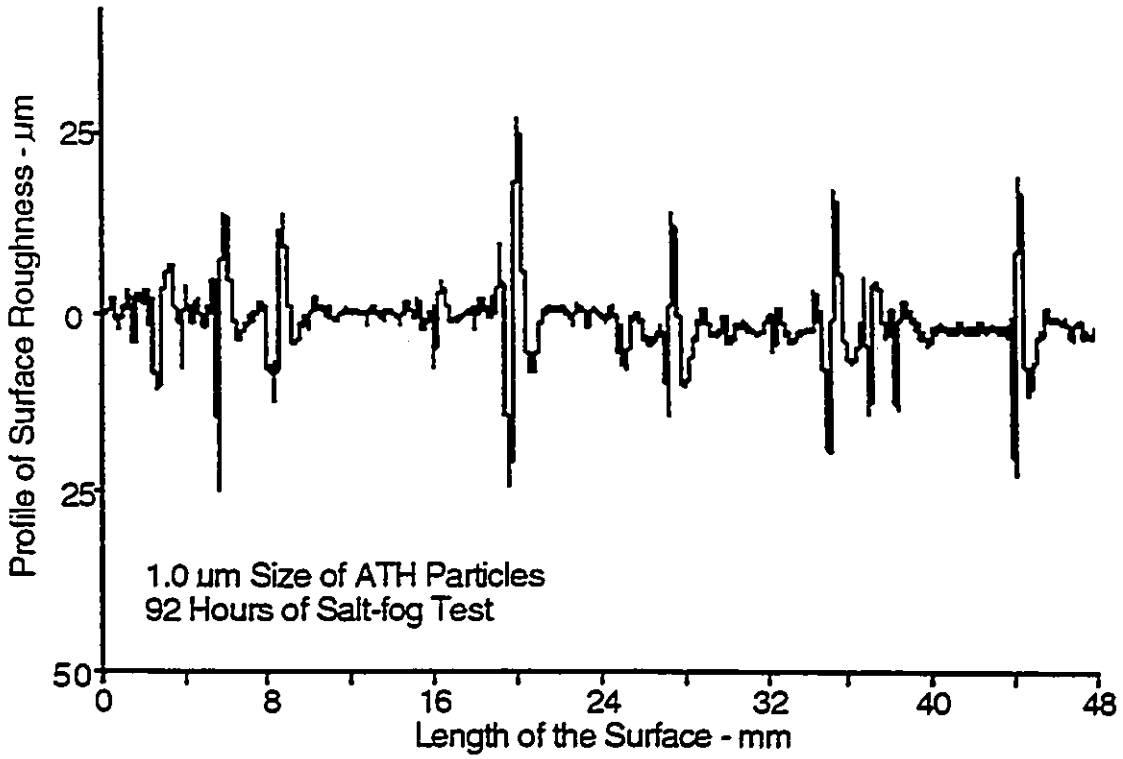

Figure 4.12 Typical roughness of the surface of RTV with 1.0µm particles of ATH after 92hr of salt-fog test. Conditions of test are as in Fig.4.1.

coating was found. Typically between 1 to 2 such non-uniform locations of the like shown in Fig.4.11 were found in every 8mm scan of the surface. Fig. 4.12 shows the measured peak-to-valley heights of the roughness over an extended span of 48mm where many discontinuities are present in the coatings with 1.0μm size of ATH particles. After 92h of salt-fog the largest peak of the roughness increased from about 9.0μm to about 60μm (Fig.4.11). However, for this size of ATH particle the change in the heights of the roughness was typically from 2.5μm (Fig.4.9) to 20μm (Fig.4.12). This resulted in hot spots on the surface which accelerated the erosion on the surface and ultimately led to a shorter life of the coating. The roughness was less pronounced on the surface with 4.5 and 13μm size of ATH particles (Fig.4.7, curve C and Fig.4.13). This resulted in less damage on the surface and a longer life. This finding is consistent with the time to failure found in the present work (Fig.4.5).

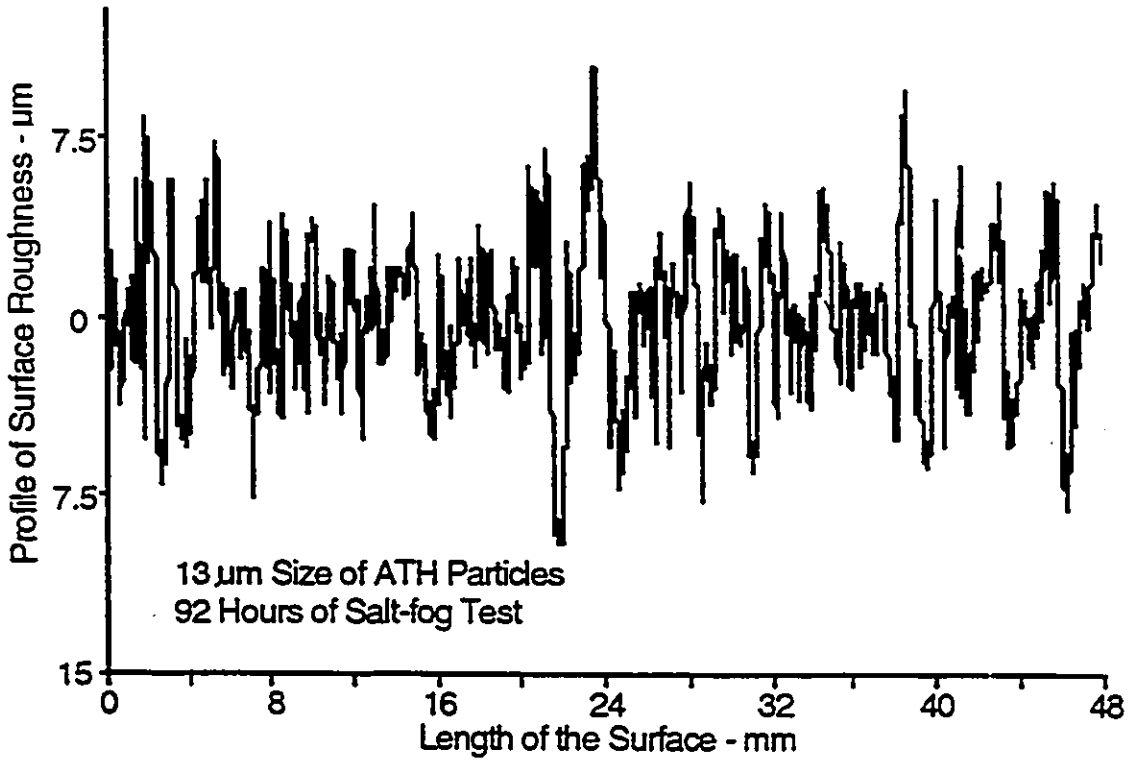

Figure 4.13 Roughness of the surface of RTV with 13μm size of ATH particles after 92h of salt-fog test. Other conditions are as in Fig.4.1.

4.2.5. SEM Studies of the Surface

Scanning Electron Microscope (SEM) studies of the surface of coatings having different sizes of particles were conducted in order to obtain independent confirmation of the results obtained from the surface roughness tester and to probe further into the physical properties of the surface. In the present study specimens (5mm x 10mm) were cut from near the top electrode where the damage to the coating ensued. These were first coated with carbon using a carbon arc, in vacuum, at a pressure of 10^{-4}-10^{-2}Pa to a thickness of about 20nm. Fig.4.14 shows a SEM microphotograph of a coating with 1.0μm size particle of ATH after it had been subjected to about 92h of salt-fog. This scan covers an area (76μm x 53.6μm) which is typical of those between successive peaks as shown in Figs.4.9 and 4.12. A region of rough surface on the scanned specimen where two discontinuities are simultaneously seen is shown in Fig.4.15 using a magnification of 60x and covering an area of 1.42mm x 1.67mm. Fig.4.16 shows a scan in the same specimen, of 1μm particle size, at the location of a large discontinuity of the type shown in Fig.4.12.

Figs.4.17 to 4.19 show SEM microphotographs of coatings having ATH particles of 4.5, 13 and 75μm, respectively. It will be observed that the surface has a larger roughness with increasing size of the ATH particles in general agreement with Fig.4.6.

Preliminary studies employing Energy Dispersive Spectroscopy (EDS) using a 15kV accelerating voltage, typical magnifications of 5000x and counting time of 60s indicate that at the locations of increased roughness of the type shown in Figs.4.8 and 4.9 for 1μm size particle the percentage values of aluminum and silicone are different than in the smooth part.

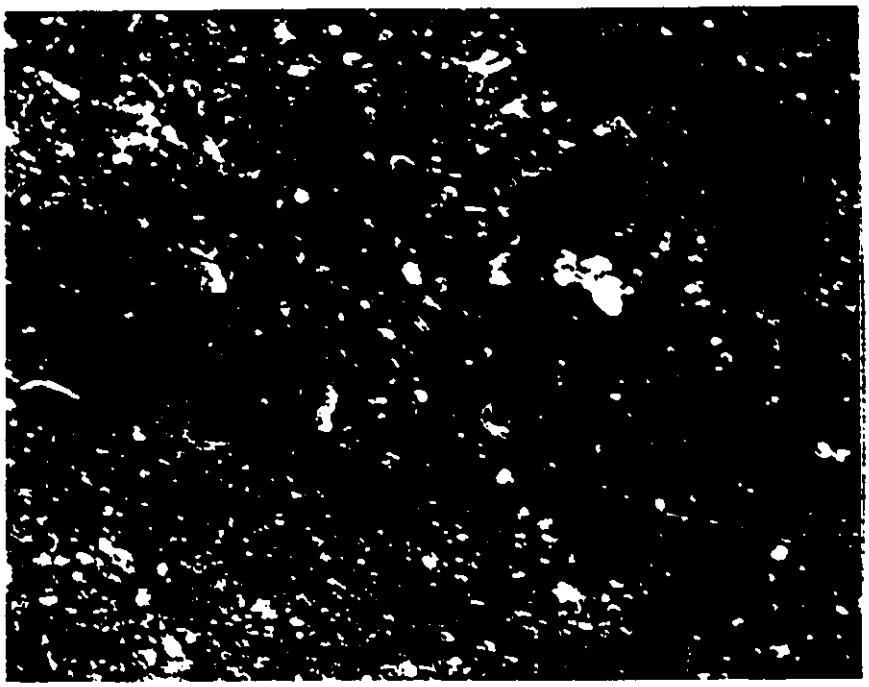

—— 10μm

Figure 4.14 SEM microphotograph of RTV coating with 1.0μm size of ATH particles on a smooth surface between the peaks of Fig.14 after 92h of test. Magnification 1125x; other conditions are as in Fig.4.1.

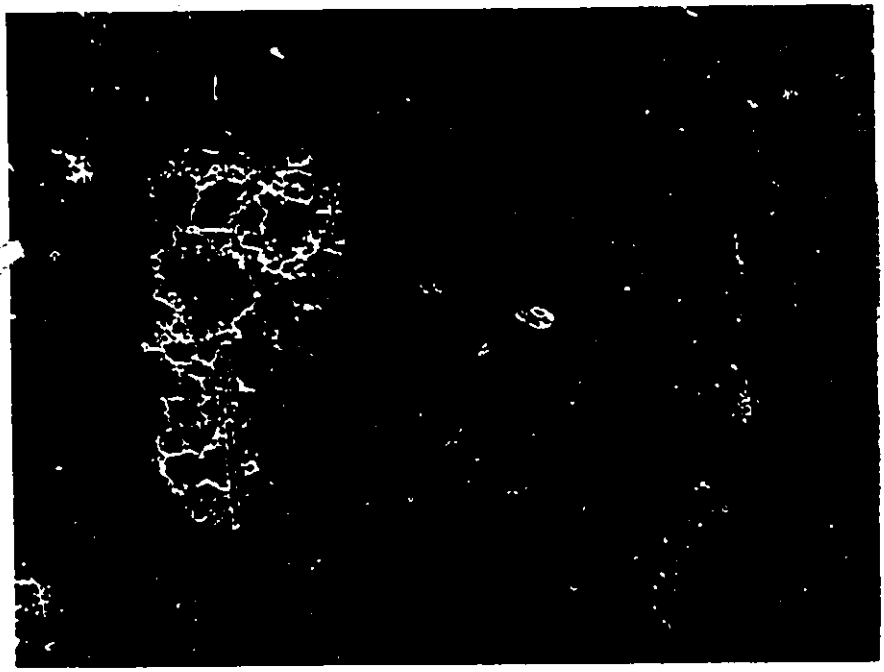

—— 200μm

Figure 4.15 SEM microphotograph of RTV with 1.0μm size of ATH particles. Magnification 60x; Other conditions are as in Fig.4.14.

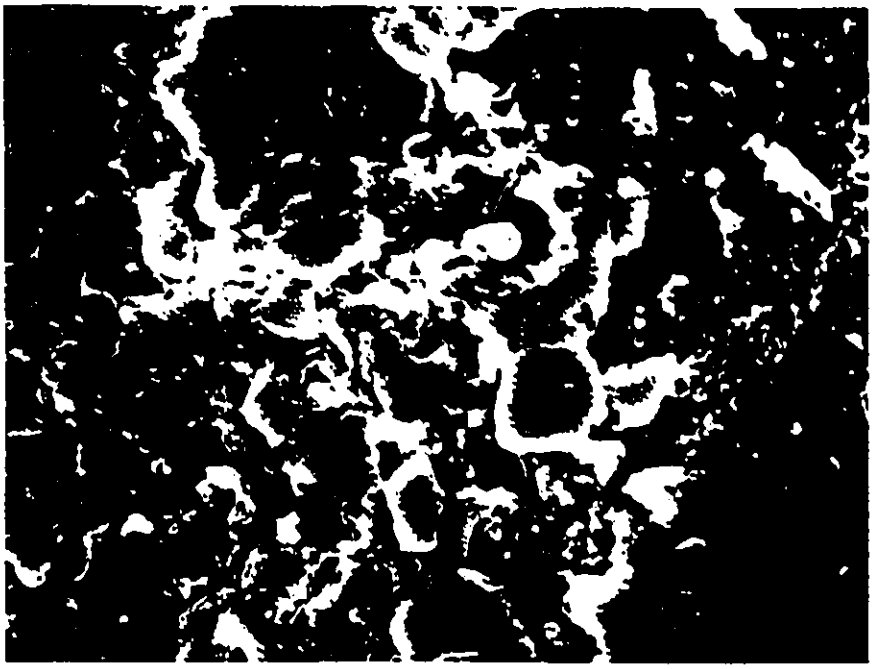

—— 10μm

Figure 4.16 SEM microphotograph of 1.0μm coating at a location of large roughness. Other conditions are as in Fig.4.14.

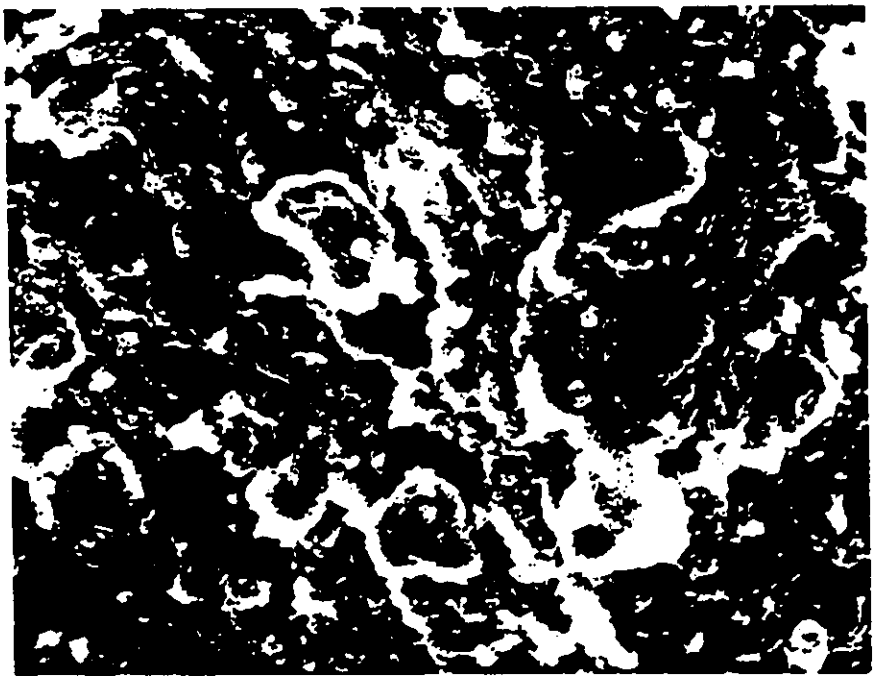

—— 10μm

Figure 4.17 SEM microphotograph of RTV with 4.5μm size of ATH particles. Other conditions are as in Fig.4.14.

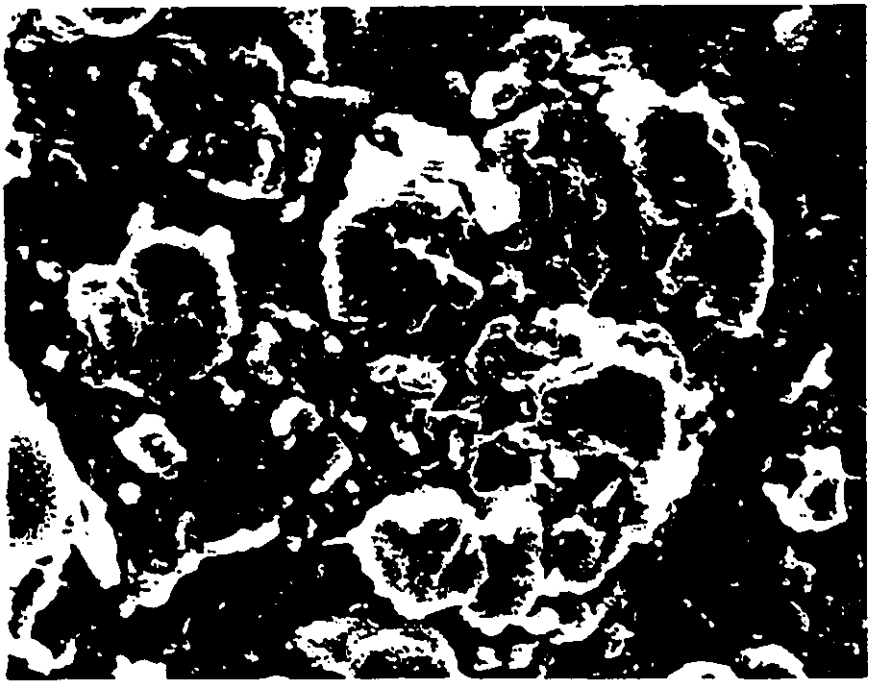

—— 10μm

Figure 4.18 SEM microphotograph of RTV with 13μm size of ATH particles. Other conditions are as in Fig.4.14.

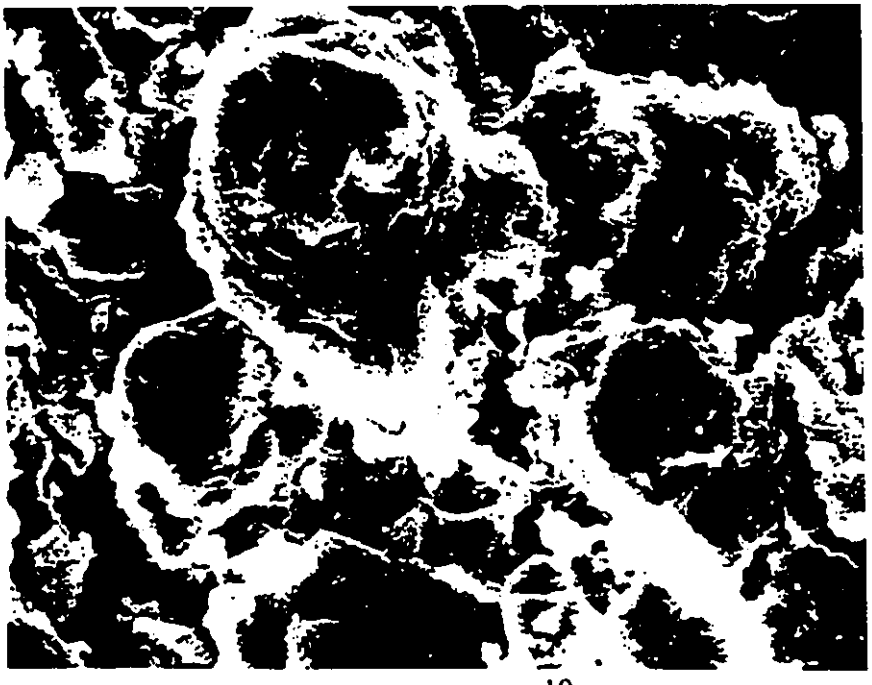

—— 10μm

Figure 4.19 SEM microphotograph of RTV with 75μm size of ATH particles. Other conditions are as in Fig.4.14.

4.2.6. Silicone Fluid on the Surface of the Coatings

To measure the amount of silicone fluid on the surface of the coating and determine its dependence on the size of ATH particles, a Nicolet 5DX Fourier Transform Infrared (FTIR) spectrometer with an attenuated total reflection (ATR) attachment was employed using a KRS-5 (Thalium Bromoiodide) crystal. The specimens were cut from the coating near the top electrode. The size of the specimen was 10 x 4 mm^2. The thickness was 0.18±0.05mm for the specimens with 17 and 75μm sizes of ATH particles and 0.26±0.08mm for the specimens with 4.5 and 13μm. The specimen with 1.0μm size of ATH particle has a thickness of 0.46±0.17mm. The variation in the thickness of the coating is not thought to affect the IR measurements.

The IR spectra of the silicone fluid on the surface of virgin specimens showed a slight increase with increasing particle size in the range 1 to 75μm. This was the case for the material before it was subjected to dry band arcing.

Figures 4.20 and 4.21 show the dependence of IR absorption of silicone fluid at three different bands as a function of size of ATH particles. Absorption is due to the silicone fluid on the surface. The band numbers in Figs.4.20 and 4.21 represent the characteristic IR absorption band. The band of CH deformation in the $SiCH_3$ groups are 1270-1255cm^{-1}, SiO band in Si-O-Si is 1100-1000cm^{-1} and $Si(CH_3)_2$, 840-790cm^{-1}[68-72]. In Fig.4.20, the specimens were tested in energized salt-fog for 14h and after the cessation of the dry band discharges were left in air for 72h. It was observed that the silicone fluid that existed or formed on the surface of ATH filled RTV coating was a function of the size of ATH particle. Fig.4.20 shows that smaller amounts of silicone fluid on the surface of the coating were found to be present with 1.0, 17 and 75μm particle sizes, compared to 4.5 and 13μm particle sizes. Similar behaviour was found on these surfaces after 92h

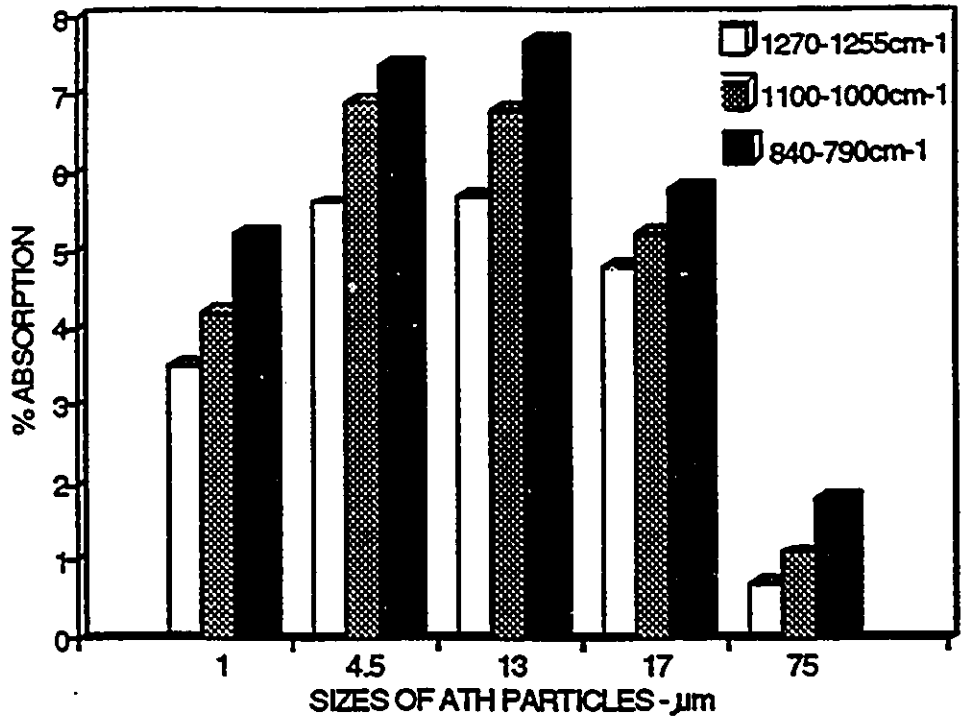

Figure 4.20 IR absorption by silicone fluid on the surface of the coating as a function of size of ATH particle after 14h of salt-fog test and 72h rest time in air. Conditions of test are as in Fig.4.1.

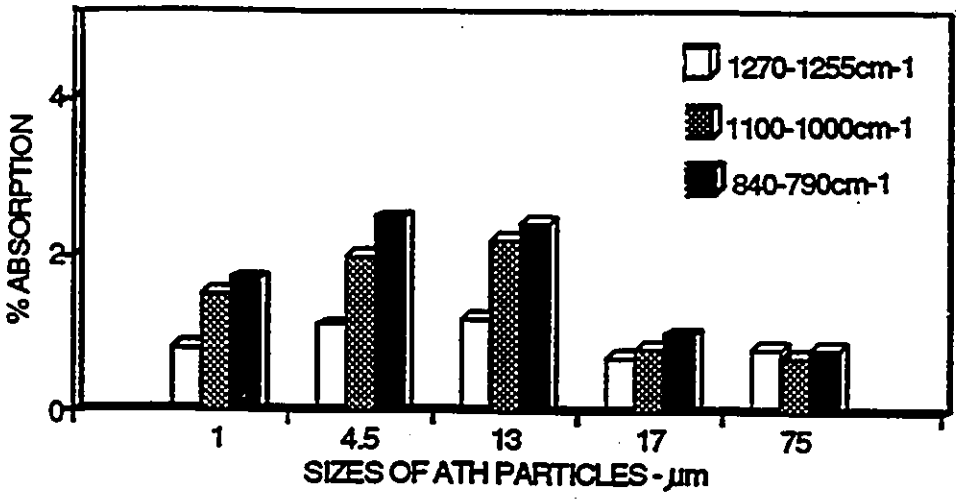

Figure 4.21 IR absorption by silicone fluid on the surface of the coating as a function of size of ATH particle after 92h of salt-fog test and 72h rest time in air. Conditions of test are as in Fig.4.1.

of salt-fog test as shown in Fig.4.21. The silicone fluid, however, was less pronounced on the surface of the coating after 92h(Fig.4.21) of test compared to that of 14h(Fig.4.20). This is because of the gradual loss of the silicone fluid due to its removal by the combined discharges and the dripping saline water on the surface of the coating.

The amount of silicone fluid detected on the surface of the coating was what remained after exposure to dry band discharges during 14h of test combined with that diffused from the bulk to the surface during the elapsed time outside the salt-fog chamber. The dry band discharges remove the silicone fluid from the surface and results in a non-equilibrium of the silicone fluid between that on the surface and in the bulk of the coating. The silicone fluid then diffuses to the surface from the bulk until equilibrium is reached. Lower leakage current indicates that less intense discharge occurs on the surface and less amount of silicone fluid is removed from the surface. The lost silicone fluid is supplanted by diffusion from the bulk to the surface. Higher leakage current removes more silicone fluid from the surface and results in subsequent depletion of the silicone fluid in the bulk. Thus the silicone fluid has to diffuse from a greater depth in the coating to the surface. This takes a longer time. Figs.24 and 25 show the silicone fluid on the surface of the coating with 13 and 75μm sizes of ATH particles after 0.33h, 25h, 72h and 168h have elapsed from the cessation of the dry band discharges. The specimens were tested in salt-fog for 14h in Fig.4.22 and 92h in Fig.4.23 respectively. Fig.4.22 shows that the amount of silicone fluid present on the coating with 13μm size of ATH particles is larger than that for 75μm for all rest times from 0.33h to 168h. This clearly establishes an important phenomenon that the smaller size particle of ATH results in larger amount of silicone fluid which is both formed (after short rest time of 0.33h) and diffused to the surface from the bulk during a long rest time(168h). Fig.4.22 also shows

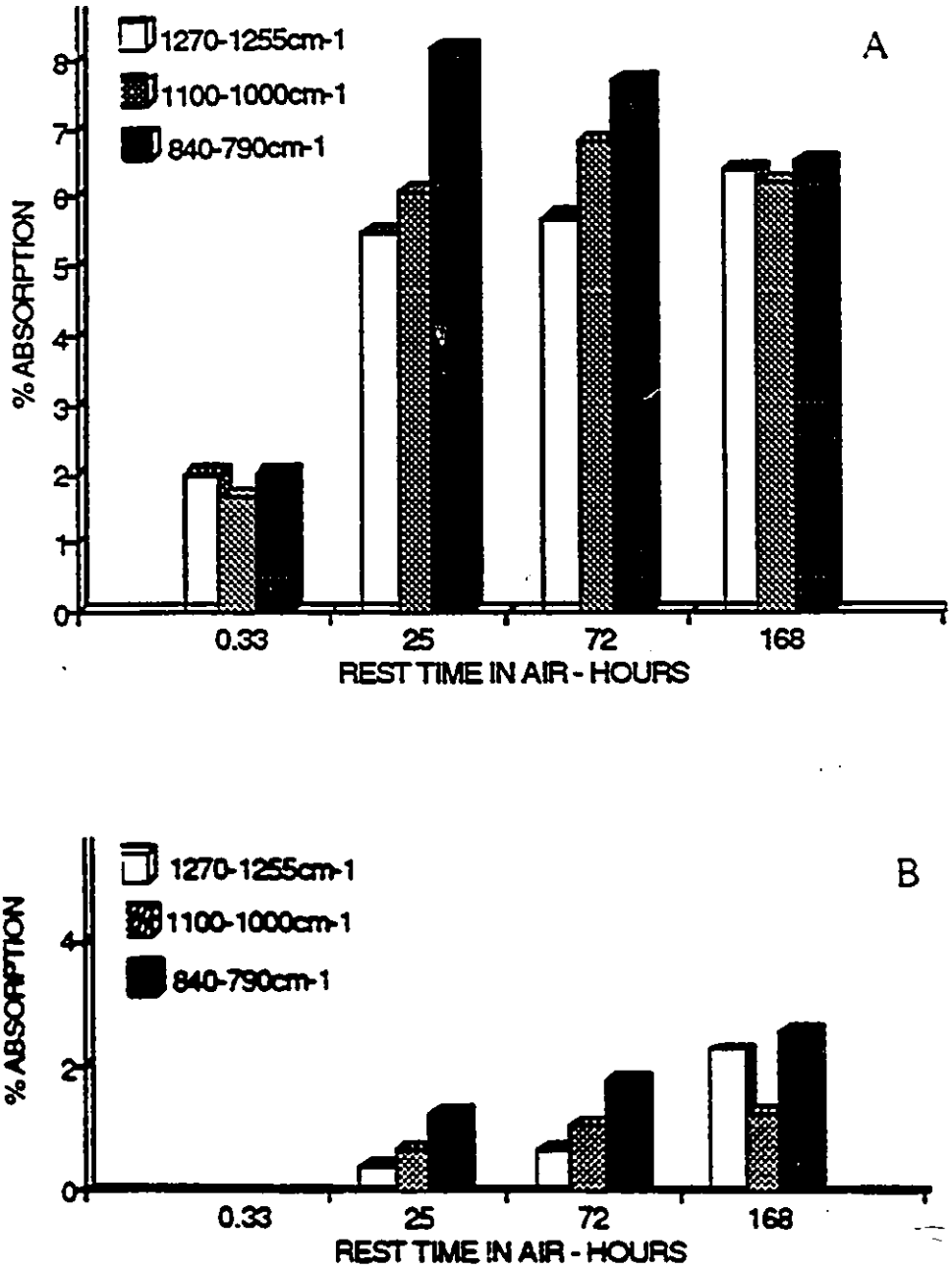

Figure 4.22 IR absorption by silicone fluid on the surface with 13 and 75μm particle sizes after 0.33h, 25h, 72h and 168h of rest time. The specimens were subjected to 14h of salt-fog test. Conditions of test are as in Fig.4.1. Abscissa is not to scale.

A: 13μm size of ATH particle; B: 75μm size of ATH particle

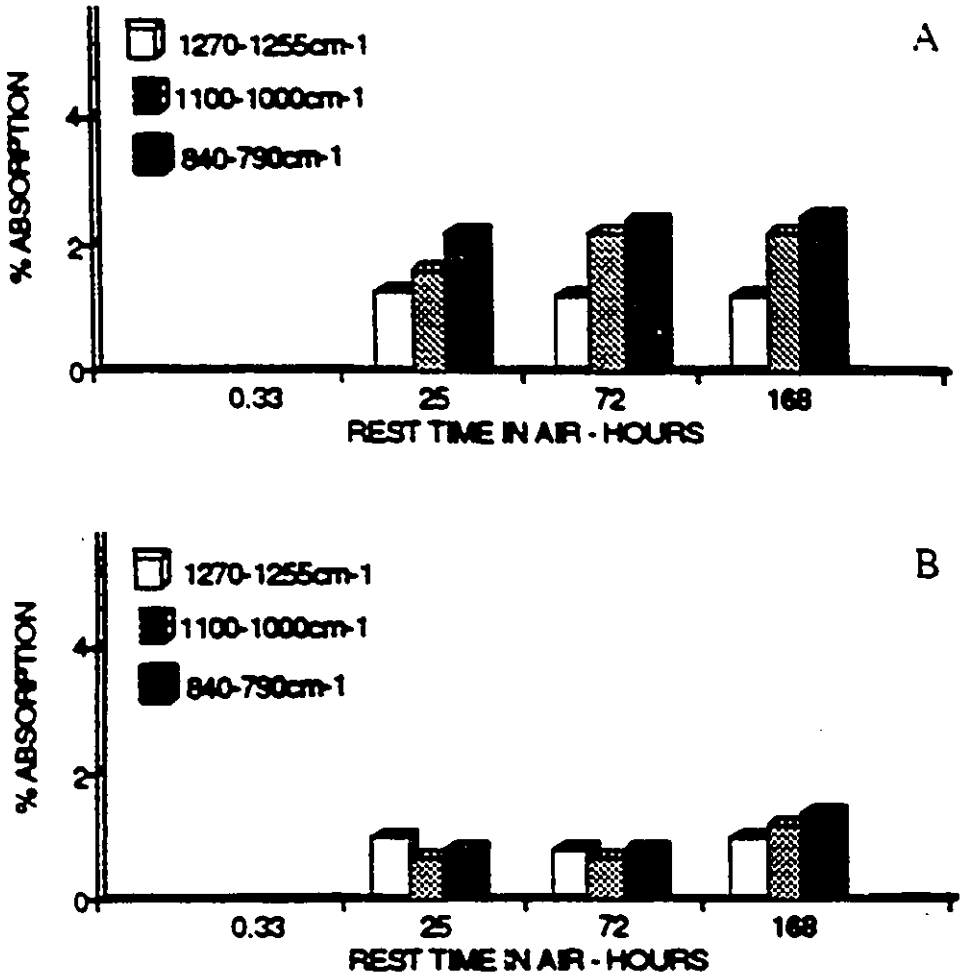

Figure 4.23 IR absorption by silicone fluid on the surface with 13 and 75μm particle sizes after 0.33h. 25h. 72h and 168h of rest time. The specimens were subjected to 92h of salt-fog test. Conditions of test are as in Fig.4.1. Abscissa is not to scale.

A: 13μm size of ATH particle: B: 75μm size of ATH particle

that increasingly more silicone oil diffused to the surface with increasing rest time for both particle sizes. Another significant observation was that for the larger particle size of 75μm there was very little or no silicone fluid left on the surface of the RTV after it was subjected to 14h of test. This was measured before significant diffusion of the fluid from the bulk could replenish this loss (Fig.4.22-B, at 0.33h after cessation of the test). On the other hand, and under the same conditions, silicone fluid was clearly present on the surface of the RTV specimens containing ATH filler with 13μm size particles (Fig.4.22-A, at 0.33h after cessation of the test). Figs.4.22-B and 4.23-A and B also show that it takes about 25h for the silicone fluid to diffuse to the surface from the bulk. This is in agreement with a previous work [38] which showed that it took about 30h for the contact angle to fully recover after the surface was subjected to lengthy discharges in salt-fog. Further, Fig.4.23 shows that a longer test time of 92h resulted in lower silicone fluid on the surface(compared to 14h) for both particle sizes. For the longer duration of 92h of dry band discharges the smaller particle size of 13μm also resulted in larger amounts of silicone fluid than for 75μm particle and this was consistent throughout the rest duration from 25 to 168h(Fig.4.23).

The amount of silicone fluid remaining on and that diffused from the bulk to the surface depends on the development of leakage current across the surface of the coating which was also a function of the size of ATH particle. The leakage current increased with increasing test time(Fig.4.1) and this resulted in less silicone fluid remaining on the surface right after the salt-fog test, as observed in the present study (Figs.4.22 and 4.23).

The diffusion of silicone fluid is responsible for providing the hydrophobicity on the surface of the coating. After heavy and prolonged dry band arcing in salt-fog, the surface of the coating temporarily lost its water repellency. More silicone fluid diffused

to the surface of the coating with 4.5 and 13μm sizes of ATH particles after a rest time in air and without electric stress than did with the other particle sizes(Fig.4.21). This resulted in a quicker recovery of water repellency on the surface and thus leading to a longer time to failure.

4.2.7. Dependence of Heat Conduction on Particle Size

Failure of the ATH filled RTV silicone rubber coating in salt-fog is due to erosion of the coating by the heat generated from dry band discharges. The heat conduction in the RTV coating is affected by ATH particle size. This is likely to be a critical factor in determining the role of the ATH filler which imparts tracking and erosion resistance to the surface and thus increases the lifetime of the coating.

When dry band arcing occurs on the surface of the coating placed on insulators, the heat from the arc evaporates water at the root of the arc and transfers thermal energy to the RTV coating. The heat transfer is largely by conduction. The rate of heat flow, Q(in J/s), by conduction, is proportional to the temperature gradient in the direction of heat flow[73],

$$Q=-k\cdot S\cdot\frac{dT}{dx}\quad\ldots\ldots(1)$$

where K(in J/sm°C) is the thermal conductivity of the RTV coating with ATH filler, S the area through which the heat flows by conduction(in m^2), T the temperature (in°C) and X (in m) is the distance in a direction perpendicular to the surface of the coating.

Equation (1) shows in a lower temperature on the surface with increasing thermal conductivity and increasing area of conduction. Thus the damage to the coating can be reduced by increasing both S and K.

The thermal conductivity of the filled RTV coating depends on the concentration of the filler and on the thermal conductivities of ATH and of the RTV silicone rubber[74]. For a given filler level(say 90 parts of filler per hundred parts of silicone rubber in weight which is used in the present work), the area of the heat conduction depends on the particle size.

The ATH particle within the RTV material is surrounded by silicone rubber. Suppose the ATH particle is a sphere of radius R (in m) and consider that there are N ATH particles. The area S (in m^2) of conduction through the cross sections of the ATH particles is $(\pi R^2/2)N$. The concentration of filler C is the ratio of the weight of the ATH filler to the weight of the silicone rubber.

$$C=\frac{N\cdot\frac{4}{3}\pi R^3\cdot n_2}{(V-N\cdot\frac{4}{3}\pi R^3)\,n_1} \quad \ldots\ldots (2)$$

where, n_1(kg/m^3) and n_2(kg/m^3) are the densities of the silicone rubber and of the ATH filler, respectively, V(in m^3) is the total volume of RTV coating including the filler which is participating in the conduction of heat. then,

$$S=\frac{3C\cdot V\cdot n_1}{n_2+C\cdot n_1}\cdot\frac{1}{8R} \quad \ldots\ldots (3)$$

Equation(3) shows that, for a given filler concentration(fixed C) the area S of heat conduction through the ATH particles is inversely proportional to the radius of the ATH particle. The area into which the heat is conducted in the RTV coating decreases with increasing the size of ATH particle. This leads to a higher temperature on the surface because the flow into the volume from the source of heat of discharges decreases with

increasing radius of the particle and hence more damage ensues. Thus a shorter life of the coating is expected with a larger size of ATH particle as was observed in this work(Fig.4.5). However, and as was shown in Fig.4.5 the coating with 1.0μm size of particle gives a shorter life than for 4.5μm particle. It is suggested and as mentioned in Section 4.2.4, that this is due to the non-uniform dispersion of these filler particles leading to aggregation and hot spots on the surface.

4.2.8. Mechanisms Suggested for Observed Effects of the Size of the Particle of ATH on the Life of RTV Coatings

The roughness of the surface of ATH filled RTV coating depends on the size of the ATH particle. Generally the surface becomes rougher with increasing particle size. Higher leakage current develops on the rougher surface which removes more silicone fluid from the surface. This leads to quicker loss of water repellency and earlier initiation of the formation of water film on the surface. Dry band discharges then develop on the surface. The heat from the discharge is transferred to the coating by conduction and results in increasing the temperature of the surface. The heat conduction into the volume of RTV coating is a function of particle size. A higher temperature develops on the surface with a larger size of particle. This may result in more damage to the surface. The higher temperature may also cause more release of water (H_2O) from ATH filler ($Al_2O_3 \cdot 3H_2O$) resulting in a rougher surface with a larger size of particle. The aging of the coating is then accelerated and it ultimately fails by erosion and subsequent tracking of the FRP.

The diffusion of the silicone fluid from the bulk to the surface provides the recovery of the water repellency of the coating [38,75]. The amount of silicone fluid

diffused to the surface depends on the leakage current which is a function of the size of the ATH particle. Lower leakage current develops on the surface with smaller particle size and this results in less damage to the surface because more silicone fluid is diffused to the surface. The combined benefits lead to a longer life of the coating.

4.3 RTV PERFORMANCE WITH VARYING COATING THICKNESS

4.3.1. RTV Coating on Polyester FRP Rods

4.3.1.1. Experimental conditions

The RTV was formulated with average 13μm particle size ATH filler in a carrier solvent of 1,1,1 trichloroethane. The use of 13μm particle size in the formulation gave a near optimum electrical performance as characterized by a lower leakage current and a longer time to failure[45]. The RTV was coated on FRP rods(polyester resin). Five coating thicknesses of 0.15, 0.38, 0.57, 0.69 and 1.40mm were studied. At least three specimens of each thickness were tested simultaneously. The conductivity of the saline water was adjusted continuously to maintain a conductivity of 1000±3% μS/cm. A saline water flow rate of 1.6±0.1 l/min and an air pressure of 0.54±0.02MPa (79±3psi) was used to generate the fog. The temperature in the fog chamber was 25±2°C during the test.

4.3.1.2. Dependence of leakage current

Measurements of the contact angle before the energized salt-fog test showed that it was within 99.5±0.5°. The average and the maximum roughness were 0.37±0.08μm and

3.33±1.03μm, respectively, for all coating thicknesses from 0.15 to 1.40mm. This clearly shows that at the start of the salt-fog test, the hyurophobicity and the roughness of the surface of all coatings were independent of the coating thickness. This resulted in a similar development of leakage current at the beginning of the test for up to 10h. Fig.4.24 shows the average leakage current as a function of test time in salt-fog for various

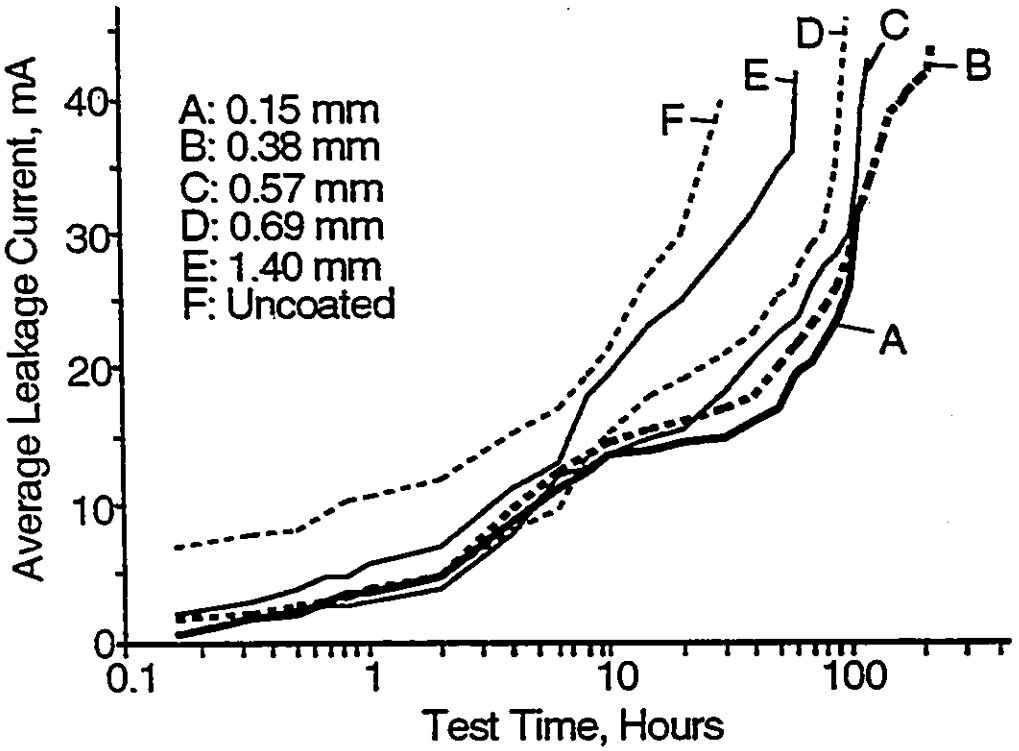

Figure 4.24 Average leakage current of RTV specimens having different coating thicknesses as a function of test time in salt-fog. Conditions: conductivity of saline water, 1000μS/cm; electric stress, 0.5kV$_{rms}$/cm; saline water flow, 1.6 l/min; compressed air pressure, 0.54MPa;ATH filler level, 90pph; size of ATH particles,13μm; substrate, polyester FRP. 3 specimens were used for each thickness.

coating thicknesses. It will be seen from Fig.4.24 that, as the test continued(>10h), the leakage current depended on the coating thickness and increased with increasing coating thickness. This was because a thinner coating transferred the heat from the dry band arcing to the FRP substrate more effectively than a thicker coating and therefore resulted in a lower temperature on the surface and a lesser damage. As the test continued the leakage current in the coating of 0.15mm exceeded that in the coating of 0.38mm. This was due to the erosion of the RTV in the thinner coating which led to an earlier exposure of the FRP in which the leakage current was higher and developed more rapidly. Fig.4.24 also shows that the leakage current of uncoated polyester FRP rod developed quicker than RTV coatings in salt-fog and reached about 40mA after 29h and thus failed sooner. The leakage currents shown in Fig.4.24 were recorded for times extending up to the onset of failure of the specimens.

Figs.4.25 and 4.26 show typical current pulse counts per second in the ranges of 31-37mA and 75-80mA, respectively, for thicknesses from 0.15 to 1.40mm. Other pulse current ranges were also determined and found to show a similar behaviour. It will be seen from Fig.4.25 that from the beginning and up to 110 hours into the test a higher current pulse rate was found with increasing coating thickness. This shows that dry band discharges were initiated at an earlier time and were more intense in the thicker coating. It is suggested that this is because the thicker coating conducted the heat from the dry band arcing to the substrate less effectively than the thinner coating. This resulted in a higher temperature on the surface and more damage to the RTV. This in turn reduced the water repellency on the surface, increased the surface roughness, leading to further growth of dry band discharges in the thicker coating. After 110 hours of test in salt-fog and when the coating of 0.15mm had sufficiently eroded to expose the substrate to the salt-fog, the

specimen developed a higher current pulse rate, as shown in Fig.4.25. As the dry band discharges developed more readily on the substrate, higher levels of discharge current pulse rates were produced which quickly led to failure by tracking on the substrate(Figs.4.25 and 4.26, curve A). Fig.4.26 shows that the current pulses in the higher range of 75-80mA developed in the coating of 0.15mm much earlier than in the coatings of 0.38 and 0.57mm until the substrate became partially exposed to the salt-fog causing failure of the rod by tracking. Monitoring of the number of current pulses is seen to demonstrate the effect of the thickness of the RTV coating on its electrical performance in salt-fog.

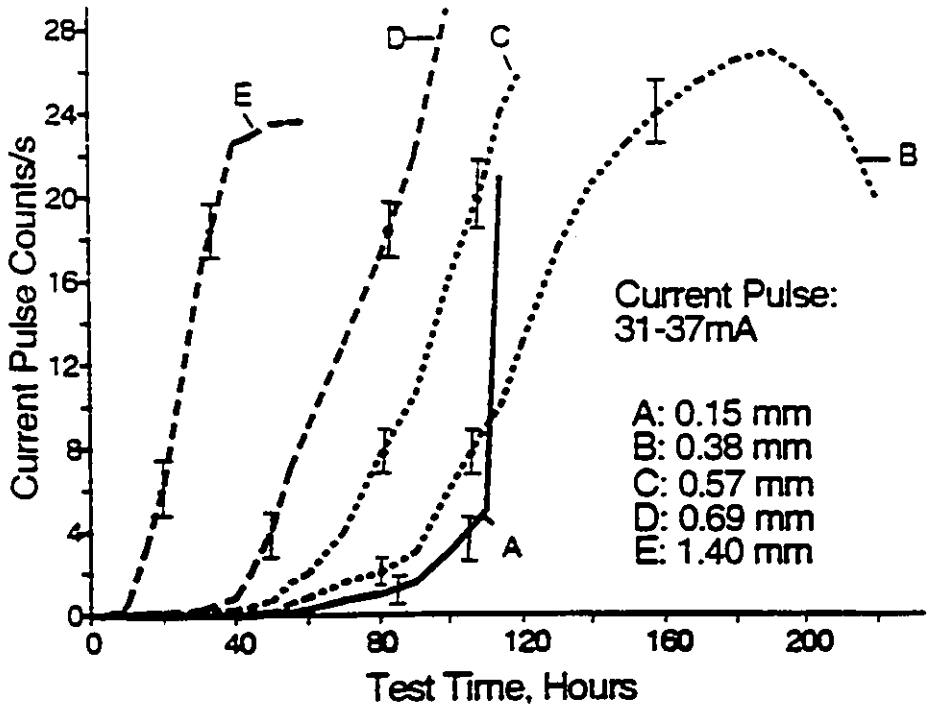

Figure 4.25 Dependence of current pulse count per second in the range of 31-37mA on test time in salt-fog for coating thicknesses from 0.15 to 1.40mm. Conditions are as in Fig.4.24.

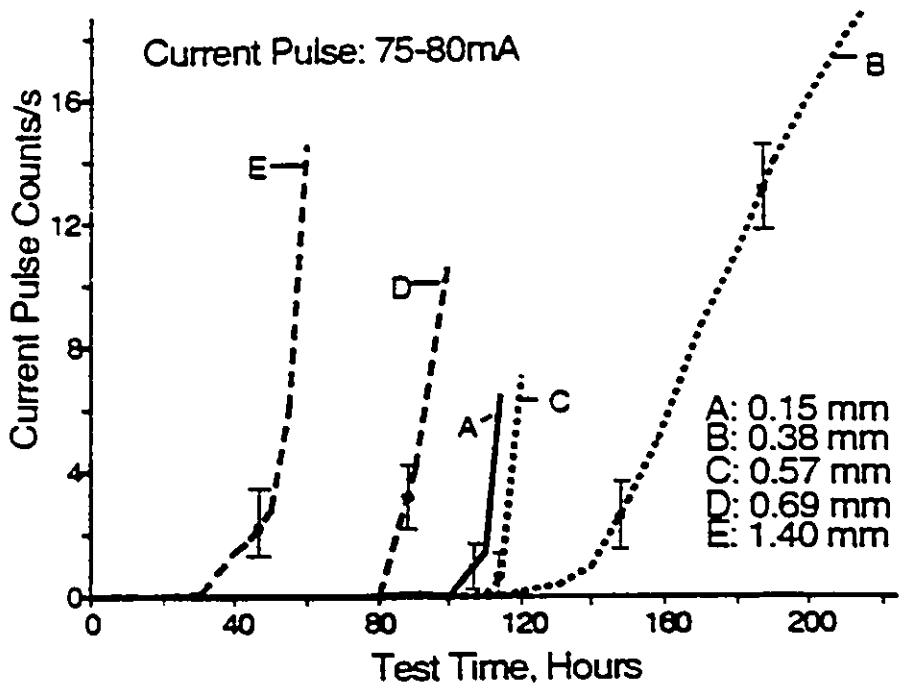

Figure 4.26 Dependence of current pulse count per second in the range of 75-80mA on test time in salt-fog for coating thicknesses from 0.15 to 1.40mm. Conditions are as in Fig.4.24.

Curve B of Fig.4.26 shows that the coating of 0.38mm leads to the development of current pulses after the longest time into the test and sustains a higher pulse rate before it fails than all other coating thicknesses investigated. Therefore it is the optimum thickness for this specific substrate. This finding is further supported by additional measurements described in the section below.

4.3.1.3. Dependence of time to failure

The accumulated damage from the heat of dry band discharge determines the life of the coating. The onset of failure of the specimens was determined when the leakage current exceeded 150mA causing a rupture of the fuse in series with each specimen. Fig.4.24 shows that the current grows very rapidly with time near the onset of failure. The

failure occurred due to substantial erosion of the RTV along a narrow channel where the dry band discharges developed and gradually extended along the surface, and subsequent tracking of FRP rods. Fig.4.27 shows the time to failure of the RTV coating as a function of thickness. The bars indicate the variation within each coating thickness using three specimens. All other conditions of electrical stress, salinity level, the rate of compressed air pressure and thus the fog droplets impinging on the specimens and the formulation were kept constant for all thicknesses. It will be seen from Fig.4.27 that the coating thickness affects the time to failure of the RTV coating. The coating of 0.38mm had a superior resistance to erosion and yielded the longest lifetime. This was because the coating of 0.38mm had a lower average leakage current than either the thicker or the thinner coatings (Fig.4.24) and lower pulse current rate at sufficiently long time into

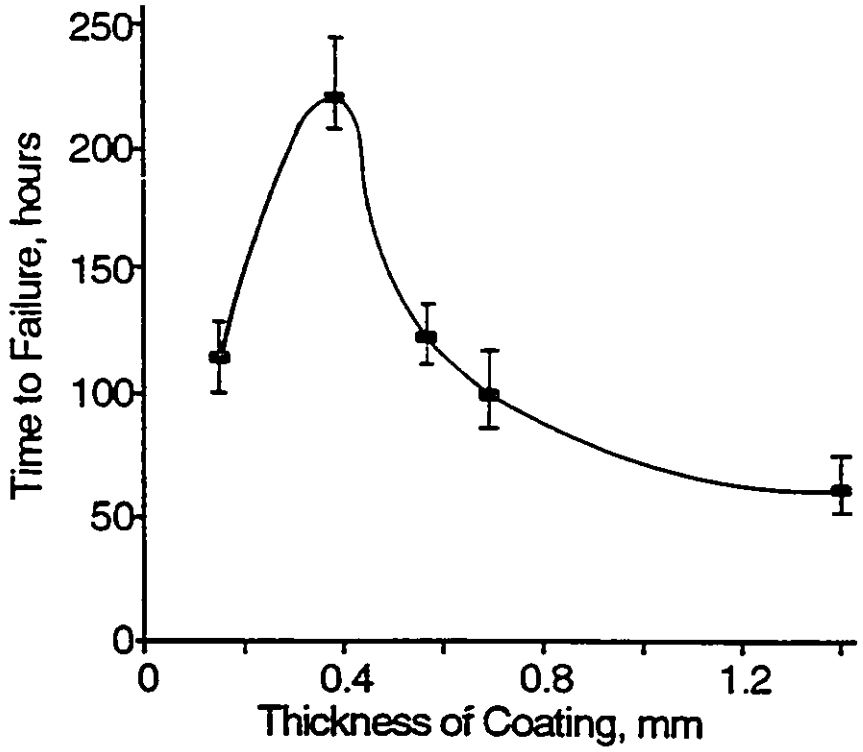

Figure 4.27 Time to failure of RTV as a function of coating thickness. Conditions are as in Fig.4.24. 3 specimens were used for each thickness.

the test(Figs.4.25 and 4.26). This led to a lower erosive damage rate and therefore gave the longest time to failure. The optimum thickness is determined by a balance between a rapid transfer of the heat generated from the dry band discharges on the surface of the RTV to the substrate, which requires a thin coating, and the provision of sufficient silicone rubber to withstand the erosive damage of the discharges for as long as possible, which requires a large thickness.

Fig.4.28 shows a photograph of RTV specimens having 0.15 and 0.38mm coating thicknesses, of the top area of the rods near the high voltage electrode, after 100 hours of test in salt-fog. The specimens were removed from the salt-fog, washed with a mild acetic acid(5%) in an ultrasonic vibrator for about 2 min and thoroughly rinsed with distilled water to remove the salt deposits from the surface. This treatment was previously

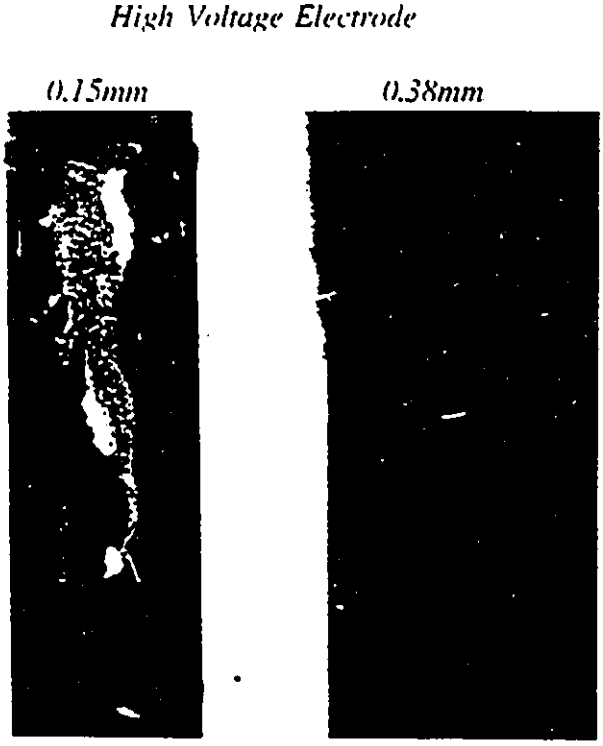

Figure 4.28 RTV specimens having 0.15mm and 0.38mm coating thicknesses, of the top area near the high voltage electrode, after 100h of test in salt-fog. Conditions are as in Fig.4.24.

shown to be very effective in removing the salt deposit from the surface without causing any deleterious effects[53]. This cleaning was necessary in order to examine the surface roughness and erosion damage beneath the salt deposits. It may be observed from Fig.4.28 that a substantial loss of material occurred from the coating of 0.38mm. Although the surface of RTV became rougher from the effect of the dry band discharges the FRP substrate was not exposed to the salt-fog after 100h into the test. This was due to the thicker coating and therefore more material was available to withstand erosion for a longer time. In the thinner coating of 0.15mm shown in Fig.4.28 the substrate was partially exposed to the salt-fog and an evidence of tracking damage is seen to have been initiated on the substrate after 100 hours of test. This shows that the coating of 0.15mm had a lower resistance to erosion and therefore led to a shorter life, as shown in Fig.4.27.

One objective of this work was to show that the electrical performance of RTV coating depends on its thickness and to suggest the mechanisms responsible for the observed phenomenon. It was not intended to tabulate the optimum values of the thickness for all possible combinations of RTV formulations and substrates. It is quite possible that the specific value of the optimum thickness might depend on the type of substrate and on the formulation as these have different thermal conductivities and therefore determine the rate of erosion of the RTV and its lifetime when dry band arcing is present.

4.3.1.4. Surface roughness of the RTV coating

The roughness of the surface of RTV silicone rubber coatings was measured, using a complete scan of the specimen, at different times during the test. Two coating thicknesses of 0.15mm and 0.60mm were studied in the test. For this purpose the test was

briefly interrupted , the specimens were removed from the salt-fog, washed with a mild acetic acid in an ultrasonic vibrator for about 2 min and thoroughly rinsed with distilled water to remove the salt deposits from the surface[53]. The measurements of the surface roughness were conducted after 0 (virgin specimen), 20h, 120 and 220h of salt-fog test.

Fig.4.29 shows the maximum and the average values of the surface roughness, of the top area of the rod near the high voltage electrode, and their dependence on testing time. The roughness of the middle region and of the bottom end of the rod changed little and essentially remained the same as for the virgin specimens in both coatings during 220h of salt-fog test.It will be observed from Fig.4.29 that the roughness of both coatings increased with increasing test time.This was due to the damage from the dry band discharges which caused a gradual roughening of the surface. The bars in Fig.4.29 indicate the variation in the values of the roughness near the top area of the two rods.

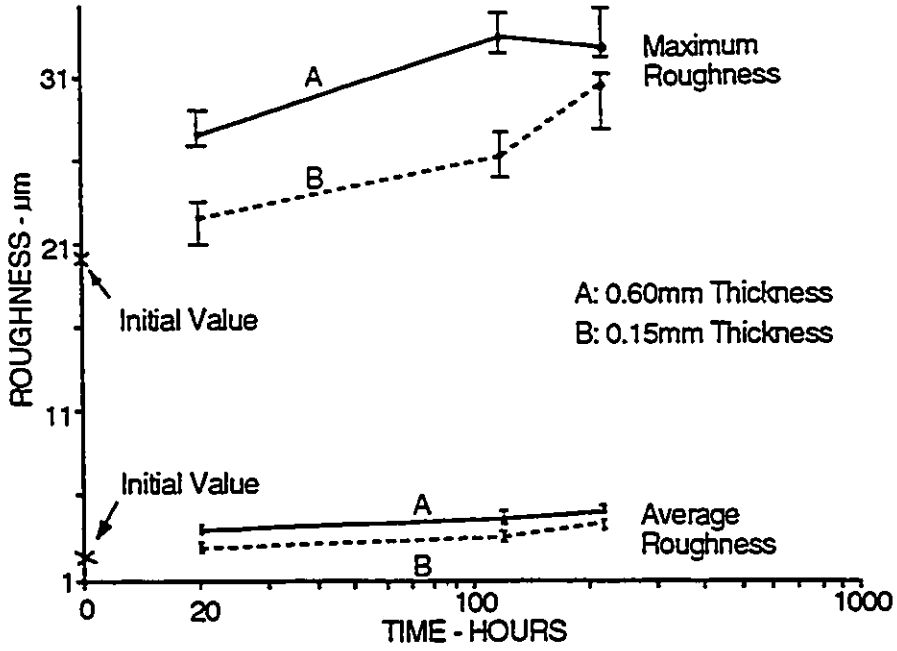

Figure 4.29 Maximum and average roughness of the surface of RTV coatings as a function of time of salt-fog test. Conditions are as in Fig.4.24.

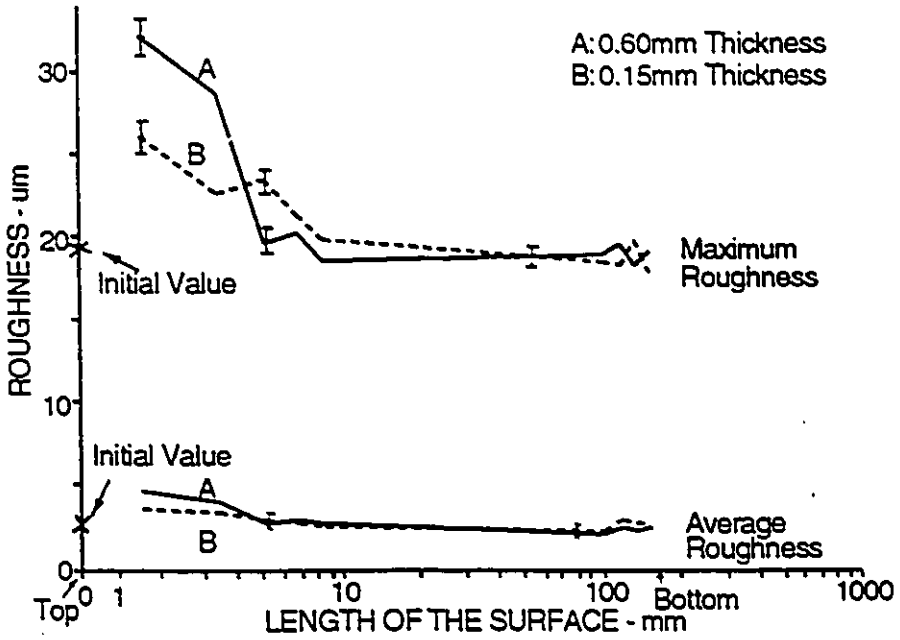

Figure 4.30 Distribution of maximum and average roughness of the surface along the length of the coated rod. The specimens were stressed for 120 hours in salt-fog. Conditions are as in Fig.4.30.

Before the test both specimens had identical values of both the average and the maximum roughness which are shown in Fig.4.29 as "Initial Value". As a result of the presence of more intense dry band discharges the thicker specimens became rougher with increasing test time. This is consistent with Figs.4.24 to 4.26 where larger leakage currents and higher current pulse counts were also measured for the thicker specimens. This indicates clearly the direct inter-relationship between the surface roughness of the insulating surface and the level of the dry-band arc current.

Fig.4.30 shows the distribution of the maximum and the average roughness of the surface along the length of the coated rod. These measurements were taken after subjecting the RTV coatings to 120h of salt-fog. It will be observed that the surface

roughness increases as the top of the vertical rod was approached where the discharges were largely concentrated. The discharges led to a rougher surface near the high voltage electrode, in both coating thicknesses. The damage to the surface of RTV from the dry band discharge is seen to be confined to about 10 mm from the top electrode(Fig.4.30).

4.3.2. RTV Coating on Porcelain Rod

4.3.2.1. Experimental conditions

The RTV was formulated with 5.5μm particle size of ATH filler in a carrier solvent of naphtha. Similar to 13μm used in Section 4.3.1, the use of 5.5μm particle size in the formulation also gave a near optimum electrical performance as characterized by a lower leakage current and a longer time to failure[45]. The RTV was coated on porcelain rods, 155mm length and 20mm in diameter. Five coating thicknesses of 0.17, 0.34, 0.43, 0.62 and 0.99mm were used. At least three specimens of each thickness were tested simultaneously. Tap water which has a typical conductivity of 275±25 μS/cm was used to produce the desired salinity. The salinity of the water forming the fog was adjusted continuously by adding distilled water (conductivity about 5.5 μS/cm) to maintain a nominal conductivity of 250±5% μS/cm. A saline water flow rate of 1.6±0.2 l/min and an air pressure of 0.54±0.02MPa(79±3psi) were used to generate the fog. The ambient temperature in the fog chamber was 23.5±1.0°C during the test.

4.3.2.2. Dependence of leakage current pulses

The development of leakage current depends on the surface conditions of the RTV

specimen. Measurement of the contact angle before the salt-fog test showed that it was within 101±0.5°.The average(Fig.4.35) and the maximum(Fig.4.36) roughness was 3.19±0.11μm and 15.00±0.98μm, respectively, for all virgin coating thicknesses from 0.17 to 0.99mm. This clearly shows that at the start of the salt-fog test, the hydrophobic properties and the roughness on the surface of all coatings were independent of the coating thickness. This resulted in a similar development of leakage current at the beginning of the test. The current pulse was in the range 0-5mA for all coating

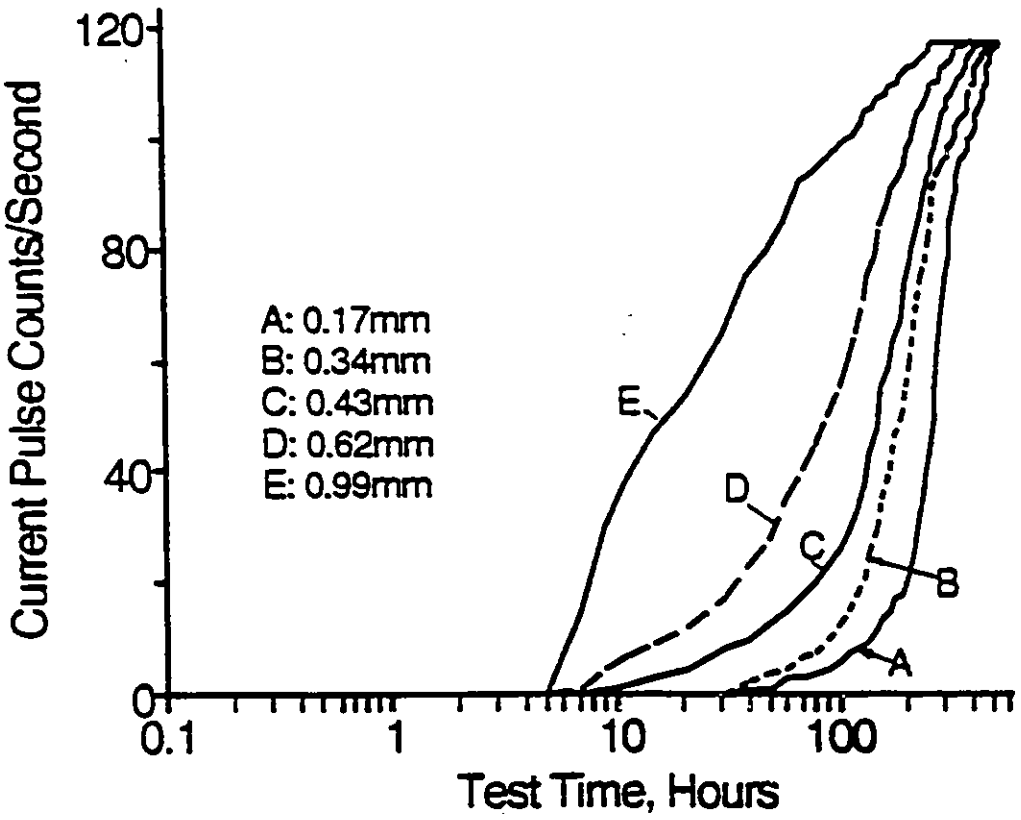

Figure 4.31 Current pulse rate having amplitude in the range 6-11mA as a function of test time in salt-fog for different coating thicknesses. Conditions: conductivity of saline water, 250μS/cm; electric stress, 0.5kV$_{rms}$/cm; saline water flow, 1.6 l/min; compressed air pressure, 0.54MPa; ATH filler level, 90pph; size of ATH particles,5.5μm; substrate, porcelain; solvent, naphtha, three specimens were used for each thickness.

thicknesses after 7h of test in salt-fog. As the test continued the RTV specimen surface gradually lost its hydrophobicity. This is believed to be due to reorientation of the hydrophobic PDMS molecular chains on the surface of RTV, in the presence of water, in response to their local micro-environment to minimize their interfacial-free energy with the surrounding water[2]. This resulted in the reorientation of the PDMS molecular chains from the surface towards the bulk resulting in a partial loss of the hydrophobicity in a prolonged salt-fog. A continuous film of water was gradually formed and dry band arcing was initiated on the surface. The maximum amplitude of current pulses produced by the dry band arcing was found to be 11mA during the test up to 570h in the moderate salt-fog of 250μS/cm. Fig.4.31 shows the current pulse rate having amplitudes in the range of 6-11mA as a function of test time for different coating thicknesses. It is shown in Fig.4.31 that as the test continued (>7h) the current pulse rate depended on the coating thickness and increased with increasing coating thickness. This indicates that more dry band arcing was present on the thicker coating. The thicker coating conducted the heat from the dry band arcing to the porcelain substrate less effectively than the thinner coating. This resulted in a higher temperature on the surface and more damage to the RTV. This in turn increased the surface roughness(Figs.4.35 and 4.36), caused more dry band discharge activity and therefore increased the rate of current pulses in the thicker coating, as shown in Fig.4.31. It should be noted that due to the low salinity of 250 μS/cm the damage to the coatings from erosion during the dry band arcing was not substantial even after 570h of test. Therefore an optimum thickness of coating on porcelain could not be discernable from Fig.4.31 at low peaks of pulse currents (6-11mA). The trend found here for the dependence of the current pulse rate on the thickness at low salinity is similar to that found at short times of tests(<100h) and low peaks of pulse

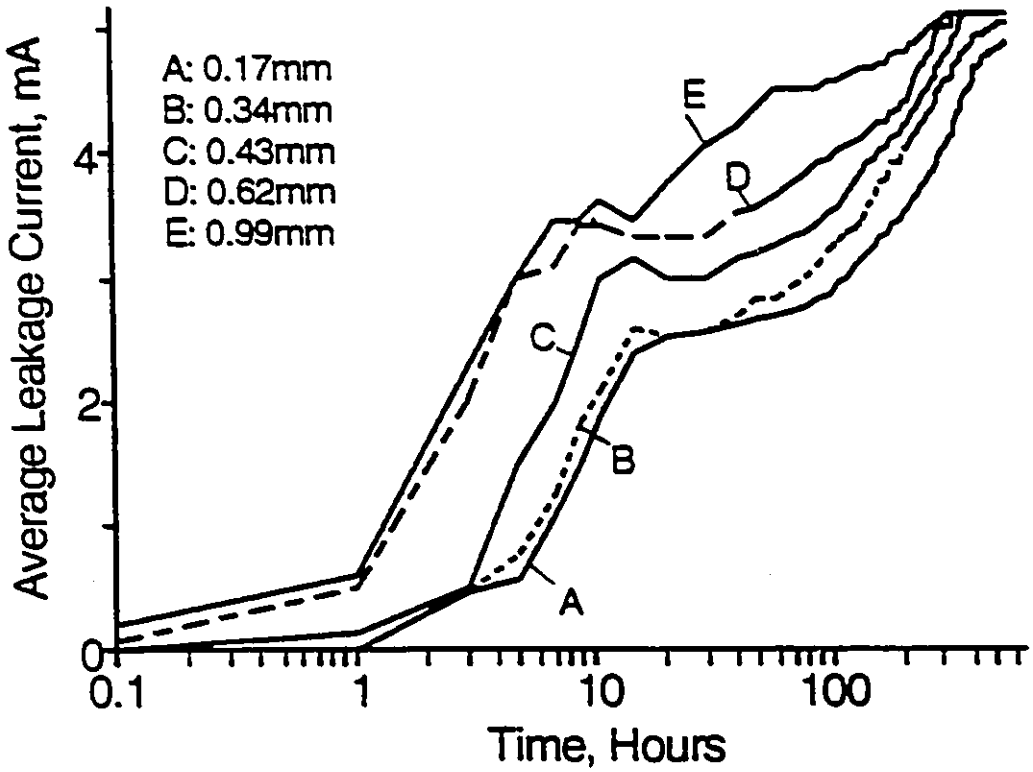

Figure 4.32 Average leakage current as a function of test time in salt-fog for different coating thicknesses. Conditions are as in Fig.4.31.

currents (31-37mA) when a higher salinity of salt-fog of 1000 μS/cm was used with RTV coatings on FRP[45].

Fig.4.32 shows the average leakage current as a function of test time in salt-fog for different coating thicknesses. It is seen from Fig.4.32 that the average leakage current increased with increasing coating thickness in general agreement with Fig.4.31.

Fig.4.33 shows the time of development of different levels of current pulse rate having amplitudes in the range of 6-11mA as a function of coating thickness. It will be observed from Fig.4.33 that it took a shorter time to develop a given level of current

pulse rate on a thicker coating. Typically at a fixed current pulse rate of 80/s having amplitude in the range of 6-11mA, the time to develop the current pulse rate decreased from 320h for coating thickness of 0.17mm to 160h for coating thickness of 0.43mm and then to 20h for coating thickness of 0.99mm.

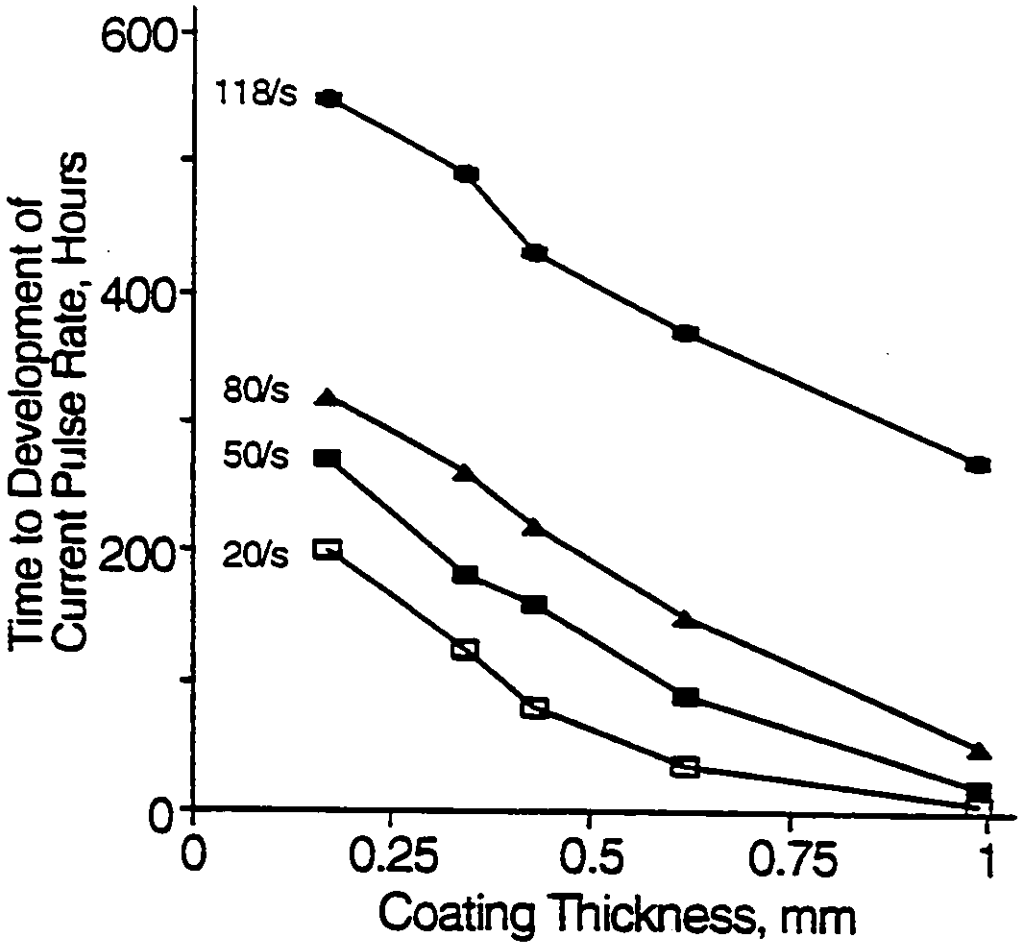

Figure 4.33 Time to development of different levels of current pulse rate having amplitudes in the range of 6-11mA as a function of coating thickness. Conditions are as in Fig.4.31.

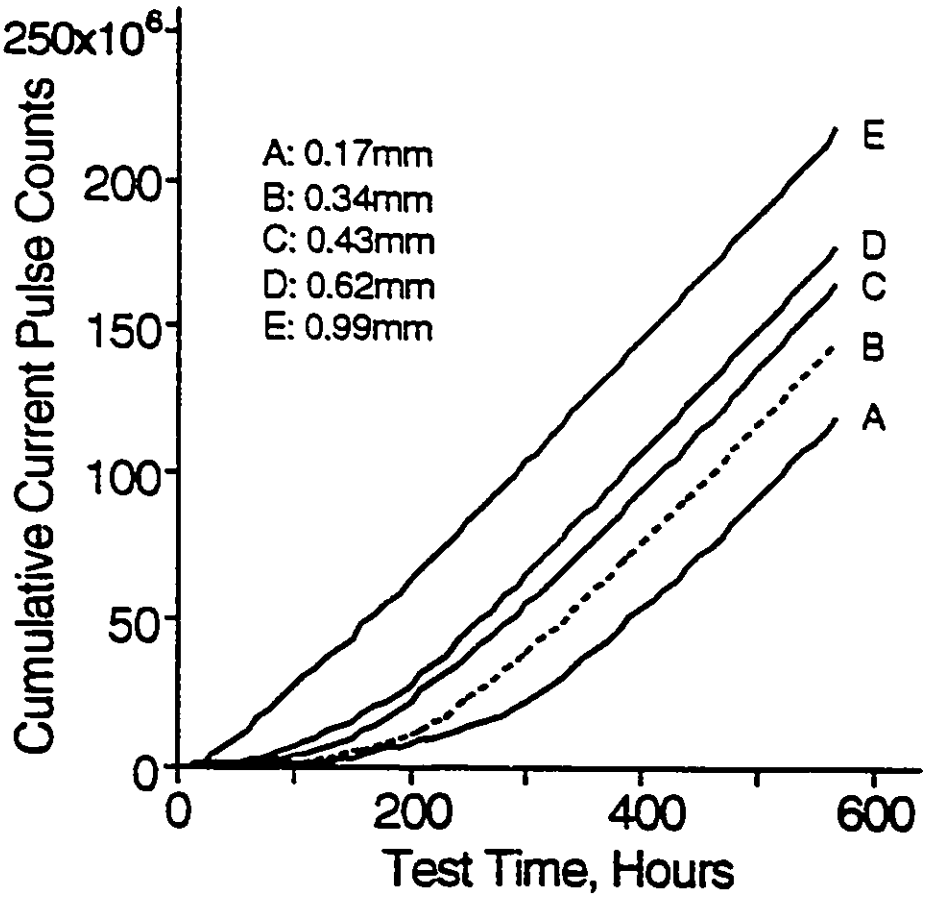

Figure 4.34 Cumulative number of current pulses having amplitudes in the range 6-11mA as a function of test time in salt-fog for different coating thicknesses. Conditions are as in Fig.4.31.

Fig.4.34 shows the cumulative number of current pulses having amplitudes in the range of 6-11mA as a function of test time for different coating thicknesses. It can be seen from Fig.4.34 that the number of the current pulses increased with increasing coating thickness. This further confirmed that the dry band arcing, as indicated by the number of current pulses, were more extensive for the thicker coatings.

4.3.2.3. Dependence of surface roughness

Figs.4.35 and 4.36 show the average roughness(Fig.4.35) and the maximum roughness(Fig.4.36) as a function of coating thickness before and after 570h of salt-fog. The measurements of surface roughness on the specimens after salt-fog were conducted at locations near the high voltage electrode. It will be seen that the average roughness and the maximum roughness were almost identical on the surface of all virgin specimens having different coating thicknesses from 0.17 to 0.99mm due to the same formulation of RTV. As the test continued and dry band arcing occurred it is postulated that the heat from the arcing severed the side chains of PDMS, deformed the short PDMS chains, crosslinked chains and removed some hydrophobic methyl groups from the surface[42]

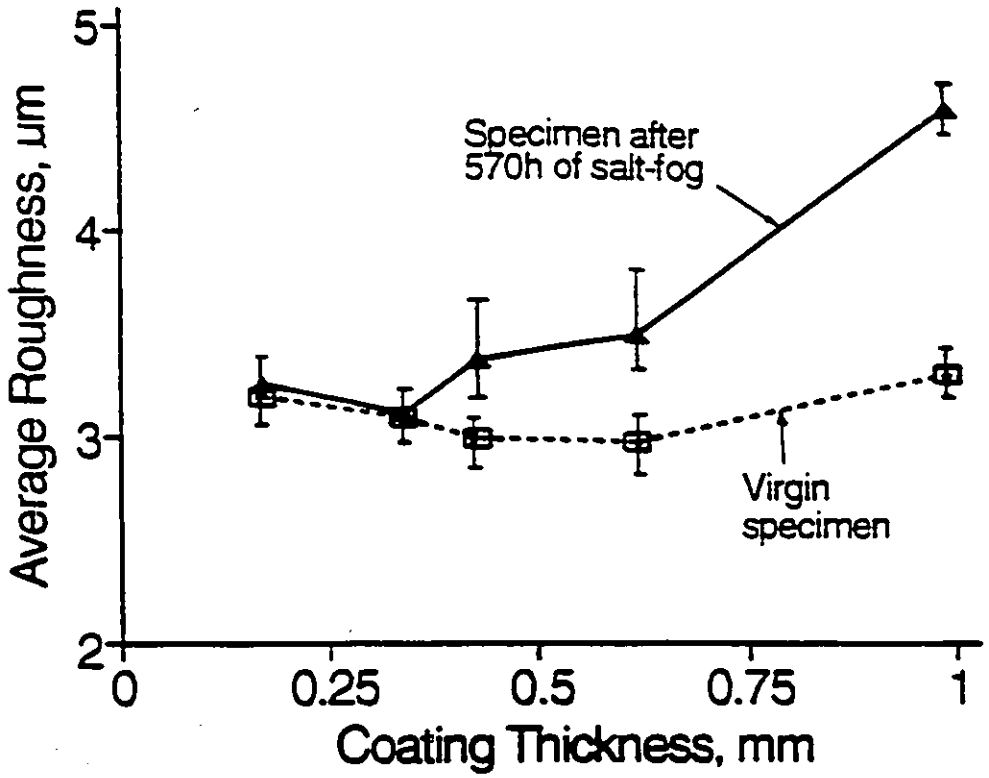

Figure 4.35 Average roughness as a function of coating thickness before and after salt-fog test. Conditions are as in Fig.4.31.

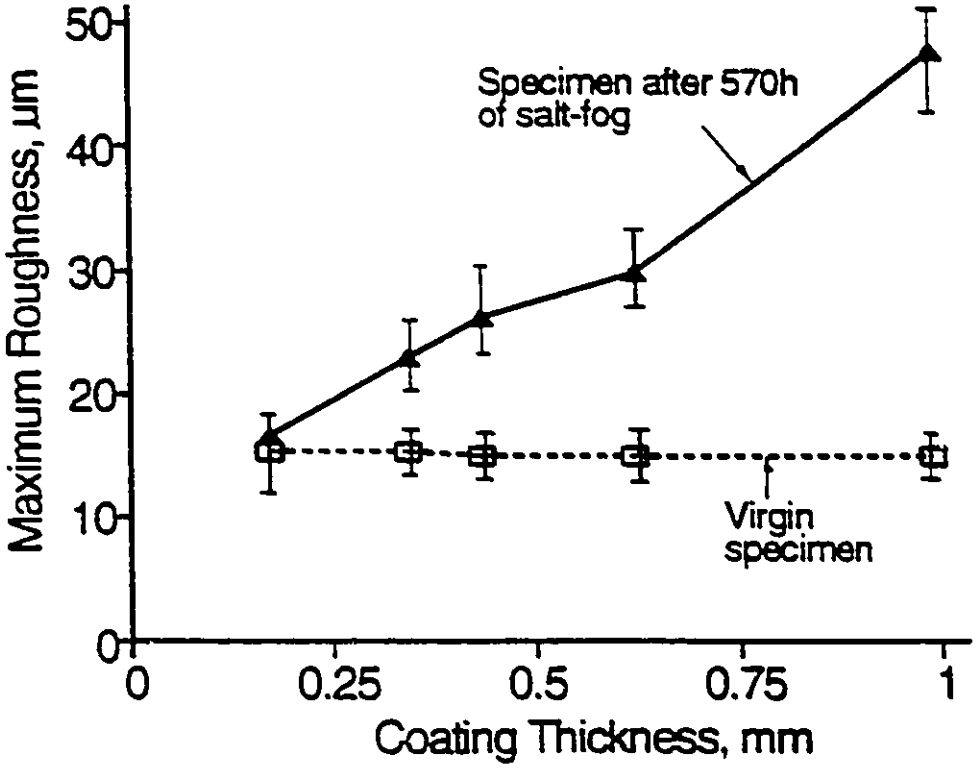

Figure 4.36 Maximum roughness as a function of coating thickness before and after salt-fog test. Conditions are as in Fig.4.31.

which ultimately led to erosion of the RTV coating. The thinner coating transferred the heat to the porcelain substrate more effectively than a thicker coating and therefore resulted in a lower temperature on the surface and less damage. The roughness increased with increasing coating thickness after 570h of salt-fog, as shown in Figs.4.35 and 4.36. The average roughness in Fig.4.35 increased slightly from 3.2µm to 3.3µm for coating thickness of 0.17mm and largely from 2.99µm to 4.60µm for coating thickness of 0.99mm after the salt-fog.test. The maximum surface roughness in Fig.4.36 increased slightly from 15.00µm to 16.50µm for 0.17mm and largely from 14.90µm to 47.60µm for 0.99mm after 570h of salt-fog. The rougher surface in turn caused a higher rate of current pulses and a larger number of current pulses on a thicker coating as shown in Figs.4.31 and 4.34.

4.4 RTV PERFORMANCE WITH THE ADDITION OF SILICONE FLUID

Silicone fluid is one of the factors responsible for the maintenance of hydrophobicity as manifested by water repellency on the surface of silicone rubber coating[35,40,44-48,75,76]. The silicone fluid is a low molecular weight of PDMS inherently present in the RTV coating. In the present study RTV coatings formulated without addition (0%) and with addition of silicone fluid of 1 and 10% by weight. The addition of silicone fluid to the RTV formulation was made in an attempt to explore the possibility of extending the lifetime of the coating under moderate conditions of contamination. The specimens were tested in the salt-fog chamber.

4.4.1. Experimental Conditions

The RTV was formulated without (0%) and with additions of 1 and 10% silicone fluid by weight in a carrier solvent of 1,1,1 trichloroethane. The viscosity of the added silicone fluid was 1000 centipoises. A median size of the ATH particles of 1μm was used in addition to the 13μm. This was in order to validate these results using two sets of formulations of RTV. The RTV was coated on FRP rods, 152mm length and 16mm in diameter. Three specimens were tested for each formulation simultaneously. Nominal conductivities of 250±5% and 1000±3% μS/cm were used in the present study. A saline water flow rate of 1.6±0.2 l/min and an air pressure of 0.54±0.02MPa(79±3psi) were used to generate the fog. The ambient temperature in the fog chamber was 25±2°C during the test.

4.4.2. Dependence of Leakage Current and Time to Failure

The surface conditions before salt-fog test as indicated by the contact angle

(98.8±2.3°), the average surface roughness (2.51±0.38μm) and the maximum roughness (22.88±3.21μm) were very close for the three types of specimens with and without additions of silicone fluid. As the contact angle was sufficiently high for the normal formulation of RTV an increase in the quantity of the silicone fluid on the surface was not expected to increase the value of the contact angle beyond its saturated level. This was also confirmed in the present work. The thicknesses were very close for the three formulations of RTV specimens of 0%, 1% and 10% silicone fluid and were 0.27±0.01, 0.26±0.02 and 0.30±0.03mm, respectively.

Fig.4.37 shows the average leakage current as a function of test time for 0%, 1% and 10% silicone fluid. It will be seen that almost an identical leakage current was developed on the three coatings at the start of the test and up to 50h due to similar initial surface conditions of contact angle and roughness. As the test continued the water repellency was gradually reduced due to the heavy and prolonged arcing in the salt-fog. The RTV coating with 10% silicone fluid was visibly covered by a thin layer of fluid. This fluid has a much lower thermal conductivity of 0.145W/m °C[77] than that of the RTV of 0.57 W/m °C [40]. The latter value was calculated for RTV and took into account the presence of the ATH filler [73]. The lower thermal conductivity of the more abundant silicone fluid on the surface than in the normal coating retarded the conduction of the heat generated by the discharges from the surface to the bulk of the coating and then on to the substrate. This caused a higher temperature on the surface resulting in decomposition of the silicone fluid. Volatile flammable materials, silica, silicon dioxide and crosslinked polymers may be formed from the decomposition of silicone fluid under high thermal and disruptive discharge conditions[77]. Silicon carbide may also be formed under arcing conditions[77]. Examination of the specimens, containing 1% and 10% silicone fluid,

13μm particle size and 90pph of ATH, showed that only after about 55h into the test a black material was formed on the surface. This was particularly more pronounced in the vicinity of the high voltage electrode, where intense discharges occurred. After failure of the coating (time shown in Fig.4.40) it was observed that the black deposits spread right across the whole specimen. It was observed that the formation of these deposits

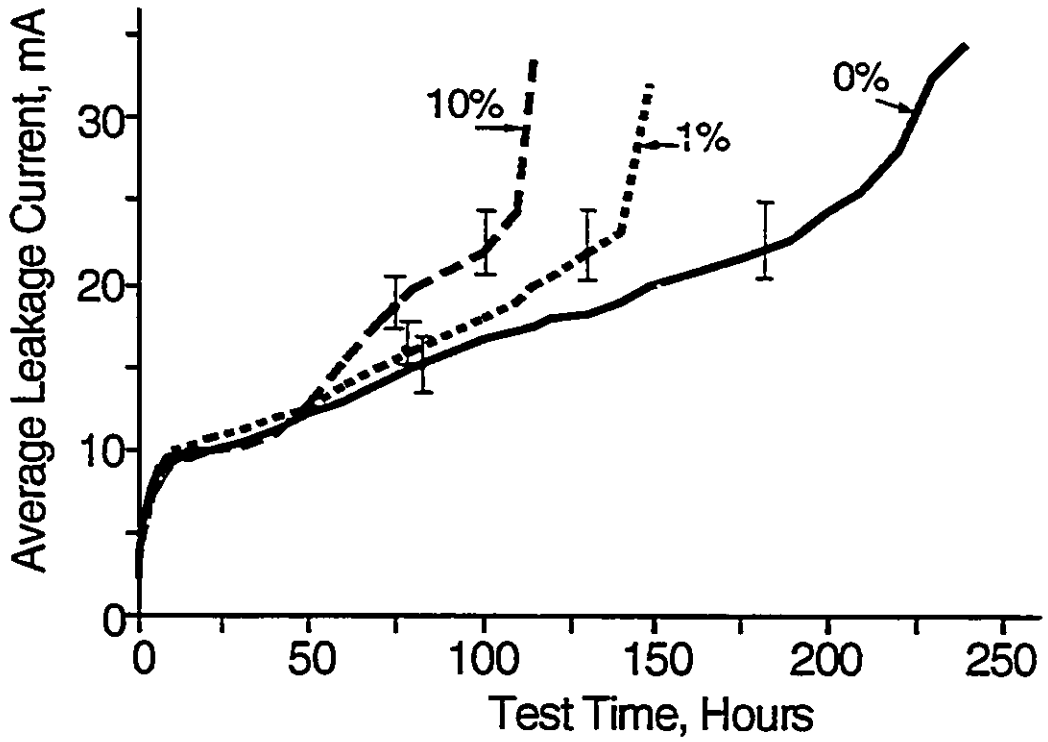

Figure 4.37 Average leakage current on RTV coated rods without (0%) and with 1% and 10% silicone fluid by weight to the formulation as a function of test time in salt-fog. Conditions: conductivity of saline water, 1000μS/cm; electric stress, 0.5kV$_{rms}$/cm; saline water flow, 1.6 l/min; compressed air pressure, 0.54MPa;ATH filler level, 90pph; size of ATH particles,13μm; substrate, polyester FRP; solvent, 1,1,1 trichloroethane. Three specimens were used for each thickness.

increased with increasing current and increasing time of test. The black material on the surface reduced the water repellency of the RTV coating resulting in increasing leakage current with increasing test time. The RTV coating with 10% extra silicone fluid is thought to have a higher temperature due to a thicker layer of silicone fluid and thus results in a larger amount of hydrophillic black material on the surface. Therefore a higher leakage current developed than in the coating with 1% extra silicone fluid, with increasing test time as shown in Fig.4.37. The RTV coating without extra silicone fluid had no black material on the surface and much less visible pitting damage due to the lower leakage current. This was directly related to the higher effective thermal conductivity of the surface of the RTV in the latter case.

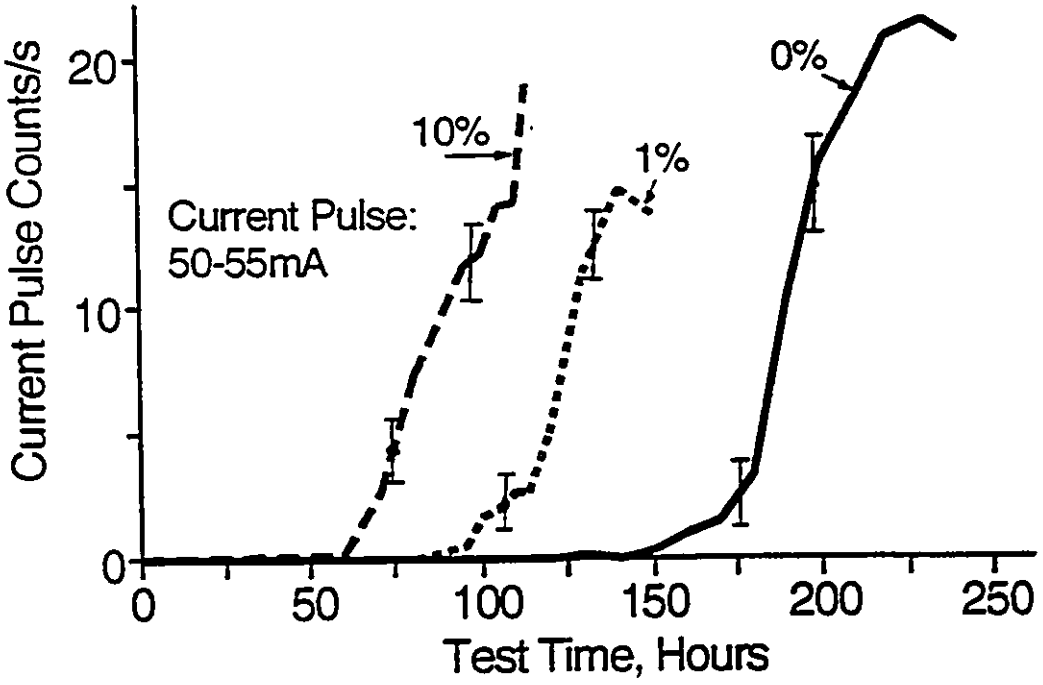

Figure 4.38 Dependence of current pulse count rates in the range of 50-55mA on test time in salt-fog for RTV coated rods without (0%) and with additions of 1% and 10% silicone fluid by weight. Other conditions are as in Fig.4.37.

Measurements of current pulses as a function of time in salt-fog also showed that the RTV specimens with 1% and 10% extra silicone fluid had higher counts of current pulses. The current pulses started at earlier times of test than the specimens without extra silicone fluid as shown in Figs.4.38 and 4.39, respectively, in the ranges of 50-55mA and 75-80mA. Figs.4.37 to 4.39 conclusively confirm that the dry band discharges were more pronounced on the surface with 1% and 10% silicone fluid than on the surface without 0% silicone fluid.

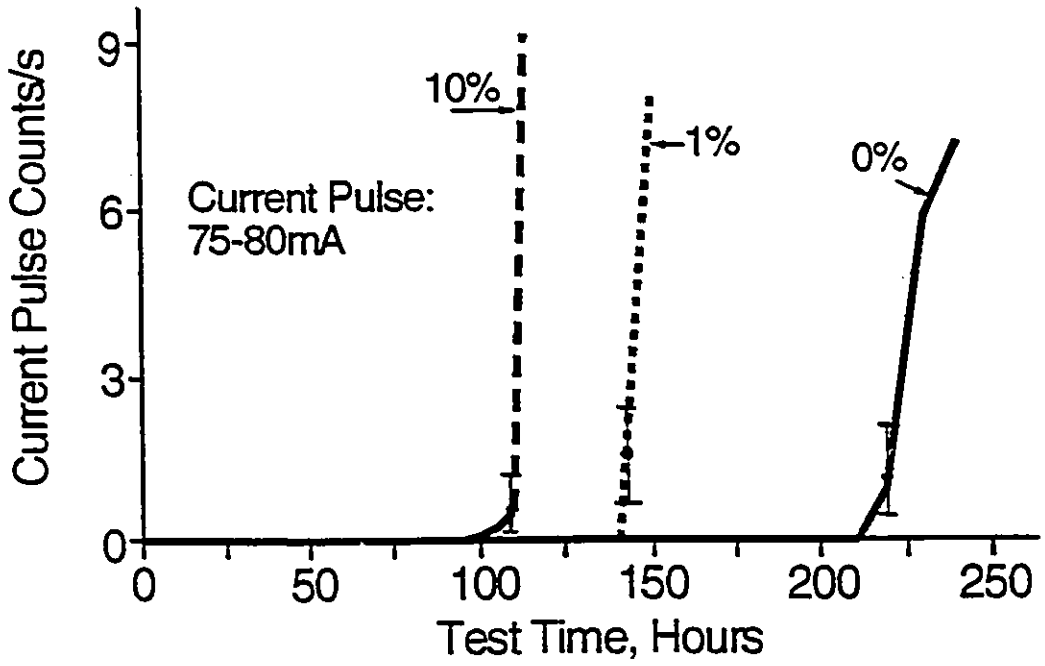

Figure 4.39 Dependence of current pulse count rates in the range of 75-80mA on test time in salt-fog for RTV coated rods without (0%) and with 1% and 10% silicone fluid by weight. Other conditions are as in Fig.4.37.

Fig.4.40 shows the time to failure in salt-fog of the RTV coatings with and without silicone fluid. The RTV coating with extra silicone fluid had a shorter lifetime than the coating without extra silicone fluid. Silicone fluid has a lower thermal

conductivity than the coating with ATH filler. Thus the extra silicone fluid on the surface is thought to retard the conduction of the heat from the surface to the bulk and therefore result in a higher temperature, larger leakage current (Fig.4.37) and larger current pulse count rate which appeared at earlier time into the test (Figs.4.38 and 4.39). The more intense dry band arcing on the specimens with 1% and 10% silicone fluid led to formation of hydrophillic material on the surface and resulted in more severe erosive damage and therefore a shorter lifetime.

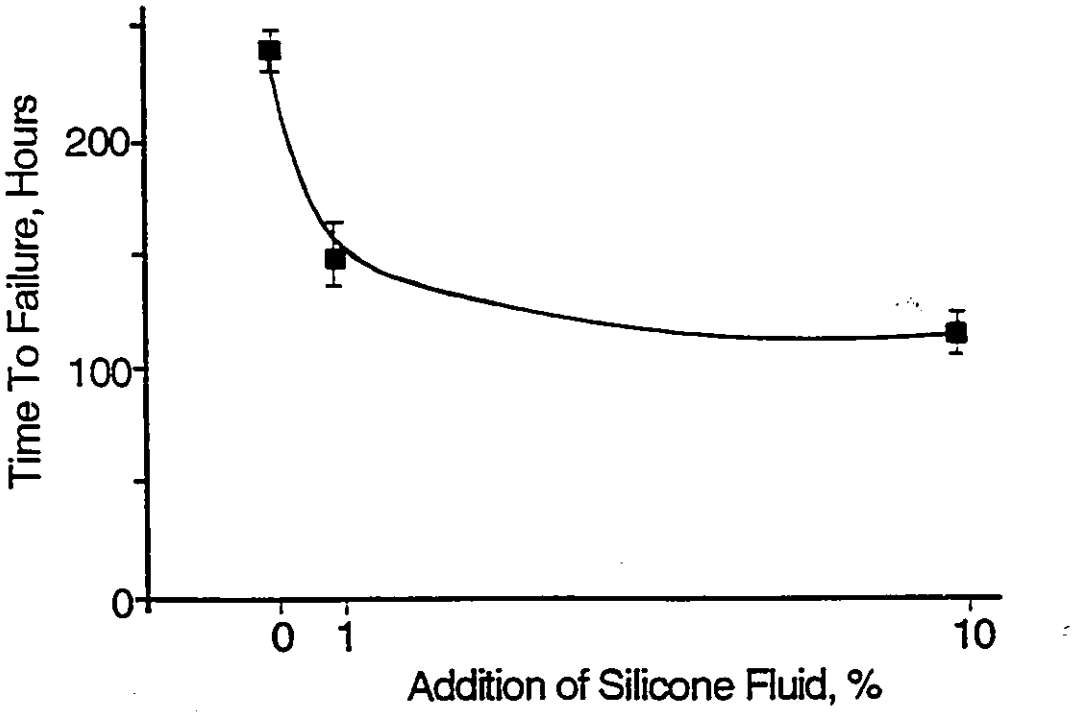

Figure 4.40 Time to failure of RTV coatings without (0%) and with 1% and 10% silicone fluid by weight to the formulation. Other conditions are as in Fig.4.37.

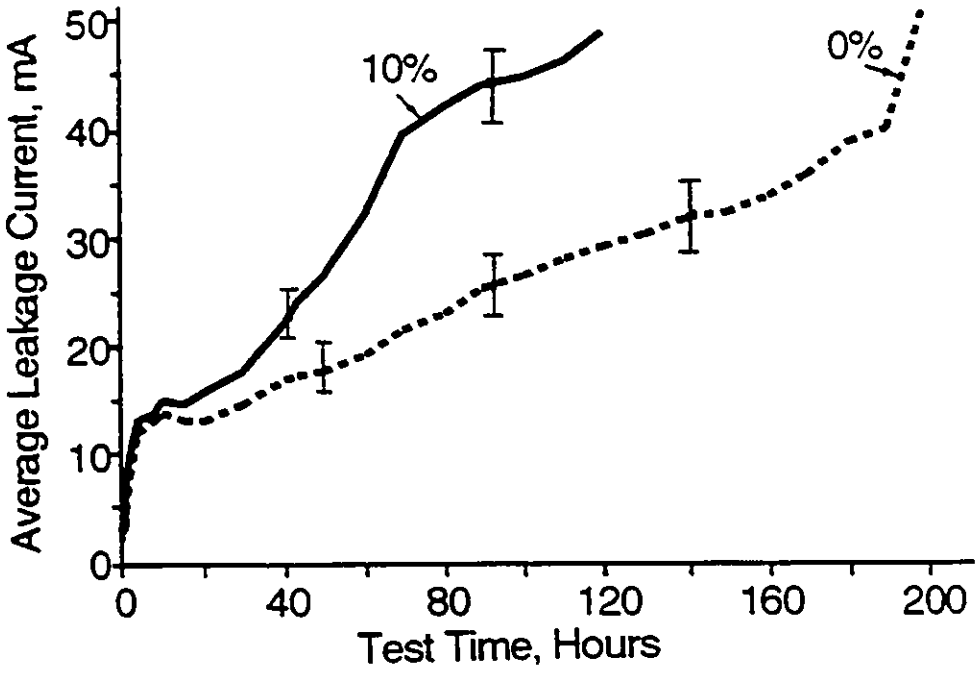

Figure 4.41 Average leakage current on RTV coated rods without(0%) and with 10% silicone fluid by weight to the formulation as a function of test time in salt-fog. Size of ATH particles, 1.0μm:. Salt-fog conditions, applied stress and other RTV formulations are as in Fig.4.37.

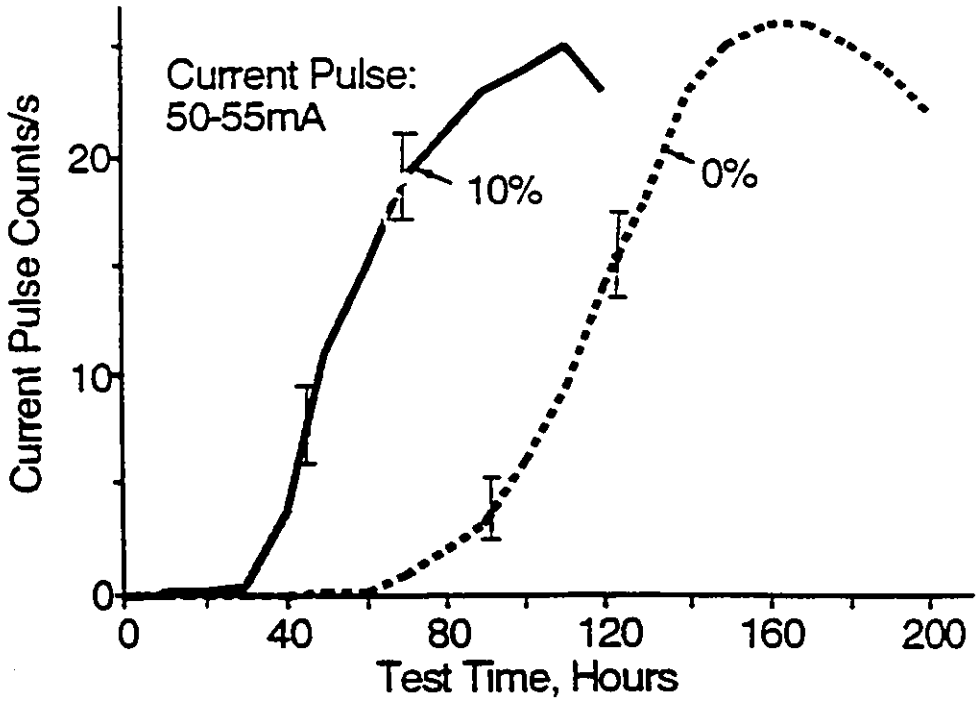

Figure 4.42 Dependence of current pulse count rates in the range of 50-55mA on test time in salt-fog for RTV coated rods without (0%) and with 10% silicone fluid by weight. Conditions are as in Fig.4.41.

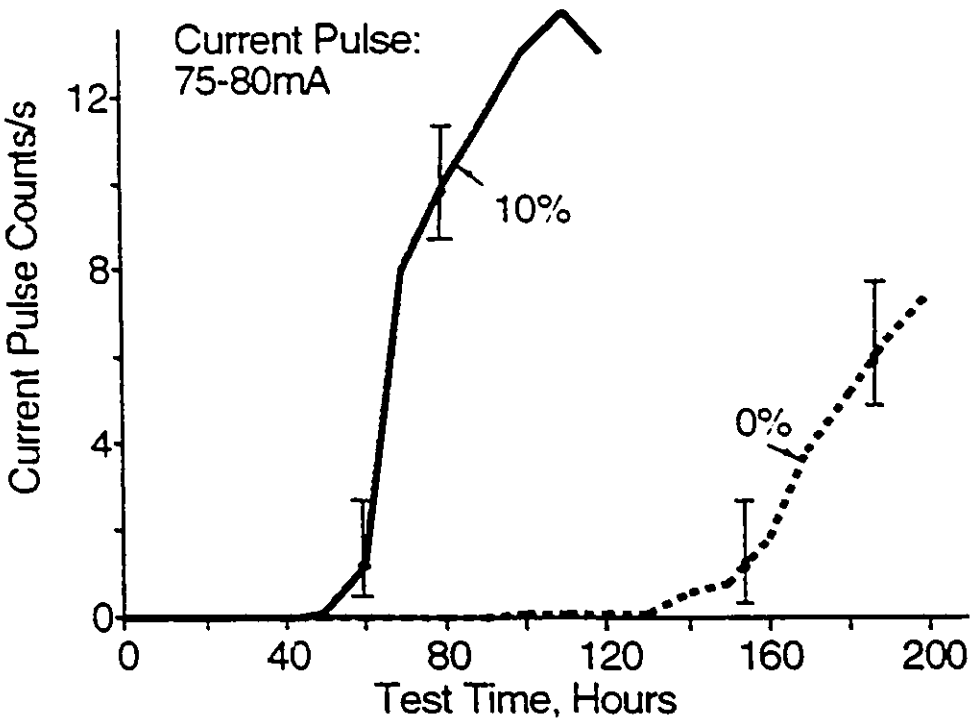

Figure 4.43 Dependence of current pulse count rates in the range of 75-80mA on test time in salt-fog for RTV coated rods without (0%) and with 10% silicone fluid by weight. Conditions are as in Fig.4.41.

Further confirmation that an addition of silicone fluid to the RTV coating does not improve its electrical performance was obtained using extensive tests with 1μm median particle size of ATH filler and 90pph. The surface conditions for this formulation before the salt-fog test, for all specimens, were for the contact angle 98.8±2.3°, the average surface roughness 0.43±0.14μm and the maximum roughness 3.55±1.25μm. The average current, the current pulse count rates and time to failure are shown in Figs.4.41 to 4.43 and Table 4.1. It is clearly demonstrated that the coating with addition of 10% silicone fluid had a higher leakage current (Fig.4.41), a higher rate of current pulse counts (Figs.4.42 and 4.43) and a shorter time to failure (Table 4.1) than the coating without (0%) extra silicone fluid. In this formulation (1μm particle size and 90pph of ATH and

10% added silicone fluid by weight) the black deposits on the surface were visible near the high voltage electrode after 7h into the test. This was much earlier than in the formulation containing 13μm particle size and for both 1% and 10% added silicone fluid (>55h). After failure of the coating (Time shown in Table 4.1) the black deposits were found to spread right across the whole specimen. These deposits were completely absent when silicone fluid was not added to the formulations.

Table 4.1 Time to failure of RTV coatings without(0%) and with 10% silicone fluid by weight to the formulation. Conditions are as in Fig.4.41.

Silicone Fluid in RTV Coatings	**10%**	**0%**
Coating Thickness, mm	**0.82 ± 0.07**	**0.80 ± 0.08**
Time to Failure, hours	**120 ± 25**	**200 ± 5**

4.4.3. X-ray Diffraction Study of the Surface

An X-ray diffractometer (type Rigaku DMAX-1200) employing 1.542×10^{-10}m wavelength from CuKα radiation was used in an attempt to identify the black deposits found on the RTV specimens with added silicone fluid. The X-ray diffraction pattern of Fig.4.44 appears to be different for the virgin specimens containing an added 10% of low molecular weight of PDMS (curves C) from that without added silicone fluid (curves A). At this stage the identification of the peaks is still inconclusive.

Fig.4.44 shows a difference in the X-ray diffraction patterns between the virgin (curves A and C) and the aged specimens (curves B and D) for both 0% and an addition

of 10% silicone fluid to the RTV formulation. On an expanded scale of the diffraction angle 2θ, the areas under the peaks are clearly seen to have decreased for aged specimens compared to the virgin specimens, indicating an increase in the crystallinity. This is in qualitative agreement with a recent study by Gorur et al[78]. The presence of new peaks in the diffraction pattern in the aged RTV specimens suggests that other changes have also occurred. This will be further studied.

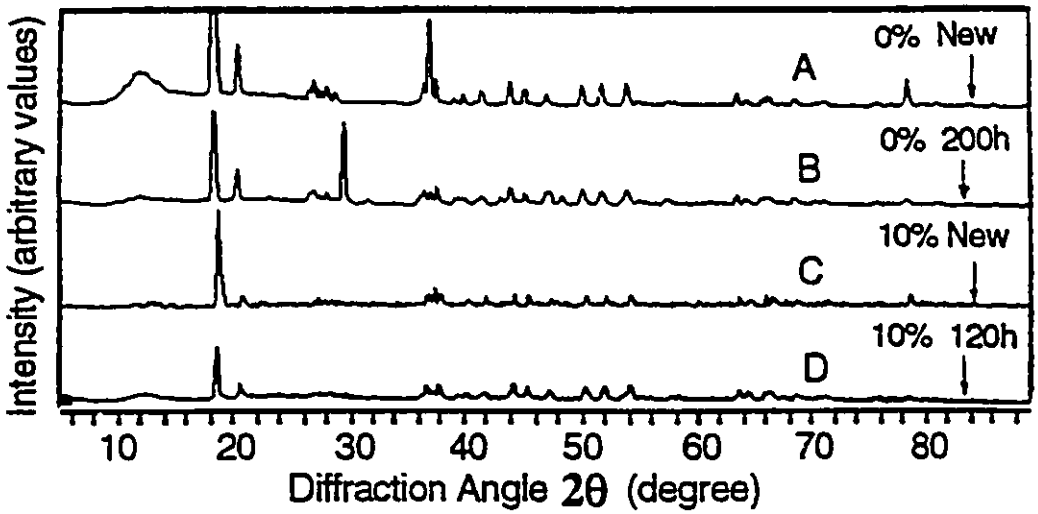

Figure 4.44 Comparative X-ray diffraction intensity patterns of RTV having different formulations before and after salt-fog test. A. virgin RTV without added silicone fluid(0%): B. RTV without added silicone fluid, after 200hr of salt-fog test: C. virgin RTV with 10% added silicone fluid by weight: D. RTV with 10% silicone fluid after 120hr of salt-fog test. 1μm particle size and 90pph of ATH. Other conditions of salt-fog, electric stress and substrate are as in Fig.4.37. The thicknesses of coatings are as in Table 4.1.

4.4.4. FTIR-ATR Study of the Surface

The surface of the virgin coatings without (0%) and with additions of 1% and 10% silicone fluid were examined using a ATR-FTIR spectrometer type Nicolet 5DX using Thalium Bromoiodide KRS-5 crystal[40]. Fig.4.45 shows the IR spectra on the surface

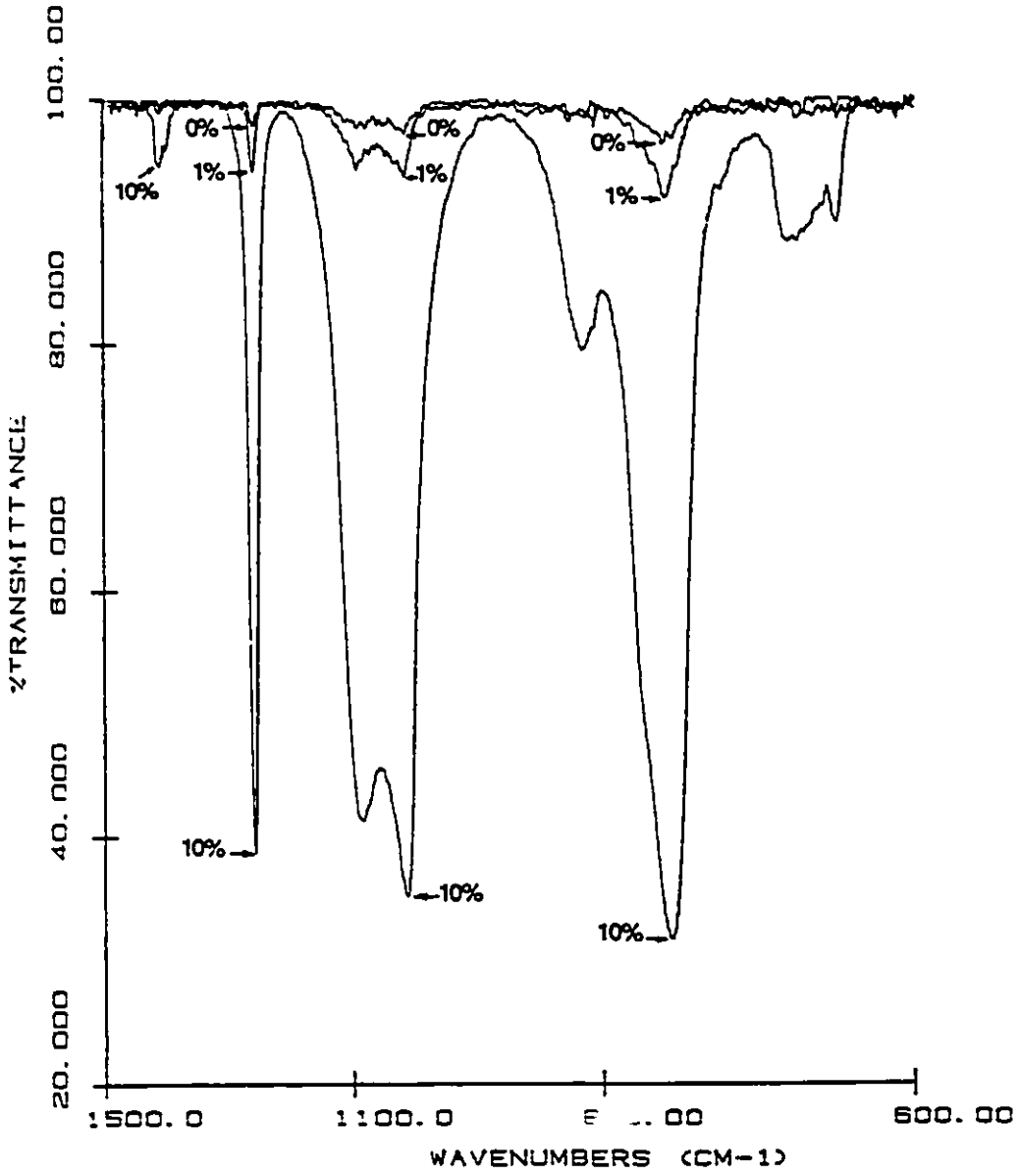

Figure 4.45 IR spectra on RTV coated rods without(0%) and with 1% and 10% silicone fluid by weight to the formulation. Other formulations of the coatings are as in Fig.4.37.

without (0%) and with additions of 1% and 10% silicone fluid before the salt-fog test. Absorption was due to the silicone fluid on the surface. The peaks in Fig.4.45 represent the characteristic IR absorption bands[40,45]. It can be seen from Fig.4.45 that more silicone fluid was present on the surface of the specimens with 1% and 10% silicone fluid. The amount of silicone fluid on the surface of the coatings increased with increasing the amount of addition of silicone fluid by weight to the RTV formulation.

Fig.4.46 shows the IR spectra on the surface of RTV coatings without (0%) (Fig.4.46A) and with addition of 10% silicone fluid (Fig.4.46B) before salt-fog test and after 0.5h, 22h and 95h have elapsed after the cessation of salt-fog test in a low salinity of 250μS/cm. It can be seen from Fig.4.46 that the silicone fluid on the surface with 0% silicone fluid (Fig.4.46A) increased after 395h of salt-fog test and rest time of 0.5h compared to the virgin specimen and no further increase of silicone fluid was found on the surface for all rest time from 0.5h to 95h. The rest time of 0.5h constitutes the total time which has elapsed between the removal of the specimens from the salt-fog chamber at which the dry band arcing ceased and the start of the IR measurements. The silicone fluid on the surface with added 10% silicone fluid (Fig.4.46B) is seen to have decreased after the test (0.5h rest time) and then increased with increasing rest time from 0.5h to 22h and no further increase of silicone fluid was found on the surface thereafter. The amount of silicone fluid on the surface with 10% silicone fluid was still less than in the virgin specimen even after 95h of rest time as shown in Fig.4.46B. The observed increase of the silicone fluid on the surface after cessation of the dry band arcing is due to the diffusion of the fluid from the bulk to the surface.

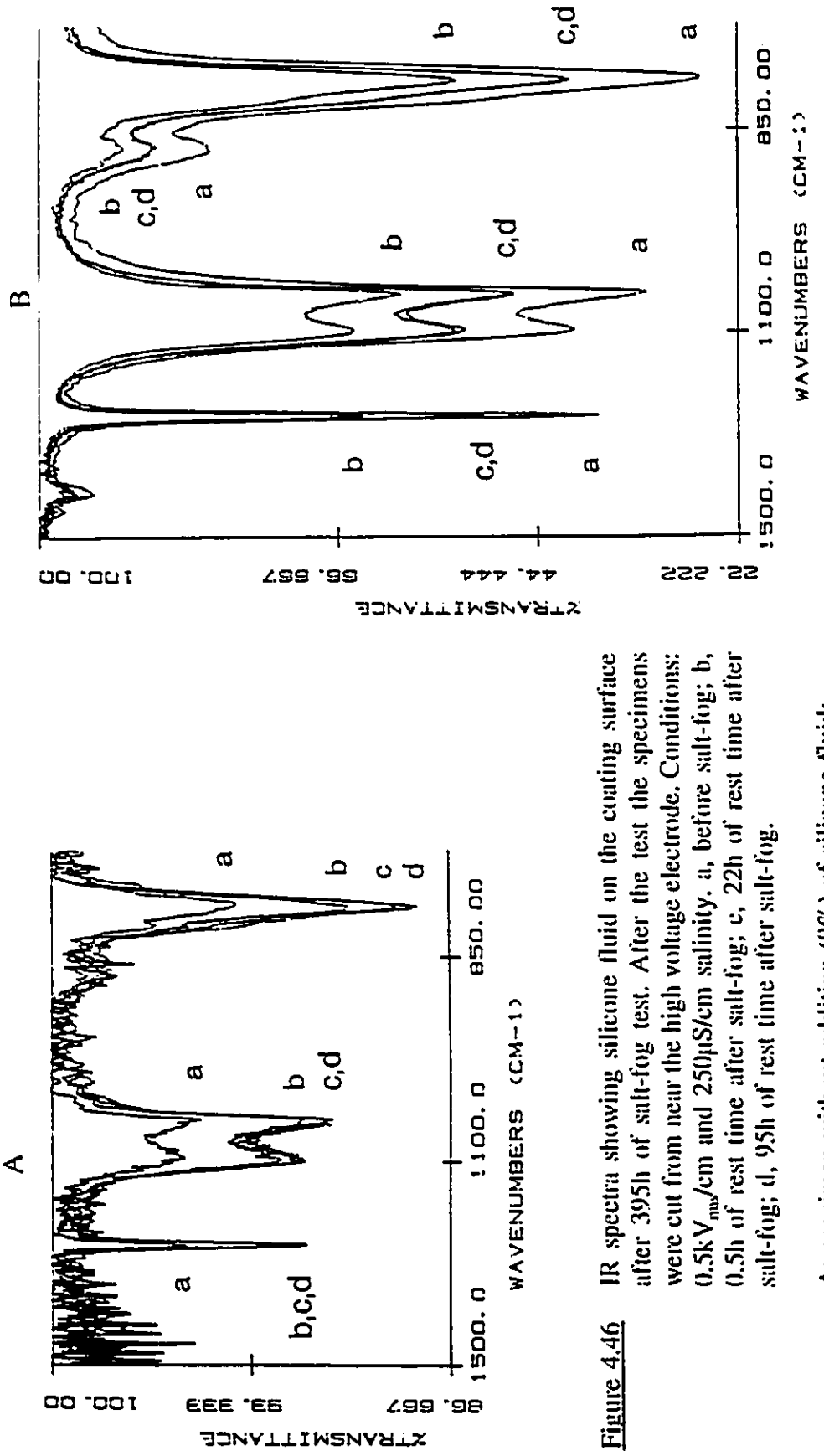

Figure 4.46 IR spectra showing silicone fluid on the coating surface after 395h of salt-fog test. After the test the specimens were cut from near the high voltage electrode. Conditions: 0.5kV$_{rms}$/cm and 250μS/cm salinity. a, before salt-fog; b, 0.5h of rest time after salt-fog; c, 22h of rest time after salt-fog; d, 95h of rest time after salt-fog.

A: specimen without addition (0%) of silicone fluid;
B: specimen with addition of 10% silicone fluid.

4.4.5. Examination of Surface Roughness

Surface roughness was determined using a high resolution detector coupled with SEM microscope. Measurements of the surface roughness of virgin RTV specimens showed that the average roughness (2.51±0.38μm) and the maximum roughness (22.88±3.21μm) were almost identical for the specimens without and with additions of silicone fluid. This clearly shows that the addition of silicone fluid to the RTV formulation did not affect the surface roughness of RTV coating before subjecting the specimens to energized salt-fog.

The roughness of the coatings without and with 10% addition of silicone fluid was examined after 395h of salt-fog test in a low salinity of 250 μS/cm. The roughness of the coating with added 10% silicone fluid increased significantly in the top area of the rod near the high voltage electrode, where extensive dry band arcing occurred. The value of the average roughness increased from 2.51±0.0.38 μm before the salt-fog test to 5.09±0.41 μm after the test. Some spotty damage were visible at the top area(Fig.4.48). The maximum roughness in the spots area was measured to be in the range 62.7 - 135.6μm. The roughness of the coating without added silicone fluid changed little and essentially remained the same as for virgin specimen during 395h of salt-fog test. This resulted from the more intense dry band arcing on the surface with the added 10% silicone fluid which caused the observed damage.

Figs.4.47 and 4.48 show SEM micrographs of RTV specimens without (0%) and with added 10% silicone fluid after 395h of salt-fog test. It will be observed that much larger roughness is present on the specimens with 10% silicone fluid, in general agreement with the roughness measurements.

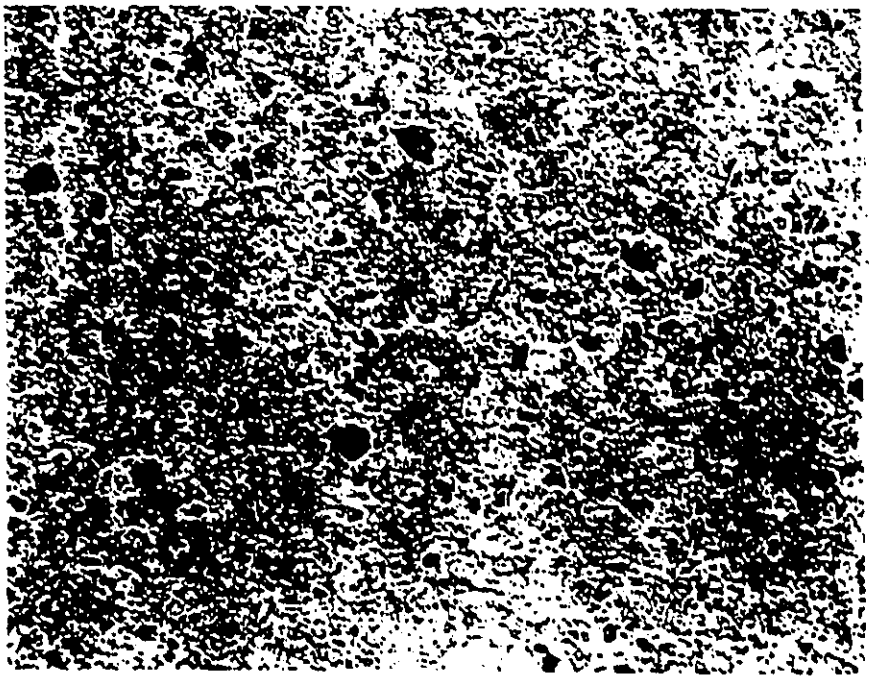

—— 80μm

Figure 4.47 SEM microphotograph of RTV coating without silicone fluid in the top area near the high voltage electrode. Magnification, 125; 0.5kV$_{rms}$; 250μS/cm; ATH filler level, 90pph, size of ATH particle, 13μm; 395 h of salt-fog testing.

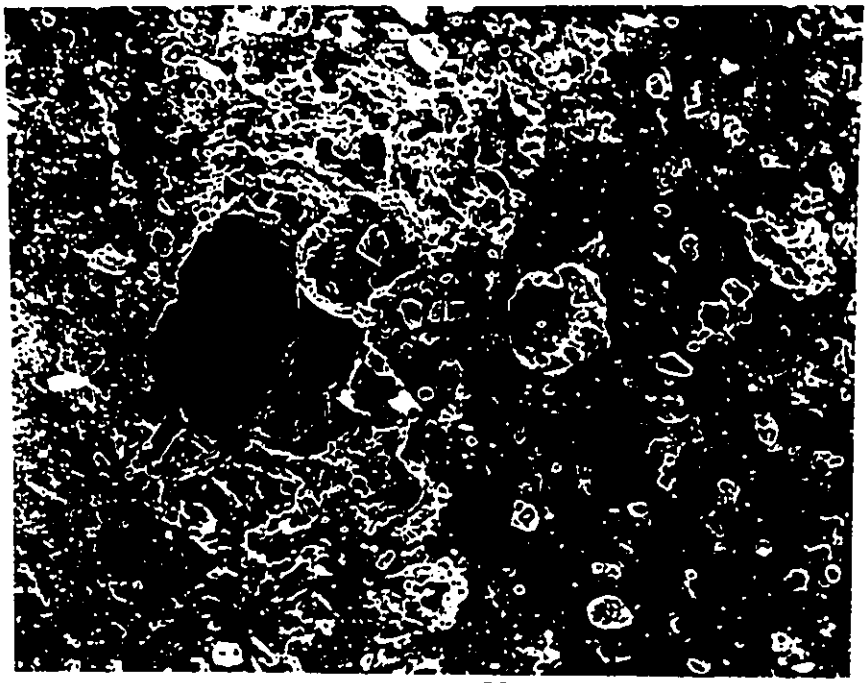

—— 80μm

Figure 4.48 SEM micrograph of RTV coating with 10% silicone fluid in the top area near the high voltage electrode. Other conditions are as in Fig.4.47.

4.5 RTV PERFORMANCE WITH SUBSTRATE TYPE

It might be noteworthy to mention here that this study was not intended to evaluate specific substrate materials as possible insulators, but to show the influence of substrate materials on the ultimate performance of the RTV coating.

4.5.1. Experimental Conditions

The RTV was formulated in a carrier solvent of 1,1,1 trichloroethane. Three types of substrate materials were used in the present work. They were FRP (epoxy resin), FRP (polyester resin) and glass (7740 Borosilicate). The graphite electrodes were attached to the FRP rods using stainless steel screws and to the glass tubes using a thin smear of silicone sealant. The glass tubings were also partially filled with silicone gum to prevent moisture ingress to the inside walls. The RTV coating was contained with 90pph level of ATH having 13μm median size of particles. The thickness of the coating on the three substrates was kept constant (0.37±0.05mm). Salt-fog was produced from having conductivity of 1000±3% μS/cm.

4.5.2. Surface Roughness Before Salt-fog Test

Surface roughness was determined on the three substrates with and without RTV coating. Typical variations of the roughness of the surface before and after coating as a function of distance within 8mm on the specimens are shown in Figs.4.49 and 4.50, respectively. It will be seen from Fig.4.49 that the substrate of epoxy FRP had a higher surface roughness than polyester FRP and glass. The average values of the roughness were 3.62±0.71μm, 0.23±0.035μm and 0.05±0.0μm, respectively, for uncoated epoxy FRP, polyester FRP and glass substrates. The maximum roughness values were 28.53±4.79μm,

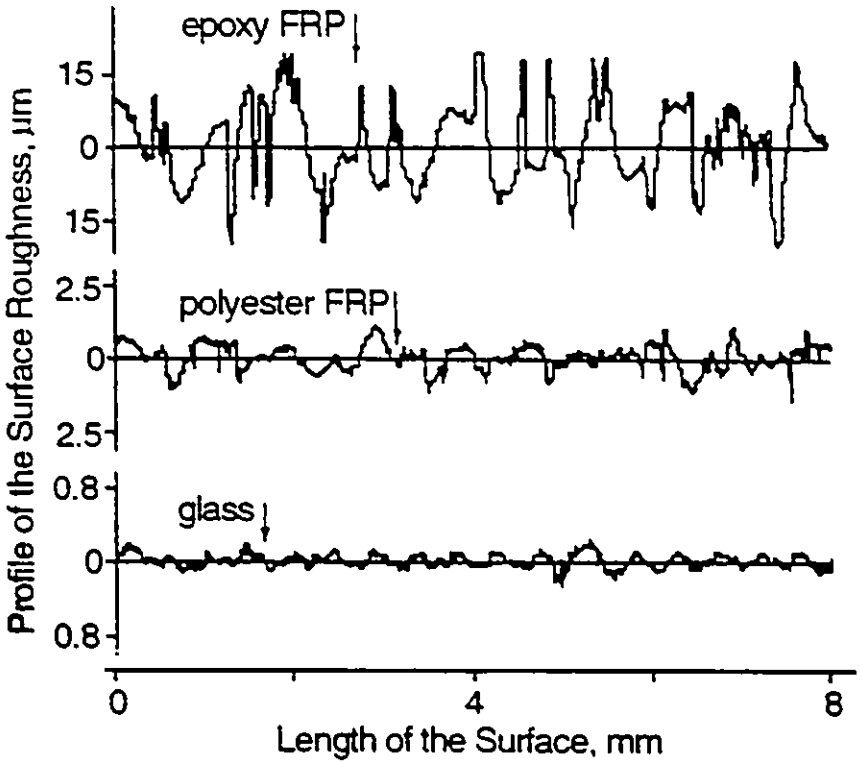

Figure 4.49 Typical variation of the roughness as a function of distance within a region of 8mm length on surfaces of epoxy FRP, polyester FRP and glass before coating with RTV.

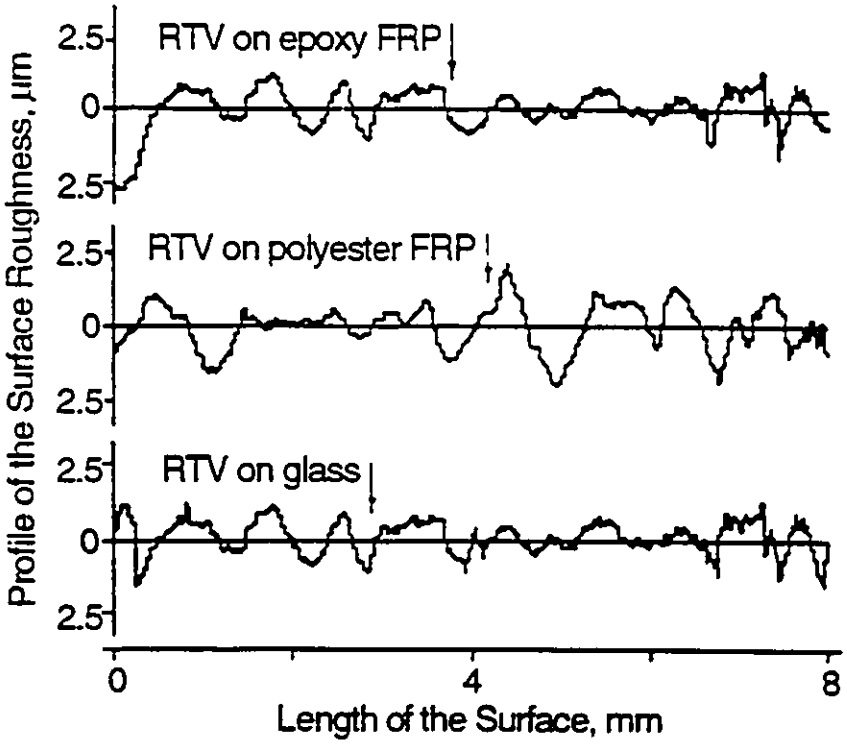

Figure 4.50 Typical variation of the roughness as a function of distance within a region of 8mm length on the surface of epoxy FRP, polyester FRP and glass after coating with RTV and before test in the salt-fog test. Thickness of coating, 0.37±0.05mm.

2.81±0.41μm and 0.33±0.07μm, respectively, for uncoated epoxy FRP, polyester FRP and glass substrates. After the substrates were coated with RTV silicone rubber having a fixed size of ATH particles (13μm) and a fixed thickness (0.37±0.05mm), the surface showed a close roughness variation for the three substrates. The average and maximum values of the roughness were in the ranges of 0.44±0.11μm and 4.19±0.54μm, respectively, for all three coated substrates.

4.5.3. Dependence of Leakage Current and Time to Failure on Substrate Type

Fig.4.51 shows the average leakage current as a function of test time for coated substrates on epoxy FRP, polyester FRP and glass. It will be observed that, at the start of the test and up to 70h, almost an identical leakage current was developed for the three substrates. This was believed that the RTV coatings on the three substrates had a similar water repellency on the surface and a similar surface roughness, due to the same formulation of RTV, at the start of the salt-fog test. As the test continued and when dry band arcing occurred, the coatings transferred the heat from the dry band arcing to the substrate equally for epoxy FRP, polyester FRP and glass due to the same coating thickness. This resulted in a similar damage on the surface and led to a similar leakage current development for the three substrates, at the initial stage of the test as shown in Fig.4.51.

After 70h of test in salt-fog, the leakage current increased rapidly on epoxy FRP. This is because in the latter substrate the coating had more erosion and thus the substrate began to be partially exposed to salt-fog resulting in more intense discharge current developing on the hydrophillic epoxy FRP. The higher leakage current flowing on the exposed epoxy FRP (Fig.4.51) quickly eroded the RTV coating in the vicinity of the

exposed area and this resulted in a rapid failure by tracking on the substrate in a short time. The exposed polyester FRP and glass substrates had a lower leakage current and a higher resistance to erosion and tracking and therefore yielded a longer lifetime. The time to failure in salt-fog for the coatings on epoxy FRP, polyester FRP and glass are given in Table 4.2.

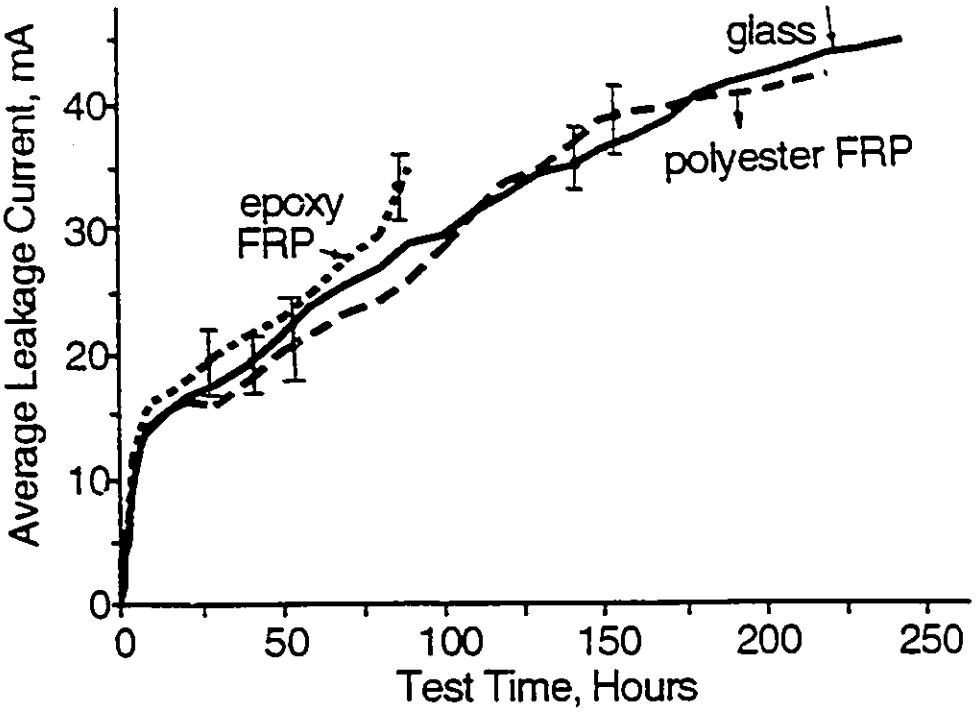

Figure 4.51 Average leakage current of RTV specimens as a function of test time in salt-fog for different coated substrates. Conditions: conductivity of saline water. 1000μS/cm: electric stress. 0.5kV$_{rms}$/cm: saline water flow. 1.6l/min: compressed air pressure. 0.54MPa: thickness of RTV coating. 0.37±0.05mm. Three specimens were used for each thickness.

Table 4.2 Time to failure of RTV coatings on different substrates. Conditions are as in Fig.4.51. 3 rods were used for each case.

Substrates	Epoxy FRP	Polyester FRP	Glass
Coating Thickness, mm	0.38 ± 0.05	0.36 ± 0.04	0.39 ± 0.03
Time to Failure, hours	90 ± 39	220 ± 36	244 ± 22

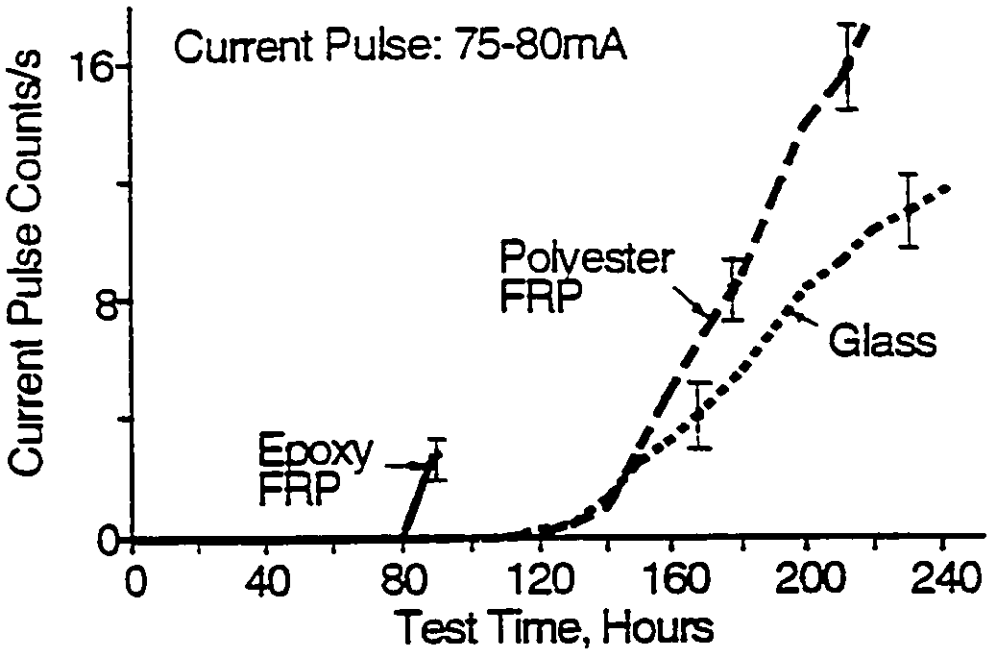

Figure 4.52 Dependence of current pulse count rates in the range of 75-80mA on test time in salt-fog for different coated substrates. Conditions are as in Fig.4.51.

Similar conclusions were derived from measuring the number of current pulses in salt-fog for the coated substrates. Fig.4.52 shows typical current pulse rates in the range of 75-80mA as a function of test time in salt-fog for the three coated substrates. It will be seen that the coatings on epoxy FRP, polyester FRP and glass initially did not show current pulse count in the range 75-80mA up to 80h into the test and just before the onset of failure of the coating on epoxy FRP. Thereafter the epoxy FRP had a higher number of current pulses than polyester FRP and glass due to its higher discharge current on the substrate which was partially and more readily exposed by the action of the dry band arcing.

4.5.4. Dependence of Leakage Current and Time to Failure on Uncoated Substrates

In order to simulate the conditions for development of the discharge current during the period before the failure of RTV coating but after it had undergone sufficient erosion and partially exposed the substrate to salt-fog, uncoated epoxy FRP, polyester FRP and glass specimen rods were also tested in energized salt-fog. Three specimen rods of each substrate type having 16mm in diameter and 152mm in length were used. Graphite disks electrodes of the same size discussed in Section 4.5.1 were affixed to the uncoated rods. Fig.4.53 shows the average leakage current as a function of test time in salt-fog for the three substrates. It will be seen that epoxy FRP had a larger leakage current right from the start of the test and reached 16.5mA after 10 min. The leakage currents on polyester FRP and glass developed slowly and were in the range of 4.7-6.8mA after 10 min of test. This was due to the larger inherent roughness on the surface of the epoxy FRP rod (Fig.4.49) which enhanced the localized field and resulted in a higher leakage current until failure occurred.

Fig.4.53 also shows that the uncoated epoxy FRP and polyester FRP rods developed a larger leakage current with increasing test time in salt-fog and yielded a shorter lifetime than glass. This was because the inorganic specimens of epoxy FRP and polyester FRP had a low thermal stability and were readily damaged by the intense heat generated on the surface by the dry band arcing. The Pyrex glass can withstand substantial heat without serious damage due to its high melting temperature of 1252°C[79] and larger thermal capacity of 837.4 J/Kg °C[80]. These desired properties rendered a lower leakage current and a longer time to failure as shown in Table 4.3. The glass was energized in salt-fog for 350h without failure as shown in Fig.4.53 and Table 4.3. It is noted from Figs.4.51 and 4.53 and Tables 4.2 and 4.3 that the coated glass had a worse performance than the uncoated glass. This is due to a larger leakage current development leading to a shorter lifetime of the coating on glass. This was because the glass without RTV maintained its smooth surface (Fig.4.49) due to, and as mentioned already, its superior thermal properties and therefore accumulated little salt contamination on the rods which were vertically placed in the salt-fog chamber. The absence of adhered contamination further reduced the development of the discharge current. On the other hand the RTV coating on glass was damaged by the heat from dry band discharges, the surface became rougher thus resulting in enhanced localized electric field and a larger leakage current. This ensued a further damage to the surface. The coating eventually failed when the discharge current pulses exceeded 150mA. In outdoor insulation the glass and porcelain insulators accumulate dust and salt contaminants on their skirts which may not be washed away. Under severe conditions of contamination and wetness, flashover may occur after the development of a large leakage current.

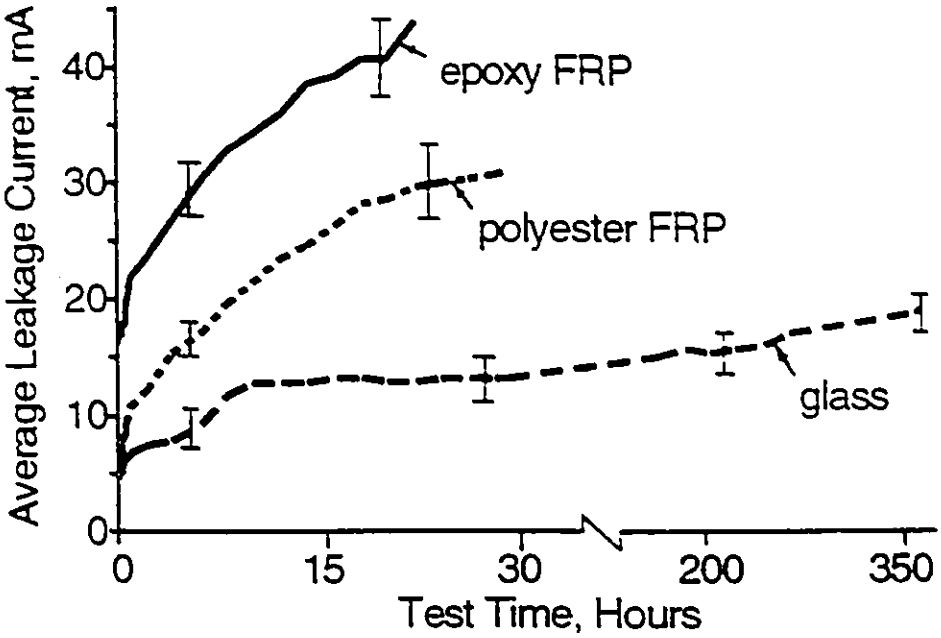

Figure 4.53 Average leakage current as a function of test time in salt-fog on uncoated rods of epoxy FRP, polyester FRP and glass. Conditions: conductivity of saline water, 1000μS/cm; electric stress, 0.5kV$_{rms}$/cm. Rod dimensions are given in Table 4.3.

Table 4.3 Time to failure on uncoated cylindrical rods in energized salt-fog. Conditions: 1000μS/cm and 0.5kV$_{rms}$/cm electric stress. Diameter of rods 16mm, length 152mm. Diameter of graphite electrodes 31.7mm.

Materials	Time to Failure, hours
Epoxy FRP	**22 ± 9**
Polyester FRP	**29 ± 9**
Glass	**> 350**

4.6 RTV PERFORMANCE WITH DIFFERENT SOLVENTS

4.6.1. Experimental Conditions

The RTV is dispersed in a carrier solvent for coating on porcelain and glass insulators. The solvent evaporates from the coating during and subsequent to its vulcanization in the presence of moisture. Solvents such as naphtha and 1,1,1 trichloroethane are used. Naphtha is a flammable material and coating systems dispersed in this solvent can not be applied to insulators while energized[10]. 1,1,1 trichloroethane solvent is non-flammable and coating systems which are dispersed in this solvent may be applied to insulators while energized [10]. In the present study RTV specimens were formulated using both of these solvents in order to determine their effects on the electrical performance. About 90pph concentration of ATH filler was used with both solvents. The median size of the particles of the ATH filler was 13μm. Polyester FRP rods were dipped twice (one dip from each end) in the RTV liquids. Because of the different viscosity of the two coating systems the thicknesses of the coatings were 0.79±0.10mm and 0.50±0.06mm, respectively, for naphtha and 1,1,1 trichloroethane as shown in Table 4.4. The coating using naphtha was dull and rough while the coating using 1,1,1 trichloroethane was bright and smooth. Both coating systems were allowed to vulcanize and the solvents evaporated to reach a steady state by leaving the coated rods in air for about 3 months before being tested in the salt-fog chamber. Salt-fog was produced from having conductivity of 1000±3% μS/cm.

4.6.2. Dependence of Leakage Current and Time to Failure on Solvents

Measurement of the surface roughness showed that the average and the maximum roughnesses were 2.23±0.21μm and 15.32±1.95μm, respectively for naphtha. For 1,1,1 trichloroethane the average and the maximum roughnesses were 0.24±0.06μm and 3.86±0.35μm, respectively. Typical profiles of the roughness of the surface as a function of distance within 8mm on the virgin coating using both solvents are shown in Fig.4.54. Measurement of contact angle on the surface of the virgin specimens showed that the contact angle was in the range of 101±0.5° on the coatings with both solvents. This indicated that the initial water repellency was identical on both coating surfaces using either naphtha or 1,1,1 trichloroethane solvents.

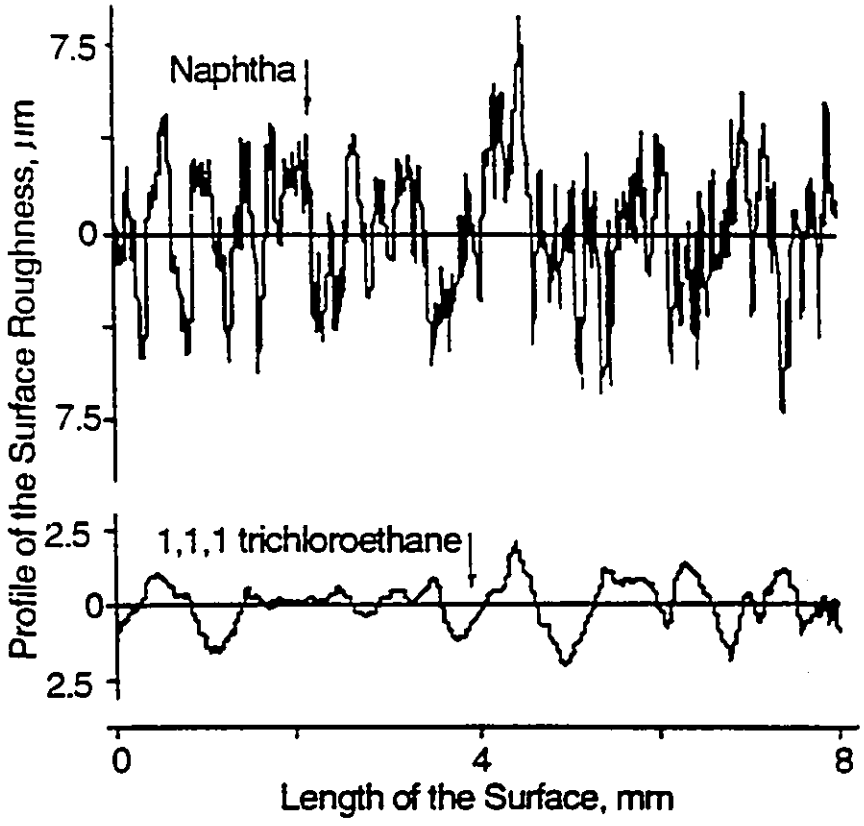

Figure 4.54 Typical variation of the roughness within a distance of 8mm on a surface of virgin RTV coatings with different solvents. Conditions: thickness of coating for naphtha, 0.79mm and for 1,1,1 trichloroethane, 0.5mm.

Fig.4.55 shows the average leakage current as a function of test time in salt-fog in the RTV coating with different solvents. It will be seen that from the start of the test and up to about 7h the coating using naphtha had a slightly larger leakage current than the coating with 1,1,1 trichloroethane. This was due to the rougher surface of the coating with naphtha. As the test continued (>7h) a higher leakage current was observed in the coating using 1,1,1 trichloroethane. This suggests that the latter coating has a lower resistance to degradation by the heat from dry band discharges resulting in a decrease of water repellency on the surface and an increase of surface roughness and therefore an increase in the leakage current. Figs.4.56 and 4.57 show the current pulse count rates in the ranges of 50-55mA and 75-80mA, respectively, for the two solvents. It can be seen that in the coating with 1,1,1 trichloroethane the dry band discharges were initiated earlier and had a larger number of current pulses than the coating with naphtha. This led to a larger erosion of RTV on the coating and a shorter time to failure by tracking on the polyester FRP substrate. The time to failure for both coatings is given in Table 4.4, where it was found to be much shorter with 1,1,1 trichloroethane.

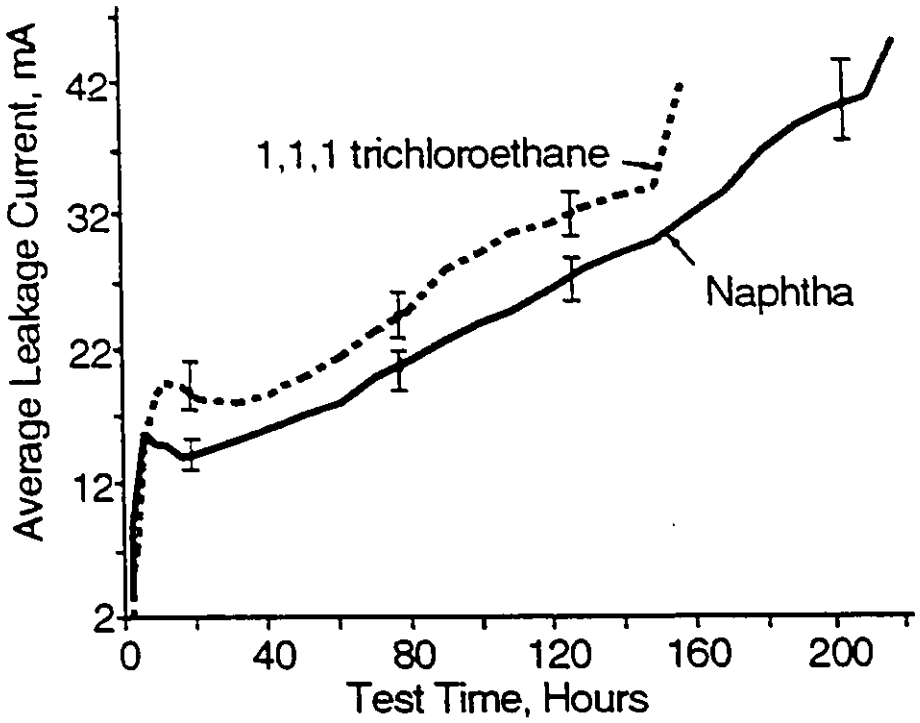

Figure 4.55 Average leakage current as a function of test time in salt-fog in the specimens of RTV coating with different solvents. Conditions: conductivity of saline water, 1000μS/cm; electric stress, 0.5kV$_{rms}$/cm; saline water flow, 1.6 l/min; compressed air pressure, 0.54MPa. Formulation of the RTV specimens are as in Fig.4.54.

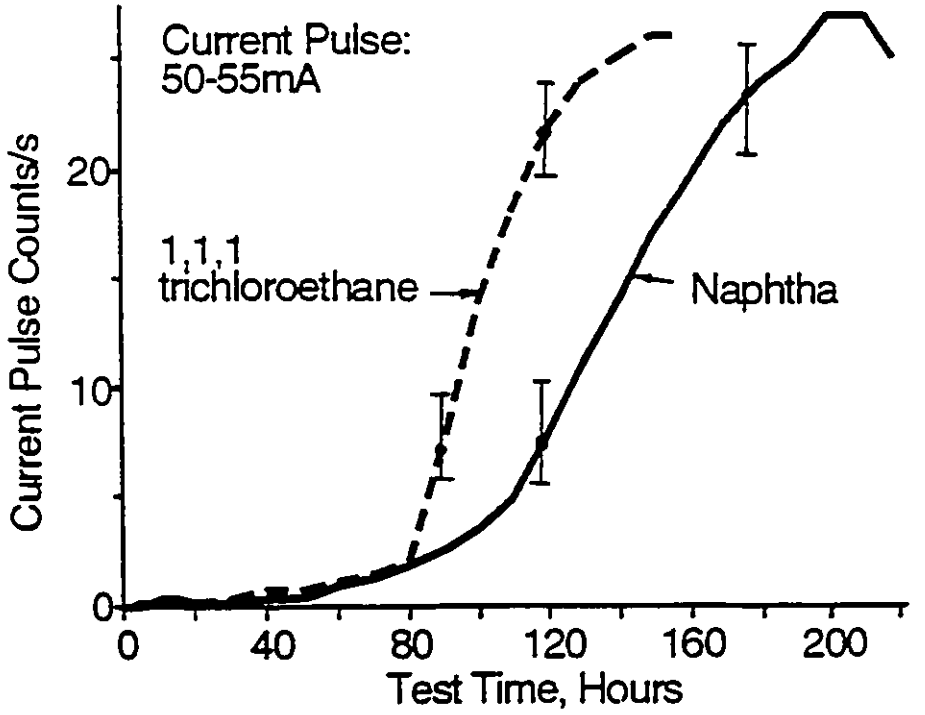

Figure 4.56 Dependence of current pulse count rates in the range of 50-55mA on test time in salt-fog for RTV coated rods containing different solvents. Conditions are as in Fig.4.55.

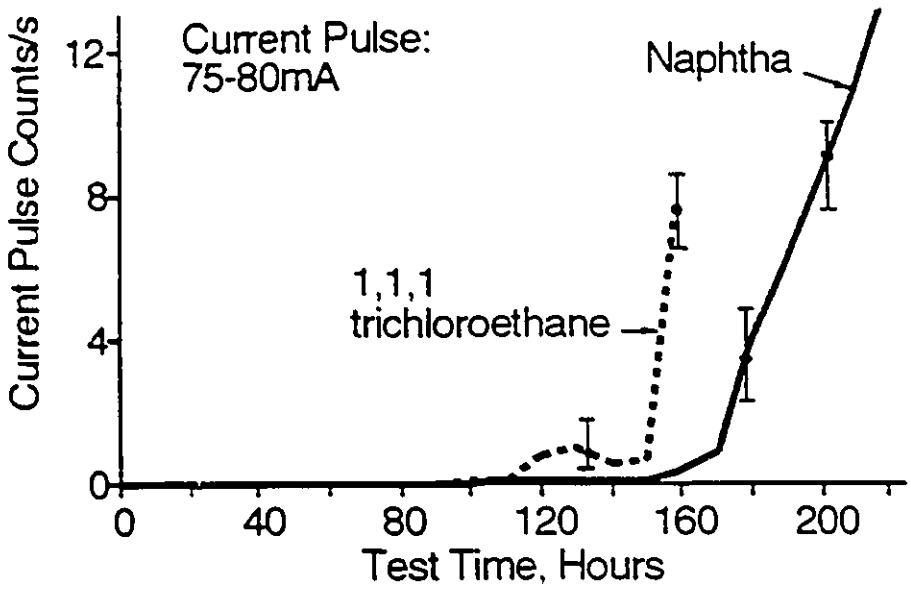

Figure 4.57 Dependence of current pulse count rates in the range of 75-80mA on test time in salt-fog for RTV coated rods containing different solvents. Conditions are as in Fig.4.55.

Table 4.4 Time to failure of RTV coating with different solvents. Conditions are as in Fig.4.55. 3 specimens were used in each case.

Solvents in RTV Liquid	Naphtha	1,1,1 trichloroethane
Coating Thickness, mm	0.79 ± 0.10	0.50 ± 0.06
Time to Failure, hours	218 ± 10	158 ± 20

CHAPTER V

SILICONE FLUID CONTENT AND ITS DIFFUSION IN RTV COATINGS

5.1 INTRODUCTION

The RTV coating provides water repellency which suppresses the development of leakage current. The hydrophobic surface is maintained even after a layer of contamination has built up on the surface. This has been attributed to the diffusion of the low molecular weight (LMW) silicone fluid from the bulk to the surface of the RTV and then on to the surface of the polluted deposits[35,46,47,49]. Therefore the presence of sufficient quantity of LMW silicone fluid in the bulk of RTV coating and its ability to diffuse to the surface are of paramount interest to maintain the hydrophobic surface of the coating and thus to the life of the coating.

This chapter attempts to explore the role of the silicone fluid in the lifetime of RTV coating. Alumina trihydrate (ATH) filled RTV coatings with various formulations were used. The content of LMW silicone fluid and its diffusion from the bulk to the surface were determined in the coatings with various sizes of ATH particles from 1.0 to 75μm, various coating thicknesses from 0.17 to 0.99mm and different carrier solvents by using extraction techniques in analytical hexane. The role of the LMW content and diffusion in the lifetime was evaluated for different formulations of RTV coatings.

5.2 EXPERIMENTAL TECHNIQUES

The polydimethyl siloxane (PDMS) chains in RTV silicone rubber generally have molecular weights in the range 10^4-10^5, of which those less than 25000 are free-flowing liquids [81]. The LMW silicone fluid can be extracted in hexane[48,76,82]. Fig.5.1 shows the percentage of LMW silicone fluid extracted from RTV specimens by weight as a function of immersion time in hexane at 40°C. The difference in weight of the RTV specimen before and after being immersed in analytical hexane is the amount of silicone fluid extracted from the specimens. The weight loss of the RTV specimen was measured using a high precision balance(0.01mg). The room temperature was 24±1°C and the relative humidity was (47±2)% during the measurements. The thickness of the specimen was 0.99mm. It was found from Fig.5.1 that the weight percentage of LMW fluid extracted by hexane increased rapidly with increasing immersion time up to about 90 hours and reached saturation thereafter. Extension of immersion time beyond 90h(in Fig.5.1) to 165h in fresh hexane failed to show additional fluid from the RTV specimen. This confirms that about 90h of immersion in hexane at 40°C is sufficient to remove all of the mobile LMW silicone fluid from the specimen having thickness of 0.99mm. Immersion at 40°C for 96h was used in the present work in determining the total content of LMW fluid in RTV specimens with different coating thicknesses from 0.17 to 0.99mm. After removal from hexane the RTV specimen was left in air at an ambient temperature of 24±1°C in order to remove all the hexane which had been absorbed in the specimen during the immersion phase.

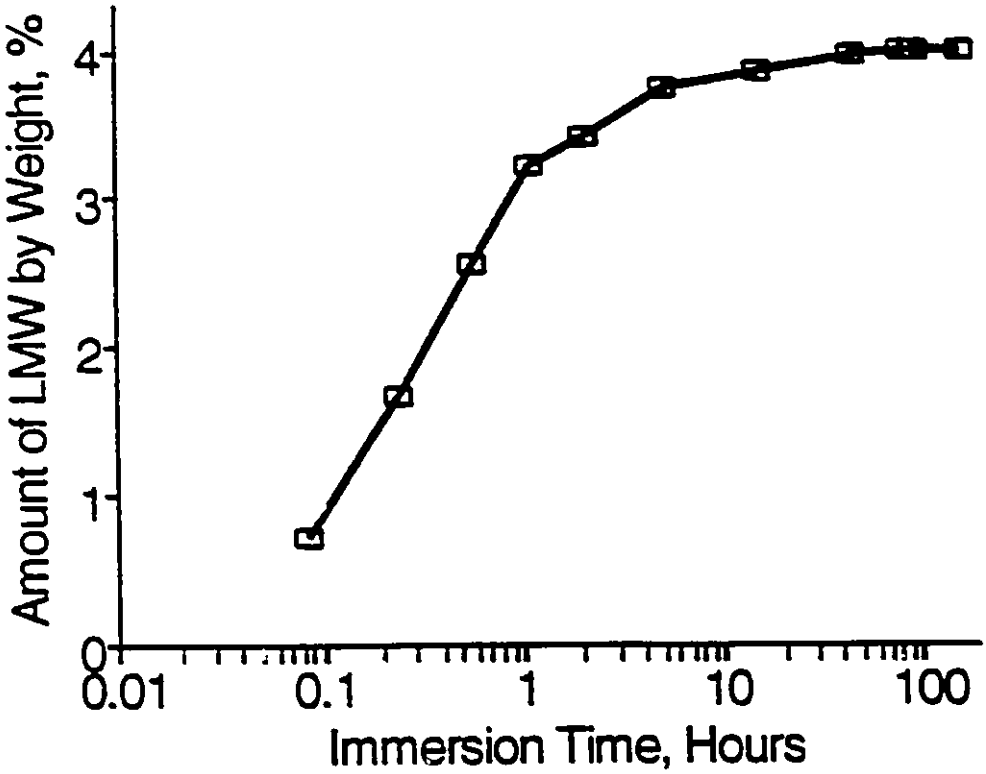

Figure 5.1 Percentage of LMW silicone fluid extracted from RTV specimen by weight as a function of immersion time in analytical hexane at 40°C. Virgin specimen which was not subjected to electrical stress in salt-fog were used. The thickness of the specimen was 0.99mm.

Fig.5.2 shows the weight loss due to the removal of hexane from the specimen as a function of rest time in air at 25°C. The thickness of the specimen was 0.99mm. It can be seen from Fig.5.2 that the hexane was completely removed from the specimen by evaporation after about 1.5h of rest in air at 25°C. About 12h of rest time was used to remove the hexane from the RTV specimens with different thicknesses from 0.17 to 0.99mm.

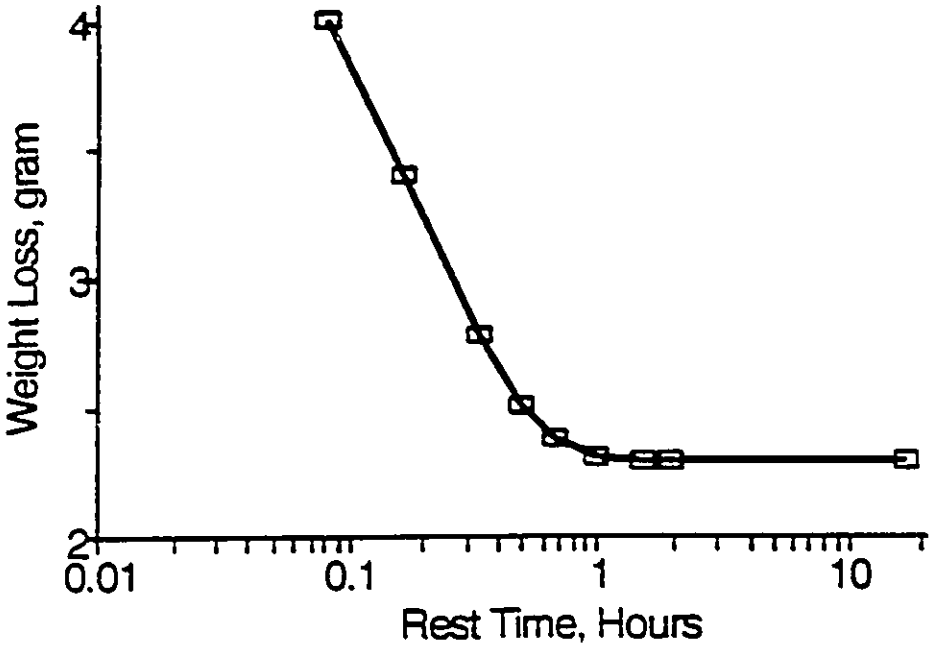

Figure 5.2 Weight loss due to evaporation of hexane from RTV specimen as a function of rest time in air at 25°C. Specimen thickness, 0.99mm; specimen weight after immersion in hexane, 2.30±0.30g.

To determine the rate of the diffusion of LMW silicone fluid from the bulk to the surface, the RTV specimens were first immersed in hexane for 1 min at 25° to remove the silicone fluid from the top surface. After removal of the specimens from hexane it was left in air for 24h at 25° to allow the LMW silicone fluid to diffuse from the bulk to the top surface to replenish the earlier loss during the 1 min immersion in hexane. The RTV specimen was then immersed in hexane again for one minute at 25°. The weight loss after the second immersion was the amount of silicone fluid diffused from the bulk during the proceeding 24h. The larger the amount of loss of silicone fluid during the fixed duration of immersion(1 min) the higher was the rate of the diffusion. The specimen was left in air at 25° for 24h before the next immersion. This procedure was repeated 10 times after the second immersion to determine the rate of diffusion for different thicknesses of RTV coatings.

5.3 LMW CONTENT AND DIFFUSION WITH COATING THICKNESS

The RTV specimen was formulated with a median size of 5.5μm of ATH particles, a filler level of 90pph and in a carrier solvent of naphtha. Five coating thicknesses from 0.17 to 0.99mm were used. RTV silicone rubber was coated on porcelain rods, 155mm length and 20mm in diameter. A saline water flow rate of 1.6±0.2 l/min and an air pressure of 0.54±0.02MPa(79±3psi) were used to generate the fog. The conductivity of the saline water (nominal) was 250 μS/cm ±5%.

5.3.1. LMW Content of RTV

Fig.5.3 shows the percentage of the total content of LMW silicone fluid by weight as a function of coating thickness of RTV specimens before and after the salt-fog test. The specimens for curve A (Fig.5.3) were cut from virgin coatings. The specimens for curves B and C (Fig.5.3) were cut from the area near the bottom electrode and the area near the high voltage electrode, respectively, after 570h of salt-fog test. It is observed from Fig.5.3 that the LMW content by weight in the virgin specimens (curve A) was not a constant percentage for all coating thicknesses. The LMW content by weight in the virgin RTV decreased from (4.49±0.04)% for the thickness of 0.17mm to (4.0±0.02)% for 0.99mm. Fig.5.3 also shows that the percentage of LMW content by weight decreased after 570h of salt-fog and depended on the locations of the specimens. In the region near the high voltage electrode where intense discharges were observed the specimens had a larger percentage decrease of LMW content by weight for all coating thicknesses. This was believed that the heat from the extensive dry band discharges broke and removed more PDMS molecular chains from the surface resulting in the loss of LMW silicone fluid(see Fig.5.4).

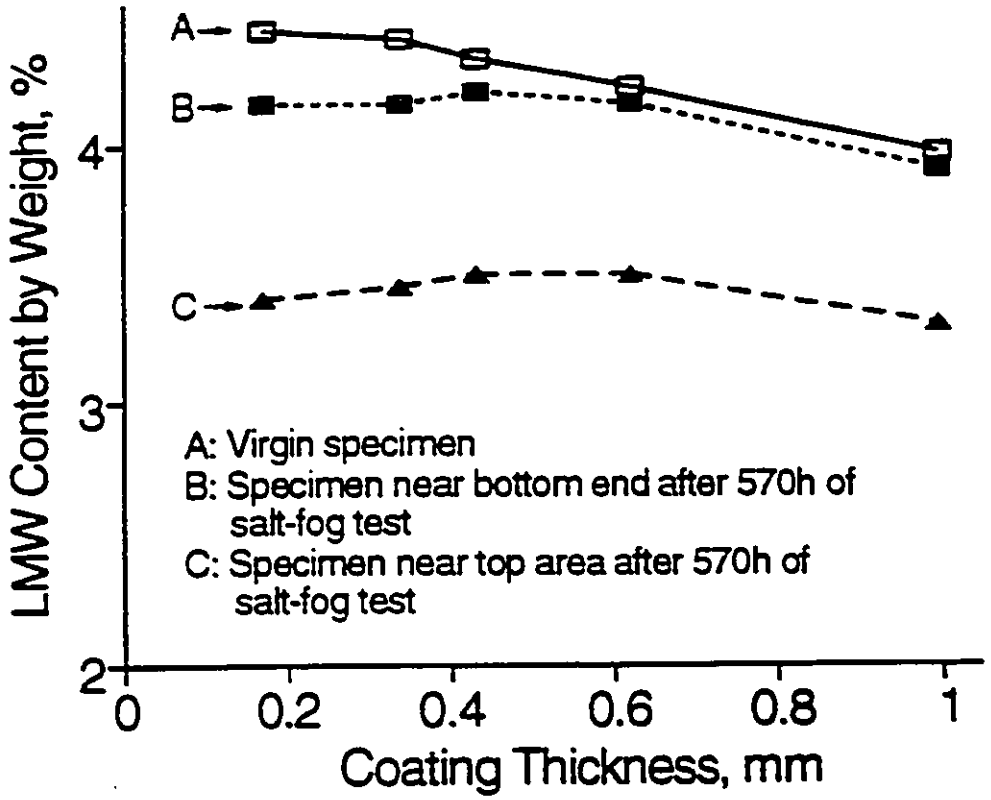

Figure 5.3 Percentage of total content of LMW silicone fluid by weight as a function of coating thickness before and after(remaining content) salt-fog test. Conditions: conductivity of saline water, 250μS/cm; electric stress, 0.5kV$_{rms}$/cm; saline water flow, 1.6 l/min; compressed air pressure, 0.54MPa; ATH filler level, 90pph; size of ATH particles,5.5μm; substrate, porcelain; solvent, naphtha.

The total content of LMW fluid in the RTV specimens near the high voltage electrode decreased to (3.43±0.07)% by weight for all coating thickness from 0.17 to 0.99mm after 570h of salt-fog test(Fig.5.3, curve C). More extensive discharges indicated by a higher rate and a larger number of current pulses (Figs.4.31 and 4.34) and a rougher surface (Figs.4.35 and 4.36) on a thicker coating did not cause a larger loss of total content of LMW silicone fluid. This was because more extensive discharges broke more long PDMS molecular chains into short chains which replenished the loss of silicone fluid in the thicker coating (see Fig.5.5). Near the bottom electrode, which was at ground potential

and where no discharge activity was visible, the LMW content had decreased only slightly for all coating thicknesses after 570h of salt-fog test(Fig.5.3, curve B). The decrease of LMW content in the specimen near the bottom electrode is thought to be due to the washing of silicone fluid from the surface by the salt-fog.

In order to investigate further the loss of LMW silicone fluid from and the production of silicone fluid in RTV coating by the action of heat produced by dry band arcing, RTV specimens were subjected to heat inside an electric oven at temperatures of 150, 240 and 370°C. The specimens were heated for 3 hours at each temperature. The thickness of the coating was 0.50mm. Fig.5.4 shows the percentage of the total content of silicone fluid by weight before (at 25°C) and after the specimens were subjected to heat. It is clearly shown from Fig.5.4 that the total silicone fluid content decreased after the application of heat. The reduction was more pronounced with increasing temperature. The total percentage of silicone fluid by weight decreased from 5.15% before heat to 4.60% after 150°C, to 4.43% after 240°C and then to 3.43% after 370°C. This is thought that the heat at high temperatures caused scissions of short chain PDMS molecules into volatile substances which evaporated at high temperatures thus resulting in a reduction of the total silicone fluid content. Fig.5.5 shows the production of silicone fluid by percentage of weight in RTV coating in an electric oven at different temperatures. The RTV specimens were first immersed in hexane for 96h at 40°C to remove all the fluid from the specimens. The specimens were left at 25°C in air for a duration of 24h to allow the hexane to completely evaporate and the specimens were weighed. The specimens were then subjected to heat. It is evident from Fig.5.5 that the silicone fluid could be produced by heat.The present work confirms the observation that silicone fluid increased on the surface of RTV specimen after it was exposed to 240°C [83]. Fig.5.5 also shows that the

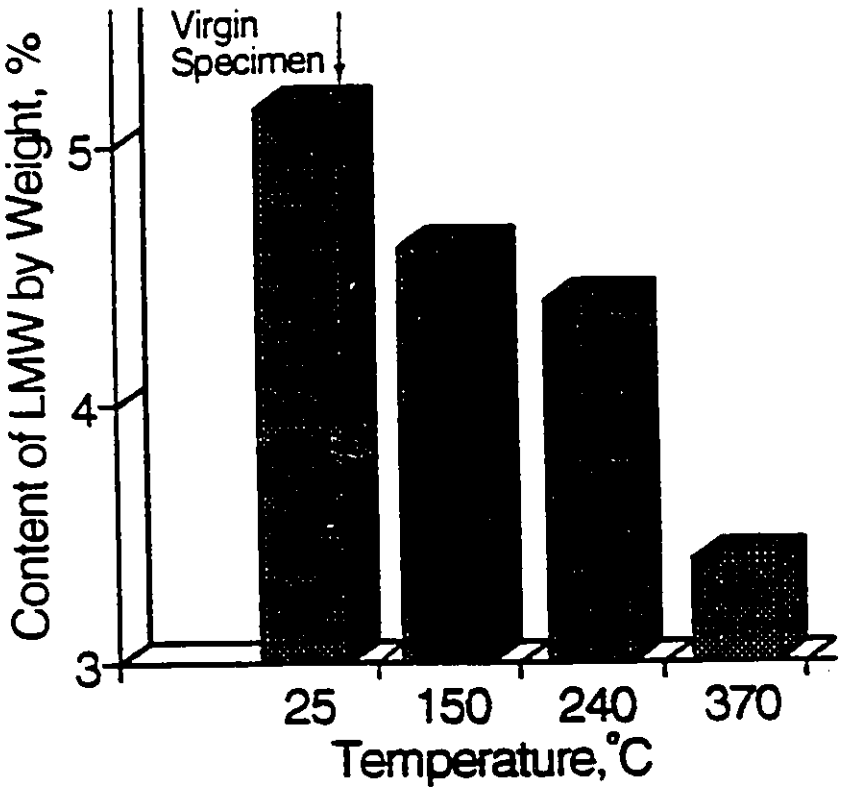

Figure 5.4 Percentage of the total content of silicone fluid by weight from RTV virgin specimens before and after exposure to different temperatures in air in an electric oven(60Hz). The duration of exposure of RTV specimens at each temperature was 3 hours. Virgin specimens were used which were not immersed in hexane before heat treatment.

production of silicone fluid in RTV depended on the temperature. More silicone fluid was produced at higher temperatures for a duration of 3 hours(Fig.5.5). The production of silicone fluid by percentage of weight increased from 0.13% at 150°C to 0.75% at 240°C and then to 5.12% at 370°C. The production of silicone fluid could be due to either the release of short cyclic chains that were trapped in the structure of the polymer and/or the scissions of long PDMS molecular chain into short chains at the high or temperatures.

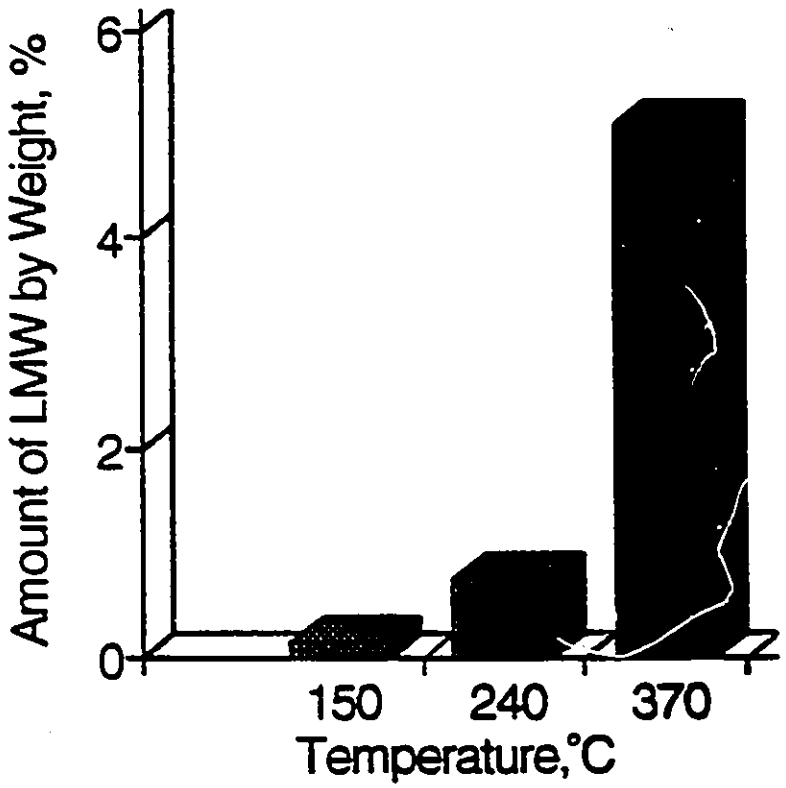

Figure 5.5 Production of LMW silicone fluid by percentage of weight in RTV virgin specimens at different temperatures. The specimens were placed in an electric oven in air for three hours at each temperature. Specimens were initially devoid of LMW silicone fluid which was extracted by immersing in hexane for 96 hours.

5.3.2. Diffusion of LMW in RTV

Fig.5.6 shows the variation of the weight loss of LMW silicone fluid with coating thickness after 1. 2. 3. 5. 7 and 10 immersions for a short duration of 1 minute in hexane and 24h recovery in air between the successive immersions. The weight loss of LMW after 4. 6. 8 and 9 immersions and recovery was found to show a similar behaviour to that depicted in Fig.5.6 and is omitted here for brevity. A larger weight loss means a higher diffusion rate from the bulk to the surface which is then removed during the brief duration of immersion of 1 minute. It can be seen from Fig.5.6 that the weight loss of

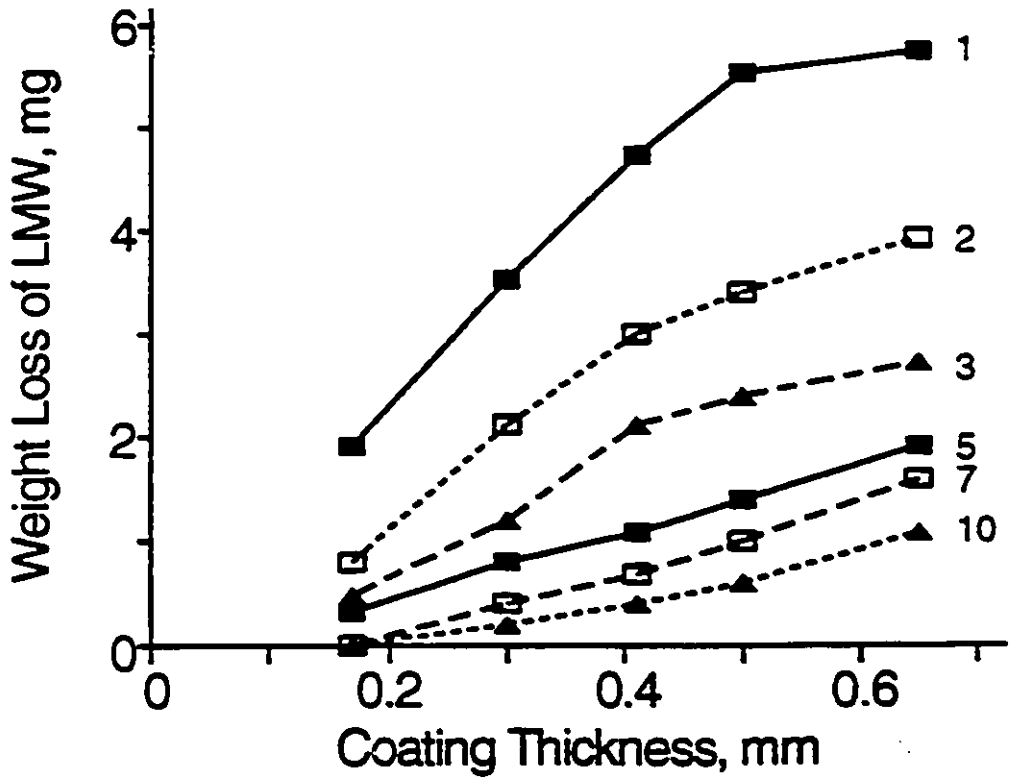

Figure 5.6 Variation of the weight loss of LMW silicone fluid with coating thickness for 10 successive immersions in hexane. Duration of each immersion. 1 min: recovery time between immersion. 24h. Size of specimen. 25x50mm^2. Size of ATH particle. 5.5μm: ATH filler level. 90pph.

LMW depends on the coating thickness. A thicker coating has a larger weight loss for the same cross-sectional area. This suggests that the thicker coating has a higher diffusion rate from the bulk to the surface. This is consistent with the evidence that a higher wetting angle was observed on a thicker silicone rubber plate after being subjected to a constant layer of contamination and after being left in air at 20° for 16 days[84]. Fig.5.6 also shows that after the 10th immersion in hexane the thicker coating of 0.65mm(1015.2mg) can still provide an amount of 1.1mg of LMW silicone fluid to diffuse to the surface. The thinner coating of 0.17mm has depleted completely its LMW content after the seventh

immersion. This indicates that the thicker coating is able to last a longer time to maintain a hydrophobic surface than the thinner coating. On the other hand the thicker coatings develop more intense discharges for the same applied electric stress(Figs.4.31, 4.32 and 4.34) which occur at progressively shorter times into the test(Fig.4.33) and therefore incur larger surface erosion(Figs.4.35 and 4.36) and a slightly larger loss of silicone fluid(Fig.5.3) from the surface which is replenished at a faster rate from the bulk(Fig.5.6). Therefore it is anticipated that an optimum thickness of RTV coating is also likely to be present in the case of porcelain insulators. This is consistent with the previously reported finding of an optimum coating thickness on polyester fibre reinforced plastic (FRP) insulating rods[85].

5.4 LMW CONTENT AND DIFFUSION WITH SIZE OF ATH PARTICLES

The RTV coatings were formulated with a constant level of ATH filler of 90pph and different median sizes of the filler particles in a carrier solvent of 1,1,1 trichloroethane. Five sizes of ATH particles of 1.0, 4.5, 13, 17 and 75μm, were used in the present study. The thickness of the coating with different sizes of ATH particles was in the range of 0.39±0.06mm. Fig.5.7 shows the total content of LMW as a percentage of weight as a function of the size of ATH particles. The bars indicate the variation within each size using 3 specimens. It is observed that the total content of LMW silicone fluid in the RTV coating depends on the size of ATH particles. The coating with 1.0μm has the lowest content of 2.74±0.01% by weight while the coating with 75μm has the highest content of 4.65±0.20% by weight. The content of LMW does not increase linearly with increasing size of ATH particles, as shown in Fig.5.7. The coatings with 4.5 and 13μm particle sizes in Fig.5.7 have a similar content of LMW (4.15±0.13%, Fig.5.7) and

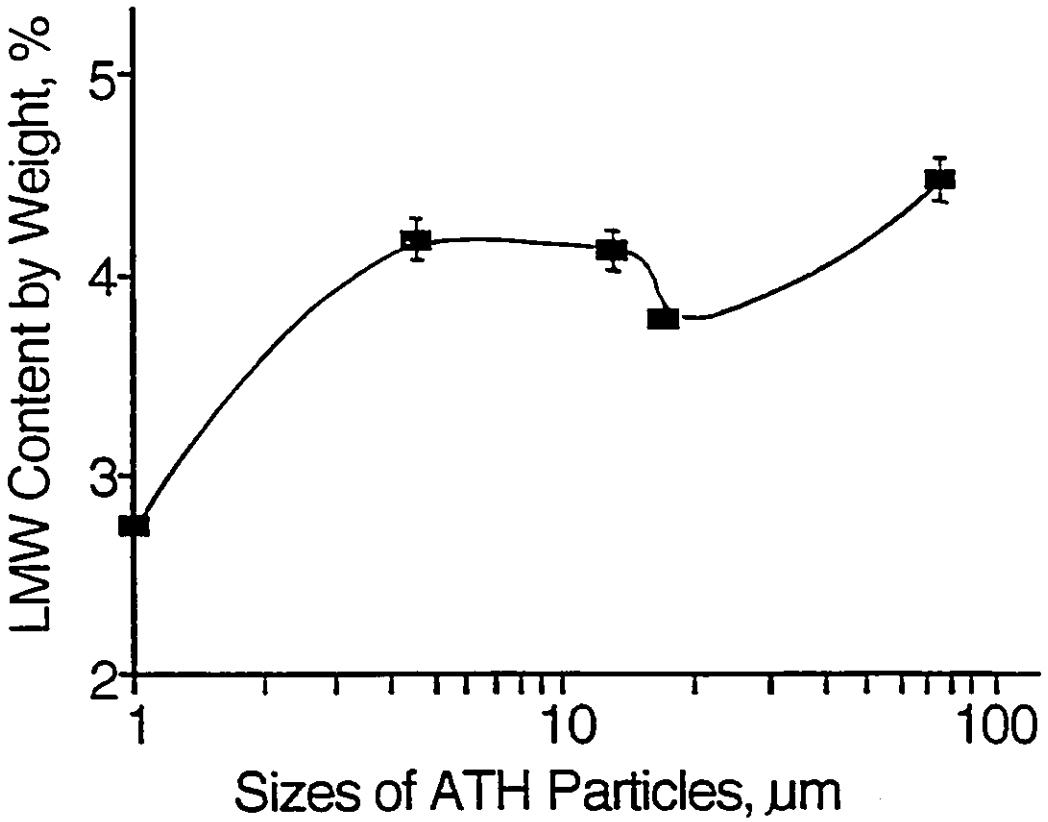

Figure 5.7 Dependence of total content of LMW silicone fluid as a percentage of weight on size of ATH particles in RTV coating. Duration of immersion. 96h: thickness. 0.39mm. Carrier solvent. 1.1.1 trichloroethane: ATH filler level. 90pph.

both coatings have more content of LMW silicone fluid than that of the coating with 17μm(3.80±0.03%. Fig.5.7).

Fig.5.8 shows the variation of the loss of LMW silicone fluid with size of ATH particles after 1. 2. 3. 5 and 10 immersions in hexane. The weight loss of LMW after 4. 6. 7. 8 and 9 immersions was found to have a similar dependence on particle size. It is shown in Fig.5.8 that the weight loss of LMW in the coatings is not strongly dependent on the size of the ATH particle from 1 to 75μm. This is the case after each immersion in hexane. It is suggested that after a prolonged recovery of 24h the diffusion of LMW from the bulk to the surface is independent of the size of ATH particles.

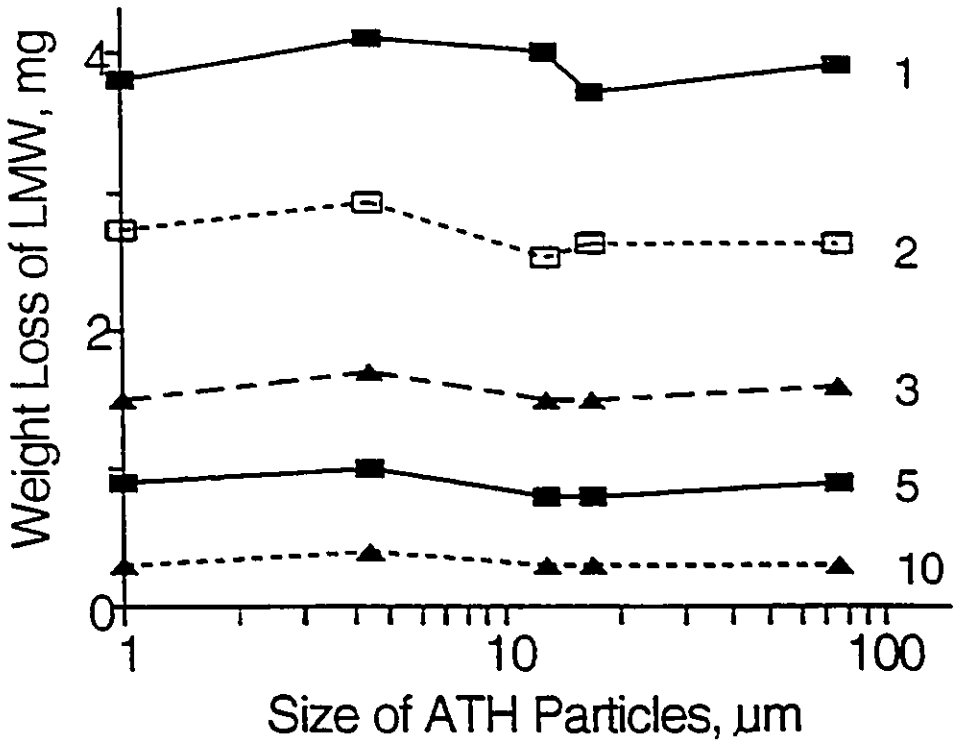

Figure 5.8 Variation of the weight loss of LMW silicone fluid with size of ATH particles in RTV coatings for 10 successive immersions in hexane. Duration of each immersion, 1 min; recovery time between immersion, 24h. Size of specimen, 25x50mm^2. Carrier solvent, 1.1.1 trichloroethane; ATH filler level, 90pph; thickness, 0.39mm.

5.5 LMW CONTENT AND DIFFUSION WITH SOLVENT TYPE

In the study, RTV specimens were formulated using two carrier solvents, 1.1.1 trichloroethane and naphtha. A composition of 90pph ATH filler was used with both solvents. The median size of the particles of ATH filler was 4.5µm in the solvent of 1.1.1 trichloroethane and 5.5µm in naphtha. The thickness of both coatings was in the range 0.43±0.02mm. After treatment in hexane for 96h at 40° it was found that the content of LMW is (4.15±0.13)% by weight in the coating using 1.1.1 trichloroethane and (4.23±0.02)% by weight in the coating using naphtha. Therefore the amount of LMW

silicone fluid in the RTV coating is independent of the carrier solvent. Fig.5.9 shows the variation of the loss of LMW silicone fluid with the number of immersions in hexane for different solvents. It can be seen that the weight loss of LMW silicone fluid for both coatings is similar for all immersions. It is suggested that the speed of diffusion from the bulk to the surface for both solvents is the same because the solvents have evaporated from the specimens.

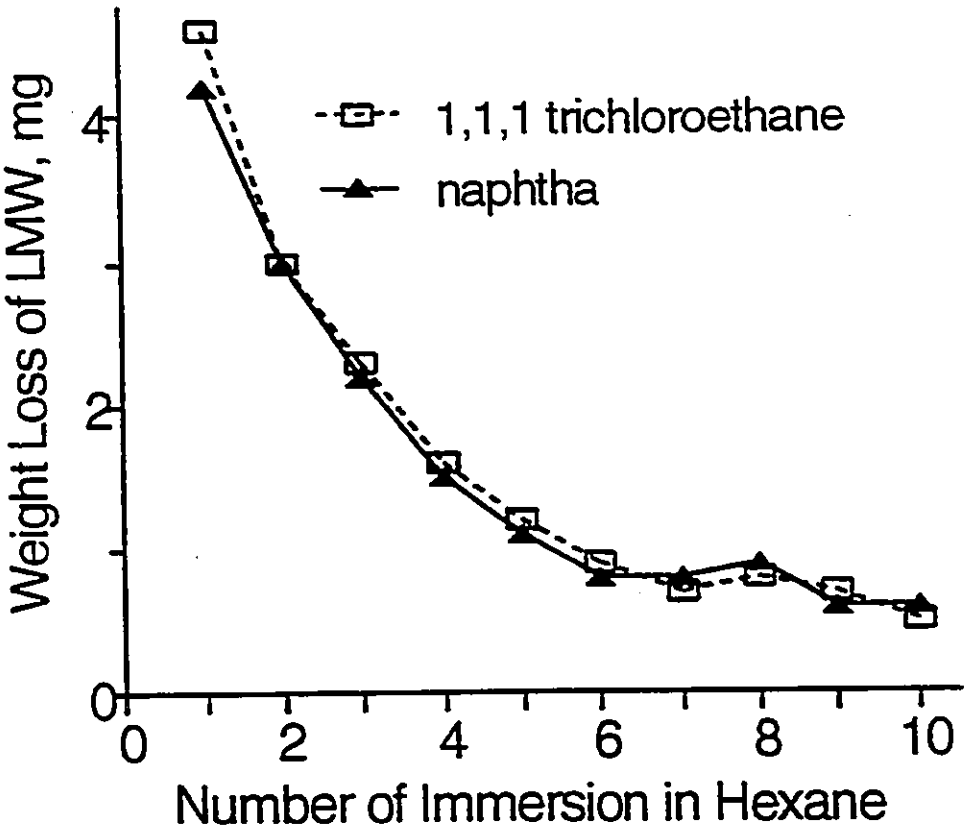

Figure 5.9 Variation of the weight loss of LMW silicone fluid from RTV with different carrier solvents with number of immersions in hexane. Conditions are as in Fig.5.8. Thickness, 0.43mm.

5.6 THE ROLE OF LMW CONTENT AND DIFFUSION IN LIFE OF RTV COATINGS

The RTV coating offers initial hydrophobicity on the surface to help prevent the formation of a continuous water filming. When the coating is polluted by hydrophillic contaminants the LMW silicone fluid diffuses from the bulk to the surface of the RTV and then surmounts the contaminants. This process of diffusion modifies the physical property of the contaminants imparting a hydrophobic quality. Therefore the LMW content and the diffusion are decisive factors in determining the lifetime of the RTV coating. The RTV coating temporally loses its hydrophobicity due to the reorientation of polymer chains in the presence of a heavy and prolonged wetting[86]. Leakage current develops and dry band arcing occurs. At this point the lifetime largely depends on the thermal property of the coating and the surface roughness.

The thicker coating has a higher speed of diffusion of LMW(Fig.5.6) and a larger amount of silicone fluid in the bulk and therefore maintains a hydrophobic surface for a longer time. On the other hand a thicker coating conducts the heat from dry band arcing slower than a thinner coating to the substrate. Therefore a higher temperature on and a larger damage result to the surface. This also leads to a shorter time to the onset of failure. Hence there expected and as was recently reported, an optimum coating thickness to give the longest lifetime [85]. It is found that the coating with 75μm particle size has the largest LMW content by weight of the five sizes from 1 to 75μm(Fig.5.7). However for this particle size the coating also has the largest surface roughness, the smallest area of heat conduction and the shortest time to failure[45]. The coatings with 4.5 and 13μm have a larger content of LMW than the coatings with 1 and 17μm(Fig.5.7). They also have a smoother surface and a larger area of heat conduction than the coating with 17μm.

This leads to the best electrical performance and the longest time to failure in the coatings with 4.5 and 13μm[45]. The coating with 1μm has the smallest LMW content(Fig.5.7) and has distinct areas on the surface where larger protruding roughness and discontinuities exist[45]. This shortens the lifetime of the coating.

There is an insignificant effect on the LMW content and the diffusion of LMW from the bulk to the surface with the solvents of 1,1,1 trichloroethane and V&P naphtha. However it has been reported that the solvent used in RTV coating affects its performance and lifetime in salt-fog condition[85]. This indicates that the influence of the solvent on the lifetime of RTV coating is not due to its LMW content and diffusion to the surface within a recovery time of 24h which is used in the present work.

CHAPTER VI

CONCLUSIONS AND SUGGESTIONS FOR FUTURE RESEARCH

6.1 CONCLUSIONS

1. The life of ATH filled RTV coatings depends on the size of ATH particle when tested in salt-fog. Generally the coating with smaller size of particle has a longer life except for very small sizes when the dispersion becomes less effective. The best performance to yield lower leakage current, lower current pulse count and the longest time to failure of the coating was obtained with 4.5μm size of ATH particles.

The role of the size of the ATH particle filler in determining the life of RTV coating is the combined effect of roughness, heat conduction into the volume, and the amount of silicone fluid on the surface of the coating. A larger particle size results in a rougher surface which leads to a higher leakage current. A higher temperature develops at the surface with larger particle size due to its poorer thermal conduction when dry band discharges occur. This results in more damage to the surface. Slower diffusion of the silicone fluid retards the recovery of the water repellency (hydrophobicity) of the surface. The aging of the coating is then accelerated and a shorter life is expected with larger size of ATH particle.

The coating with 1.0μm size of ATH particles has distinct areas on the surface where large protruding roughness and discontinuities exist. These result in hot spots on the surface which accelerate the erosion on the surface and ultimately lead to a shorter life of the coating. The coating with 1.0μm has the

smallest LMW content by weight percentage in five sizes of ATH particles from 1.0 to 75μm used. This may also shorten the life of the coating. The large roughness and discontinuities are attributed to aggregation of the particles in the RTV coating. The aggregation might occur due to poor dispersion in the liquid or during vulcanization after coating the substrate.

2. The thickness affects the electrical performance of RTV silicone rubber coating in salt-fog. Conduction of the heat generated by the dry band arcing results in more damage with a rougher surface which causes a larger leakage current and a higher current pulse counts in the thicker coatings. On the other hand the thicker coatings have a higher speed of diffusion of LMW fluid to the surface and a larger amount of silicone fluid in the bulk. This may maintain a hydrophobic surface for a longer time for a thicker coating.

An optimum thickness is obtained in the RTV coating on FRP rods by indicating the longest lifetime of coating. This is because the thinner coating has less material to erode and exposes FRP quickly. This causes the specimen to fail in a short time by tracking on the substrate. On the other hand the thicker coating has a higher current and more damage. This also leads to shorter time to failure. Hence there is an optimum coating thickness to give the longest lifetime of coating. The best electrical performance of RTV is obtained in a coating thickness of 0.38mm on polyester FRP.

For RTV coating on porcelain, the leakage current increases with increasing coating thickness and optimum thickness is not found. This is because when the RTV is sufficiently eroded to expose the surface of porcelain, the porcelain has

a large resistance to erosion and did not fail by tracking on the surface due to its high heat capacity.

3. Adding 1% and 10% silicone fluid by weight to the formulation of RTV adversely affects the electrical performance of the coating in salt-fog. The viscosity of the added silicone fluid was 1000 centipoise. Coating performance decreases with addition of silicone fluid from 1 to 10% by weight. This is thought that the more abundant silicone fluid on the surface retards the heat conduction from the dry band arcing to the bulk due to its lower thermal conductivity. This causes a higher temperature on the layer of the silicone fluid resulting in more damage, a rougher surface and therefore a larger leakage current, a higher current pulse counts and a shorter life.

4. RTV coating on epoxy FRP, polyester FRP and glass initially develops a similar leakage current in salt-fog. After the coating erodes and partially exposes the substrate to the salt-fog, the leakage current depends on the coating substrate. Coated epoxy FRP has a larger leakage current than both polyester FRP and glass after the coating is eroded and the substrate exposed to salt-fog. The higher leakage current on the partially exposed epoxy FRP causes more erosion of the coating and consequently it fails by tracking on the substrate in a shorter time. Coated polyester FRP and coated glass have a similar level of leakage current and consequently a similar erosion rate. This leads to similar times to failure on both substrates.

5. The solvent used in RTV coating affects its performance in salt-fog conditions. The coating using naphtha has a lower discharge current and a higher resistance to erosion and therefore yields a better performance than the coating using 1,1,1 trichloroethane. However, naphtha is combustible and RTV coating dispersed in this solvent can not be applied to energized insulators.

The solvent type has negligible effect on the LMW content of silicone fluid and on the diffusion of LMW to the surface.

6. The total content by weight of LMW of silicone fluid in RTV coatings decreases with increasing coating thickness. The total LMW content by weight decreases from (4.49±0.04)% to (4.00±0.02)% with increasing coating thickness from 0.17 to 0.99mm. The reason for this dependence on thickness is unknown at the present time. The diffusion of LMW silicone fluid to the surface from the bulk of the virgin RTV coating increases with increasing coating thickness.

Generally the LMW content of silicone fluid by weight in the virgin coating increases with increasing size of the ATH particles. The coating with 4.5 and 13μm have almost identical LMW content of silicone fluid and both of these coatings have more LMW of silicone fluid than the coatings with 1 and 17μm. After 24h recovery time the coatings have the same value of diffused LMW of silicone fluid to the surface for all sizes of ATH particles from 1 to 75μm.

7. The total content of LMW silicone fluid decreases after 570h of salt-fog at 0.5kV_{rms}/cm and 250μS/cm for all coating thicknesses from 0.17 to 0.99mm. The decrease is almost independent of coating thickness but depends on the

intensity of the dry band arcing on the surface of the RTV specimen. The total content of LMW decreases to (3.43±0.07)% by weight for all thicknesses of coating near the high voltage electrode. This is because more intense dry band discharges are developed near the high voltage electrode resulting in more removal of LMW of silicone fluid from the surface. This is confirmed in an electric oven, where RTV specimens are subjected to different temperatures, in that the total content of LMW decreases with increasing temperature. The total content by weight of LMW decreases slightly from 4.16 to 3.80% with increasing coating thickness, respectively, from 0.17 to 0.99mm at the bottom end of the rod near the grounded electrode after 570h of salt-fog.

8. The life of RTV coating is determined by the combined effects of LMW content of silicone fluid, diffusion to the surface, thermal conductivity, surface roughness, type of substrate, size of ATH particles, amount of ATH(pph), electric stress level, thickness of coating, salinity and velocity of the salt-fog.

6.2 SUGGESTIONS FOR FUTURE RESEARCH

The electrical performance of RTV silicone rubber coatings with various formulations has been extensively investigated in salt-fog. However, there are many aspects which may affect the performance of RTV coatings and further research is suggested to improve the performance of the coating.

1. The RTV coating with 1.0μm size of ATH particles has a poor performance

due to the aggregation of the fine particles resulting in large roughness and discontinuities on the surface. Aggregation of this size of filler particles is often encountered in polymers. It is well known that silane treatment can improve ATH dispersibility. It is suggested to study this aspect of treatment in a future work in order to improve the performance of the coating.

2. The evaluation of the RTV coatings in the present work was conducted with AC electric stress. The insulator with DC stress can accumulate more contaminants than with AC insulator due to unidirectional electric field on the surface of the insulator. Therefore the performance of the RTV coating under DC electric stress may differ from AC and future study is suggested to evaluate the RTV coating with DC electric stress.

3. The RTV coatings was evaluated in an extended salt-fog test in the present work. The coating lost its water repellency completely and formed a continuous water filming on the surface several hours after the start of the test due to the accelerated wetting and contamination conditions. The evaluation of the performance indicated by leakage current and time to failure thus largely depended on the coating resistance to erosion. Further study is needed to investigate the coatings with various formulations in practical service environments.

BIBLIOGRAPHY

[1] A.W. Adamson,"Physical chemistry of surface",4th Ed., 1982.

[2] J.D. Andrade,"Polymer surface and interface dynamics: An introduction", in Polymer Surface Dynamics, pp.1-8, Ed., J.D. Andrade, Plenum Press, 1988.

[3] S.H. Kim, E.A. Cherney and R. Hackam,"Hydrophobic behaviour of insulators coated with RTV silicone rubber", IEEE Trans. on Electrical Insulation, Vol.27, pp.610-622, 1992.

[4] C.H.A. Ely and P.J. Lambeth,"Artificial-pollution test for high-voltage outdoor insulators", Pro. IEE, Vol.111, pp.991-998, 1964.

[5] P.J. Lambeth, J.S.T. Looms, A. Stalewski and W.G. Todd,"Surface coatings for H.V. insulators in polluted areas", Pro. IEE, Vol.113, pp.861-869, 1966.

[6] P.J. Lambeth,"Effects of pollution on high voltage outdoor insulators", Pro. IEE, IEE Reviews, Vol.118, pp.1107-1130, 1971.

[7] J. Johnson, R.T. Henderson, W.S. Price, D.E. Hedman and F.J. Turner,"Field and laboratory tests of contaminated insulators for the design of the state electricity commission of Victoria 500kV system", IEEE Trans. on PAS, Vol.PAS-87, pp.1216-1228, 1968.

[8] I. Kimoto, K. Kito and T. Takatori,"Anti-pollution design criteria for line and station insulators", IEEE paper 71 TP649-PWR, pp.317-327, 1971.

[9] F. Obenaus,"Contamination flashover and creepage path length", Deutsh, Elektrotechnik, Heft4, pp.135-136, 1958.

[10] E.A. Cherney, R. Hackam and S.H. Kim,"Porcelain insulator maintenance with RTV silicone rubber coatings", IEEE Trans. on Power Delivery, Vol.6, pp.1177-1181, 1991.

[11] J.S. Forrest,"The characteristics and performance in service of high voltage porcelain insulators", Pro. IEE, Vol.89, Part 2, pp.60-92, 1942.

[12] J.J. Taylor,"Insulators to withstand air-borne deposits", AIEE Trans., Vol.67, pp.1436-1441, 1948.

[13] G.H. Gillam,"Report on the work of study committee No.5 (insulators)", CIGRE, paper 234, 1964.

[14] M.J. Billings and R. Wilkins,"Considerations of the suppression of insulator flashover by resistive surface films", Pro. IEE, Vol.113, pp.1649-1653, 1966.

[15] J.H. Moran and D.G. Powell,"Resistance graded insulators - The ultimate solution to the contamination problem?", IEEE Trans. on PAS, Vol. PAS-91, pp.2452-2458, 1972.

[16] H. Fukui, K. Naito, T. Irie and I. Kimoto,"A practical study on application of semiconducting glaze insulators to transmission lines", IEEE Trans. on PAS, Vol. PAS-93, pp.1430-1443, 1974.

[17] L. Egiziano, P.G. Orsini and V. Tucci,"On the corrosion phenomena of semiconducting glazed insulators", 4th Intern. Symp. on High Voltage Eng., paper 45.10, Athens, Greece, 1983.

[18] L. Egiziano, G. Lupo, B. Macchiaroli, V. Tucci and P.G. Orsini,"Investigation on ageing characteristics of semiconducting glazed insulators", Intern. Conf. on Properties and Applications of Dielectric Materials, pp.751-753, Xian, China, 1985.

[19] A.C. Baker, J.W. Maney and Z. Szilagyi,"Long term experience with semi-conductive glazed high voltage post insulators", IEEE Trans. on Power Delivery, Vol.5, pp.502-508, 1990.

[20] J.E. Conner and A.D. Lantz, jr."The insulator contamination problem as influenced by silicone surface coatings", Am. IEE, Vol.77, Part III, pp.1101-1112, 1958.

[21] J.S. Forrest,"The electrical characteristics of 132kV line insulators under various weather conditions", Proc. IEE, Vol.79, pp.401-423, 1936.

[22] E.A. Cherney and D.J. Stonkus,"Non-ceramic insulators for contaminated environments", IEEE Trans. PAS, Vol.PAS-100, pp.131-142, 1981.

[23] P. Ignacz,"Silicone-greasing provides excellent insulator flashover protection", Power Engineering, October, pp.56-57,1962.

[24] R. Krasa and T. Orbeck,"Development of a long-life, arc-resistant silicone insulator compound", 1975 Annual International Conference of Doble Clients, April, 1975, Boston, paper 42AIC75.

[25] R.M. Radwan and G.M. Abd El-Salam,"Effects of silicone grease on the DC electrical characteristic of polluted insulators", 3th Intern. Sym. on High Voltage Eng., paper 54.04, Milan, August 28-31, 1979.

[26] A. Leschanz and E. Steinort,"Examination of the silicone grease on epoxy resin outdoor insulators", 3th Intern. Sym. on High Voltage Eng., paper 54.09, Milan, August 28-31, 1979.

[27] H. Dietz, H. Karner, K.H. Muller, H. Patrunky, G. Schenk, P. Verma and H.J. Voss, "Latest developments and experience with composite longrod insulators", CIGRE, paper 15-09, 1986.

[28] B. Fuentes and T. Orbeck,"Evaluation of silicone elastomers for outdoor high voltage insulators", Mexicon 82, X Conf. Intern. Sobre Investigation, Desarrollo Y Aplicacion En Ingenieria Electrica, Electronica Y Comunicaciones, IEEE Mexico, October 29, 1982.

[29] F. Hammer, A. Kuchler and G. Maueler,"Behaviour of bushings with silicone rubber sheds", 6th Intern. Sym. on High Voltage Eng., paper 47-38, New Orleans, LA, USA, August 28 - September 1, 1989.

[30] J. Hall and T. Orbeck,"Evaluation of Silicone Elastomers for Outdoor High Voltage Insulators",IEEE Trans on PAS, Vol.101, pp.4689-4696, 1982.

[31] R.E. Carberry and H.M. Schneider,"Evaluation of RTV Coating for Station Insulators Subject to Coastal Contamination", IEEE Trans. on Power Delivery, Vol.4, pp577-585, 1989.

[32] R.S. Gorur, E.A. Cherney and R. Hackam,"A comparative study of polymer insulating materials under salt-fog conditions", IEEE Trans. on E.I., Vol.EI-21, pp.175-182, 1986.

[33] R.S. Gorur, E.A. Cherney and R. Hackam,"Performance of polymeric insulating materials in salt-fog", IEEE Trans. on Power Delivery, Vol.PWRD-2, pp.486-492, 1987.

[34] R.S. Gorur, E.A. Cherney and R. Hackam,"The electrical performance of polymeric insulating material under accelerated aging in a fog chamber", IEEE Trans. on Power Delivery, Vol.3, pp.1157-1164, 1988.

[35] R.S. Gorur, E.A. Cherney, R. Hackam and T. Orbeck,"The electrical performance of polymeric materials under accelerated aging in a fog chamber", IEEE Trans. on Power Delivery, Vol.3, pp.1157-1164, 1988.

[36] S.S. Low and G.R. Elder,"Experience dictates future HVDC insulator requirements", IEEE Trans. on E.I., Vol.16, pp.263-266, 1981.

[37] R.G. Niemi and T. Orbeck,"High Surface Resistance Protective Coatings for HV Insulators"IEEE PES Summer Meeting PaperC72 557- 1972.

[38] S.H. Kim, E.A. Cherney and R. Hackam,"The Loss and Recovery of Hydrophobicity of RTV Silicone Rubber Coatings", IEEE Trans. on Power Delivery, Vol.5, pp.1491-1500, 1990.

[39] A.E. Vlastos and E. Sherif,"Experience from insulators with RTV silicone rubber sheds and shed coating", IEEE PES 1989, Winter Meeting 1989, Paper 89 WM 120-7 PWRD.

[40] S.H. Kim, E.A. Cherney and R. Hackam,"Suppression mechanism of leakage current on RTV coated porcelain and silicone rubber insulators",IEEE Trans. on Power Delivery, Vol.6, pp.1549-1555, 1991.

[41] "Silicones, Chemistry and Technology", Ed: A.G. Bayer, et al, CRC Press, 1991.

[42] S.H. Kim, E.A. Cherney, R. Hackam and K.G. Rutherford,"Chemical changes at the surface of RTV silicone rubber coatings on insulators during dry band arcing",IEEE Trans. on Dielectrics and Electrical Insulation, Vol.1, pp.106-123, 1994.

[43] S.H. Kim, E.A. Cherney and R. Hackam,"Effect of Dry Band Arcing on the Surface of RTV Silicone Rubber Coatings", Conf. Record of the 1992 IEEE Inter. Symps. on Electr. & Insul., Baltimore, pp.237-240, 1992.

[44] S.H. Kim, E.A. Cherney and R. Hackam,"Effects of Filler Level in RTV Silicone Rubber Coatings Used in HV Insulators",IEEE Trans. on Electrical Insulation, Vol.27, pp1065-1072, 1992.

[45] H. Deng, R. Hackam and E.A Cherney,"Role of the size of particles of alumina trihydrate filler in the life of RTV silicone rubber coating", IEEE Trans. on Power Delivery, Vol.10, pp.1012-1024, 1995.

[46] S.M. Gubanski and A.E. Vlastos,"Wettability of naturally aged silicone and EPDM composite insulators", IEEE Trans. on Power Delivery, Vol.5, pp.1527-1535, 1990.

[47] IEEE Dielectric and Electrical Insulation Society Outdoor Service Environment Committee S-32-3 Report, "Protective coatings for improving contamination performance of outdoor high voltage ceramic insulators",IEEE Trans. on Power Delivery, Vol.10, Paper 94 WM 096-8 PWRD,1994.

[48] R.S. Gorur, G.G. Karady, A. Jagota, M. Shah and A.M. Yates,"Aging in Silicone Rubber Used for Outdoor insulation", IEEE Trans. on Power Delivery, Vol.7, pp.525-538, 1992.

[49] H. Deng, R. Hackam and E.A. Cherney,"Effects of addition of silicone fluid on electrical performance of RTV silicone rubber coating", 1995 IEEE 5th Intern. Conf. on Conduction and Breakdown in Solid Dielectrics, Leicester, U.K., pp.616-620, 1995.

[50] J.I. Kroschwitz(editor),"Encyclopedia of Polymer Science and Engineering", Vol.15, John Wiley and Sons, pp.204-308, 1989.

[51] IEC Report, Publication NO.57,"Artificial Pollution Test on High Voltage Insulators to Be Used on AC System", 1975

[52] IEEE Standard NO.4,"Standard Techniques for High Voltage Testing", 1978.

[53] S.H. Kim, E.A. Cherney and R. Hackam,"Artificial testing and evaluation of RTV coatings in a salt-fog chamber",IEEE Trans. on Electrical Insulation, Vol.26, pp.797-805, 1991.

[54] IEEE Standard Techniques for High Voltage Testing, IEEE Std 4-1978, pp.33, 1978.

[55] S.H. Kim,"Electrical performance and surface analysis of RTV silicone rubber coatings for H.V. outdoor insulators", Ph.D. dissertation, University of Windsor, Ontario, Canada, 1992.

[56] S.H.Kim and R. Hackam,"Effects of saline water flow rate and air speed on leakage current in RTV coatings", IEEE. Trans. on Power Delivery, 95Winter Meeting, 1995.

[57] S.H. Kim and R. Hackam,"Temperature distribution in RTV silicone rubber coating following dry band arcing",IEEE Intern. Symps. Electrical Insulation, Pittsburgh, pp.599-602, 1994.

[58] Y.S. Touloukian, R.W. Powell, C.Y. Ho and P.G. Klemens,"Thermal conductivity, Nonmetallic solids", Thermophysical Properties of Matters, The TPRC Data Series, Vol.2,IFI/PLENUM, New York-Washington, 1970.

[59] M. Issi and M. Komatsubara,"Hydrophobicity of organic insulating materials", CEIDP, Ottowa, pp.134-139, 1988.

[60] S.M. Gubanski,"Properties of silicone rubber housings and coatings", IEEE Trans. on Power Delivery, Vol.27, pp.374-382, 1992.

[61] E. Matijevic,"Surface and Solid Science", Vol.2, pp.85, Wiley-Interscience, 1969.

[62] S. Wu,"Polymer Interface and Adhesion", pp.11, Marcel Dekker, INC., 1982.

[63] J.D. Andrade,"Surface Infrared Spectroscopy", in "Surface and Interfacial Aspects of Biomedical Polymers", Vol.1, Surface Chemistry and Physics, Ed., J.D. Andrade, Plenum Press, 1985.

[64] N.J. Harrick,"Use of infrared absorption in Germanium to determine carrier distribution for injection and extraction", Phys. Rev., Vol.103, pp.1173-1181, 1956.

[65] N.J. Harrick,"Surface chemistry from spectral analysis of totally internally reflected radiation", J. Phys. Chem., Vol.64, pp.1110-1114, 1960.

[66] J. Fahrenfort,"Attenuated total reflection, a new principle for the production of useful infra-red reflection spectra of organic compounds", Spectrochim. Acta, Vol.17, pp.698-709, 1961.

[67] J. Fahrenfort and W.M. Visser,"On the determination of optical constants in the infrared by attenuated total reflection", Spectrochim. Acta, Vol.18, pp.1103-1116, 1962.

[68] W. Noll,"Chemistry and Technology of Silicones", Academic Press, 1968.

[69] C.N.R. Rao,"Chemical Applications of Infrared Spectroscopy", Academic Press, 1963.

[70] R.M. Silverstein, G.C. Bassler and T.C. Morrill,"Spectrometric Identification of Organic Compounds", 3rd Ed., John Wiley & Sons Inc., 1974.

[71] D.N. Kendall,"Applied Infrared Spectroscopy", Reinhold Publishing Corp., 1966.

[72] A.L. Smith,"Analysis of Silicones", John Wiley & sons, 1974.

[73] F. Kreith,"Principles of Heat Transfer", Inter. Textbook Co.,1965.

[74] S.H. Kim, E.A. Cherney and R. Hackam,"Thermal Characteristics of RTV Silicone Rubber Coatings as a Function of Filler Level", 1992 Conf.on Electrical Insulation & Dielectric Phenomenon, Victoria, pp713-718, 1992.

[75] A.E. Vlastos and S.M. Gubanski,"Surface Structure Changes of Naturally Aged Silicone and EPDM Composite Insulators",IEEE Trans. on Power Delivery, Vol.6, pp888-900, 1991.

[76] R.J. Hill,"Laboratory analysis of naturally aged silicone rubber polymer insulators from contaminated environments, 138 to 765kV",IEEE T&D Conf. and Exhibition, Chicago, 1994.

[77] A.C.M. Wilson,"Insulating liquids: their uses, manufacture and properties", Ch.6, pp.126-135, Peter Reregrinus Ltd, 1980.

[78] R.S. Gorur, G.G. Karady, A. Jagota, M. Shah and B.C. Furumasu,"Comparison of RTV silicone rubber coatings under artificial contamination in a fog chamber",IEEE Trans. PD, Vol.7,pp.713-719,1992.

[79] "The Corning Laboratory Catalogue: Glass, Plastics, Equipment and Instruments", p.T9, 1988.

[80] "Kontes Catalogue, scientific glassblowers supplies", p.34, 1985.

[81] K.J. Saunders,"Organic Polymer Chemistry", Chapman & Hall, 1986.

[82] J.W. Chang and R.S. Gorur,"Surface recovery of silicone rubber used for HV outdoor insulation", IEEE Trans. on Trans. Dielectrics and Electrical Insulation, Vol.1, pp.1039-1046, 1994.

[83] S.H. Kim and R. Hackam,"Formation of silicone fluid at the surface of RTV silicone rubber coating due to heat", Conf. on Electrical Insulation and Dielectric Phenomena, IEEE Pub. 93CH 3269-8, pp.605-611, 1993.

[84] J. Kindersberger and M. Kuhl,"Effect of hydrophobicity on insulator performance", 6th Inter. Syms. on High Voltage Engineering, Paper 12.01, New Orleans, USA, 1989.

[85] H. Deng, R. Hackam and E.A Cherney,"Influence of thickness, substrate type, amount of silicone fluid and solvent type on the electrical performance of RTV silicone rubber coatings", IEEE PES Winter Meeting, Paper 250-1 PWRD, 1995.

[86] M.J. Owen, T.M. Gentle, T. Orbeck and D.E. Williams, 8th Rocky Mountain Regional ACS Meeting, Denver, Colorado, June 1986.

PUBLICATIONS IN SUPPORT OF THIS THESIS

I. Refereed Journals:

[1] H. Deng, R. Hackam and E.A. Cherney,"The Role of the Size of Alumina Trihydrate Particle Filler on RTV Silicone Rubber Coating Life",IEEE Transactions on Power Delivery, Vol.10, pp.1012-1024, 1995.

[2] H. Deng, R. Hackam and E.A. Cherney,"Influence of Thickness, Substrate Type, Amount of Silicone Fluid and Solvent Type on the Electrical Performance of RTV Silicone Rubber Coatings",IEEE Trans. on Power Delivery, 95 WM 250-1 PWRD, pp.1-11, New York, Jan. 29 to Feb. 2, 1995.

[3] H. Deng, R. Hackam and E.A. Cherney,"Electrical Performance of RTV Silicone Rubber Coating on Porcelain with Different Thicknesses", IEEE PES Winter Meeting, January, 1995. Sent on July 28, 1995.

II. Refereed International Conferences:

[4] H. Deng, R. Hackam and E.A. Cherney,"Effects of Addition of Silicone Fluid on Electrical Performance of RTV Silicone Rubber Coatings", 1995 IEEE 5th Inter. Conf. on Conduction and Breakdown in Solid Dielectrics, Leicester, UK, pp.616-620, 1995.

[5] H. Deng, R. Hackam and E.A. Cherney,"Study of Production of Silicone Fluid in RTV Silicone Rubber Coatings due to Dry Band Arcing and Applied Heat", 1995 IEEE Conference on Electrical Insulation and Dielectric Phenomena, Virginia Beach, Virginia, paper 6-1, Oct. 22-25, 1995.

[6] H. Deng, R. Hackam and E.A. Cherney,"Low Molecular Weight Silicone Fluid Content and Diffusion in RTV Silicone Rubber Coating",1995 Inter. Symps.on Electrical Insulating Materials, Tokyo, Japan, pp.181-184, 1995.

[7] H. Deng, R. Hackam and E.A. Cherney,"Factors Influencing the Electrical Performance of RTV Silicone Rubber Coatings", 1994 IEEE Conference on Electrical Insulation and Dielectric Phenomena, Arlington, Texas, pp.669-674, 1994. IEEE Conference Proceedings 94CH3456-1.

[8] H. Deng, R. Hackam and E.A. Cherney,"Effect of Coating Thickness of RTV Silicone Rubber on Its Electrical Performance", 1994 IEEE Inter. Symps. on Electrical Insulation, Pittsburgh, PA, PP.578-581, 1994. IEEE Conference Proceedings 94 CH3445-4.

[9] H. Deng, E.A. Cherney and R. Hackam,"Effects of Particles Size of ATH Filler on the Performance of RTV Rubber Coatings", 1993 Conf. on Electrical Insulation and Dielectric Pheno.(CEIDP), Pocono Manor, PA, pp.598-604, 1993. IEEE Conference Proceedings 93CH3269-8.

[10] H. Deng, E.A. Cherney and R. Hackam,"Optimum of Particle Size of ATH Filler to Enhance Performance of RTV Rubber Coating", 25th Symps.on Electrical Insulating Materials, Nagoya, Japan, pp.99-102, 1993.

VITA AUCTORIS

Hui Deng was born in 1964 in Liaoning Province, China. He received his B.Sc. from Huazhong University of Science and Tech., China, M.Sc. from the Graduate School, Electric Power Research Institute, Ministry of Energy, China, all in Electrical Engineering in 1985 and 1988, respectively. From 1988 to 1992, he was at High Voltage Department, Electric Power Research Institute, Ministry of Energy, China. He is currently a candidate for the degree of M.A.Sc., Electrical Engineering, University of Windsor, Windsor, Ontario, Canada.